FROM IMPACTS TO IMPLEMENTATION: A SURVEY OF SAND DAMS IN SUB-SAHARAN AFRICA

A Dissertation

Submitted to the Faculty

of

Purdue University

by

Jessica A. Eisma

In Partial Fulfillment of the

Requirements for the Degree

of

Doctor of Philosophy

August 2020

Purdue University

West Lafayette, Indiana

THE PURDUE UNIVERSITY GRADUATE SCHOOL
STATEMENT OF COMMITTEE APPROVAL

Dr. Venkatesh Merwade, Chair

Lyles School of Civil Engineering

Dr. Dennis Lyn

Lyles School of Civil Engineering

Dr. Chad Jafvert

Lyles School of Civil Engineering

Dr. Indrajeet Chaubey

Dean, College of Agriculture, Health and Natural Resources, University of Connecticut

Approved by:

Dr. Dulcy Abraham

Head of the School Graduate Program

To my Eismen

ACKNOWLEDGMENTS

Dr. Venkatesh Merwade, thank you for helping me grow as a researcher and for your flexibility throughout my graduate studies. Your leadership made my graduate school experience truly enjoyable.

I would also like to thank the rest of my committee for their helpful comments and guidance: Dr. Dennis Lyn, Dr. Chad Jafvert, and Dr. Indrajeet Chaubey. Immeasurable gratitude goes to my graduate school community that helped make every day great: my CE hydro office mates, the geotech lunch crew, the tireless women in the CE main office and business office, CEGSAC, and EACC.

I would like to thank the Mennonite Central Committee of Tanzania, especially Al Wright, for the introduction to Tanzania's sand dams and their community water groups. I would also like to thank my translators, Christina Sumayani, George John Filex, and Benedict Mwiliko, for their assistance in all matters. Further gratitude goes to the Kimokouwa, Soweto, and Chididimo community water groups, without whom this research would not have been possible. Additional appreciation goes to Nelson Mandela African Institute for Science and Technology, especially Dr. Karoli Njau, for providing a home base and instrumental guidance while I was in Tanzania.

Last, but certainly not least, I would like to thank my family. Thank you to my parents for always believing in my journey and for providing a place to crash and countless meals while I finished this dissertation. I am ever grateful to my husband, RJ, for his unending support, encouragement, and for always keeping me accountable. Thank you for sticking by side throughout my unconventional PhD path, and thank you for taking care of our son, Isaiah, so I could focus on making my dreams come true! And lastly, to my son Isaiah, I cannot say how much your giggles lifted me up throughout this process, even as you tried to pull me off my chair to play with you. Mama can play now :)

TABLE OF CONTENTS

Page

LIST OF TABLES

LIST OF FIGURES

Figure Page

Figure Page

Figure Page

ABSTRACT

Eisma, Jessica A. Ph.D., Purdue University, August 2020. From impacts to implementation: A survey of sand dams in sub-Saharan Africa. Major Professor: Venkatesh Merwade.

International development projects are a massive business, with billions invested annually in the Global South. However, such projects have an unacceptably long record of high failure rates. The problem perpetuates, in part, due to the success factors by which international development projects are judged. Often, projects are assessed on the basis of donor-identified priorities that are not aligned with local impacts. One such international development project involves the construction of small-scale water harvesting structures known as sand dams. Non-governmental organizations (NGOs) continue to raise sufficient funds to build thousands of sand dams across sub-Saharan Africa, and yet 50% of sand dams are estimated to be non-functioning.

Sand dams are small, reinforced concrete dams built across an impermeable streambed. Over time, sand settles behind the dam, creating an upstream sand reservoir that fills with rainwater and surface runoff. The sand helps filter the water, protects it from evapotranspiration, and can provide water to the local community for domestic and agricultural use during the dry season. Sand dams often fail due to poor construction, inadequate siting, and siltation.

This dissertation explores methodologies for studying the regional and local impacts of sand dams and investigates the feasibility of developing model-based site selection guidelines for sand dams. Three objectives of this study are: (1) to develop a methodology to assess the ability of sand dams in improving the overall water availability in the region; (2) to examine claims made by non-scientific bodies about sand dam impacts by investigating how diverse sand dams influence macroinvertebrate

habitat, vegetation, erosion, and local water availability; and (3) to create guidelines for siting new sand dams based on a fully integrated surface and groundwater flow model.

For the first objective, two multiple regression models are developed to compare (1) water storage and (2) vegetation in an area with a high density of sand dams, termed the sand dam counties (SDC), to those in a control area. The models analyze remotely sensed datasets to assess whether evidence exists of significantly increased storage in the SDC relative to the control area. The results show that the remotely sensed water storage data is unable to consistently detect higher levels of water storage in the SDC. This is likely due to the low resolution of the dataset combined with the small magnitude of sand dams' impact on regional water storage. The results of the vegetation model show that the sand dams have a consistent, positive impact on vegetation within the SDC relative to the control area. Because vegetation health and cover is often correlated with groundwater levels, these results likely indicate that the sand dams are also increasing local groundwater levels. Overall, this study shows that remotely sensed dataset can provide a useful basis to assess the impact of international development projects, particularly those that involve the natural environment.

For the second objective, data relating to macroinvertebrates, vegetation, erosion, and water table elevations at three sand dams were collected and analyzed during a year-long field study in Tanzania. These study subjects were specifically selected to test an NGO claim that sand dams revitalize the entire ecosystem. The results of this study show that sand dams are not a suitable habitat for macroinvertebrates due to their homogeneity. The impact of sand dams on vegetation cover can be significant, but may be limited by the slope of the surrounding land. Functioning sand dams likely have little impact on streambank erosion, but non-functioning sand dams may contribute to the erosion of streambanks in unstable reaches. Lastly, the water table is locally raised by recharge from sand dams, however, the spatial and temporal extent of the impact is more limited than conveyed by NGOs and previous studies. This study adds to the limited body of knowledge on the environmental responses to sand

dams and demonstrates the importance of examining the local impacts of individual international development projects.

For the third objective, results from four different simulations of a watershed-based model with three cascading sand dams are analyzed to identify overland features that improve vadose zone storage and groundwater recharge and reduce evapotranspiration. Results from this study show that sand dams constructed in a low-lying area that collects surface runoff from adjacent steep slopes, such as in a U-shaped valley, will likely collect and store sufficient water for use by a local community. Watersheds with relatively more area cultivated with low-water-need crops will similarly be beneficial to sand dam performance. In addition, the analysis revealed that the volume of water a sand dam receives during a rainy season is less important for water storage than the duration of dry seasons. Lastly, the simulations showed that sand dams constructed in an area with sandier soils will perform better than those in an area with loamy soils. This study produced a set of guidelines that can be used to identify locations where sand dams are likely to capture and store sufficient water for community use during the dry season.

1. INTRODUCTION

One of the United Nations' Sustainable Development Goals, addressing the problem of food insecurity, poses difficulties for communities in developing nations. A food-secure community can maintain a nutritionally balanced and sufficiently calorific diet through either agricultural or economic means. Beyond the issue of widespread poverty, many developing nations face additional hindrances to food security: depleted natural resources, challenging climatic conditions, and deficient infrastructure, among others. In Tanzania and Kenya, where 80% of the population works in agriculture, many families grow most of their own food but are still food insecure. The two primary factors limiting crop yield in sub-Saharan Africa are nutrient-poor soils and water scarcity (World Bank, 2013). Tanzania and Kenya present an interesting opportunity, because the countries generally receive sufficient rainfall but lack the infrastructure to capture and store the rainfall for use during the dry seasons. Mueller et al. (2012) estimate that better water management could result in increased crop yields of up to 25%. An ancient water-capture and storage technology is revitalizing communities in the heart of Africa—sand dams.

Sand dams are simple reinforced concrete dams built atop impermeable river beds in arid regions with infrequent, high-intensity rainfall (see Figure 1.1). The high-intensity rainfall washes sand overland where it builds up behind the dam. After a few rainy seasons, the sand begins storing water, where it is naturally filtered, protected from evapotranspiration, and helps raise the groundwater level in the surrounding area (Borst & de Haas, 2006; Hut et al., 2008; Quilis et al., 2009). One sand dam can store millions of liters of water, provide clean water throughout the year to a thousand people, increase vegetation, and improve the arability of the surrounding land (Borst & de Haas, 2006).

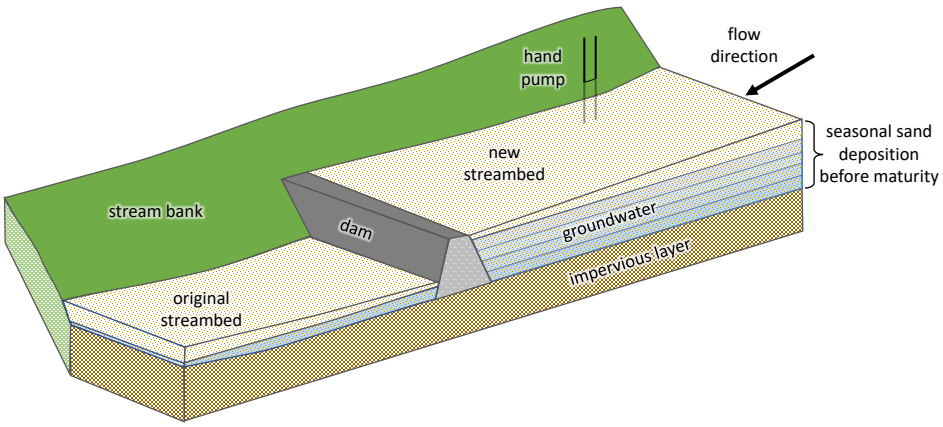

Figure 1.1. Schematic of a sand dam showing seasonal sand deposition before the dam reaches maturity.

The impacts of climate change in sub-Saharan Africa risk the food security progress resulting from sand dams in rural communities. Sand dams, however, offer a much-needed buffer against these changes. Current climate change projections indicate precipitation in the region will increase, but that it will be concentrated in high-intensity rainfall events (World Bank, 2013). This increases the likelihood of flooding, especially since many countries in sub-Saharan Africa lack adequate water infrastructure. Sand dams offer an opportunity to capture and retain large quantities of water, helping to reduce flooding and to store the water for future use. This will be increasingly important for maintaining food security, since drought, aridity, and temperature are also expected to increase gradually over time. Crop yields are predicted to decrease by 5 to 20%, and livestock production will suffer due to decreased forage material and increased heat stress (World Bank, 2013).

While acknowledging the important role of sand dams in increasing food security, this work focuses on understanding how sand dams influence the local environment. Non-governmental organizations (NGOs) are constructing sand dams throughout East Africa, but few scientific studies have investigated the ecological impact of these

structures. There is some evidence that many sand dams do not capture and store water as effectively as is commonly believed (de Trincheria, Leal, & Otterpohl, 2018; Viducich, 2015). As with any rapidly expanding project, the current pace of sand dam construction has the potential to lead to over-development and subsequent negative impacts. This is particularly true if many of the sand dams built are not functioning as intended. This dissertation aims to provide greater understanding of the benefits of sand dams as well as potential drawbacks.

1.1 Background

The first subsurface dams were built hundreds, maybe thousands, of years ago in arid and semi-arid regions of the world (Hut et al., 2008). In sub-Saharan Africa, this technology has developed into the sand dam (see Fig. 1.1). Sand dams were first popularized by a local NGO in Kenya, Utooni Development Organization. NGOs have built over 3000 sand dams since the late 1970s (de Trincheria et al., 2018; Viducich, 2015).

1.1.1 Hydrology of sand dams

Sand dams are most often constructed all at once over the course of a few weeks, rather than in stages as recommended by Nissen-Petersen (2006). During the first rainfall after a dam's construction is complete, surface runoff and streamflow will carry many soil particles to the location of the dam. Some of these soil particles will remain suspended in the water column and flow over the dam, while the heavier particles, such as sand, will settle out and form the first layer of the sand dam. When the streamflow dries after a short time, perhaps two days in these ephemeral streams, some water will remain trapped behind the dam. Here, all soil particles in the stagnant water will settle out and remain behind the dam. Sand will settle first, with silt and clay to follow, such that the top of the new sand reservoir will be covered with a thin layer of silt and clay. People and animals walk across the silt and

clay, breaking it up and allowing the material to be picked up by wind or the next streamflow (Borst & de Haas, 2006). This cycle repeats each rainfall, until the height of the sand behind the dam is level with the dam spillway. At this point, the dam has reached maturity. This process could take anywhere from one rainy season to a few years.

After maturity, the sand dam stores up to 3.8% of the runoff in the catchment area (Aerts et al., 2007). During the first few rainfalls of the season, the sand dam will fill to capacity. The water table in the sand dam rises very quickly, but there is about a three week delay in the rise of the water table in the streambanks (Borst & de Haas, 2006). However, this timeframe may vary as streambank soil texture influences the connectivity between the sand reservoir and the stream margins. Hut et al. (2008) found that a sand dam could contribute to a raised water table up to 85 m from the dam centerline. The sand dam essentially remains at full capacity throughout the rainy season, with any drawdowns being replenished by the next rainfall. Once the dry season begins, water is lost from the sand dam due to evapotranspiration, groundwater flow, seepage, and community water use (de Trincheria, Nissen-Petersen, Filho, & Otterphol, 2015). de Trincheria et al. (2015) found that 87% of the sand dams included in their study lost more than half of their stored water to evaporation. The sand dam might receive some recharge during the dry season due to lateral baseflow from water that had infiltrated on the hillslopes (Borst & de Haas, 2006). Supposedly, sand dams store water for the community's use throughout the entire dry season, but this notion has been challenged by de Trincheria et al. (2015) and Viducich (2015).

1.1.2 Impacts of sand dams

Since only 3% of agricultural land is irrigated in sub-Saharan Africa, the region is highly dependent on rainfall for maintaining crop yields. With 70-84% of growing seasons in eastern Africa experiencing a dry spell of at least 10 days, crops are signifi-

cantly stressed by lack of water (Biazin, Sterk, Temesgen, Abdulkedir, & Stroosnijder, 2012). Through the implementation of irrigation from sand dams, many farmers have been able to switch from growing low-water-use crops such as sorghum to high-value crops like rice (Biazin et al., 2012). The ability to plant a variety of crops provides for crop rotation, which decreases the rate of soil nutrient depletion and further benefits crop yields (Drechsel & Gyiele, 1999). The additional water has also enabled the keeping of fish and duck ponds and increased fodder production for maintaining livestock (Behailu & Haile, 2002; Biazin et al., 2012). Communities experience greater food security and economic gains when they have access to the additional water stored by sand dams.

Members of rural communities must often spend three to four hours every day collecting water for domestic and agricultural use (M. Henry, Baldwin, & Quathamer, 2015). With the introduction of a sand dam in a rural community, the time spent collecting water decreases to about 15 minutes daily (M. Henry et al., 2015; Lasage, Aerts, Mutiso, & de Vries, 2008). Community members spend the time saved improving other areas of their lives. A third of households dedicate this extra time to farming-related tasks, 29% spend the time on domestic tasks, and 43% spend the time generating income in a different manner, such as brick and basket production (Lasage et al., 2008). These activities directly improve food security within a community, since they result in higher food production or the economic means to obtain more food.

1.1.3 Challenges of sand dams

Sand dams are a resource for increased food and water security for the local community when the sand dam is functioning as intended. However, Viducich (2015) and de Trincheria et al. (2015) find that up to 50% of all sand dams are non–functioning. Non-functioning sand dams are typically filled with silt instead of sand as a result of being built in one stage where construction in multiple stages would have been more

appropriate (Nissen-Petersen, 2006). Nissen-Petersen (2006) recommends building the spillway of the sand dam in 30 cm stages to ensure that most of the silt suspended in the stream flows over the dam instead of settling behind the dam wall. Once the sand behind the spillway is flush with the top, the next 30 cm of the spillway can be constructed. However, most NGOs do not follow this advice when constructing new sand dams, because it significantly extends the construction process. Also, a multi-stage construction process may introduce new challenges. For example, maintaining the community's interest over a longer construction period may be difficult, especially when the community is not seeing the immediate benefits of their involvement in the project. Most African cultures hold a short-term view of planning, and people prefer to exert their energies towards whatever activity presents the clearest advantage (Maranz, 2001).

In addition to siltation, seepage of water under and around the sand dam can significantly hinder the storage of water. Some sand dams are either constructed poorly or are not constructed on impermeable river beds, allowing large volumes of water to seep from the sand dam. de Trincheria et al. (2015) found that 37% of the sand dams included in their study had severe seepage problems. A sand dam with severe seepage issues will present clear indicators downstream of the dam. For example, a small pool of water will form just downstream of the spillway when there has not been recent rainfall.

1.2 Shortcomings in the current sand dam literature

The information available on sand dams is primarily available through NGO websites, project reports from international development groups, master's theses, and peer-reviewed journal publications. Depending on the source, each provides a different view of the impacts and effectiveness of sand dams. Further, most of the master's theses and journal publications use the same set of data from the same study of just one sand dam in Kitui County, Kenya, Dam Kwa Ndunda. Dam Kwa Ndunda

is a high-functioning sand dam (Douglas Graber Neufeld, personal communication, September 13, 2016), and therefore the aforementioned publications only briefly, if at all, mention the potential issues with sand dams. This has created a fairly narrow understanding of the true potential of sand dams to serve as a solution to water scarcity in rural sub-Saharan communities.

Viducich (2015) and de Trincheria et al. (2015) performed survey studies of 11 and 30 sand dams, respectively, in Kenya. These studies are the first published studies that have really explored the factors influencing sand dam effectiveness. Viducich (2015) examined the catchment and reach-scale factors affecting sediment deposition in the sand dam and explored the impact of spillway height on sedimentation via field studies and Hydrologic Engineering Center's River Analysis System (HEC-RAS) simulations. de Trincheria et al. (2015) investigated the hydrogeological and construction design factors that impact the performance and, specifically, the cost-efficiency of sand dams.

The research performed thus far has only looked at Kenyan sand dams, but Figure 1.2 shows that sand dams have spread throughout sub-Saharan Africa, to the Middle East and south Asia. The current body of research is much too limited to understand the potential positive and negative impacts of sand dams across such wide-ranging climatic and hydrogeologic conditions. This research quantifies the impact of sand dams on water availability in Kenya, provides deeper insight into how multiple sand dams outside of Kenya are interacting with their environment, and provides model-based guidelines on siting new sand dams.

1.3 Addressing shortcomings

To answer some of the questions still surrounding sand dams and their potential for positively impacting water availability, three objectives will be investigated in this research. The first objective is to quantify the impact of sand dams on regional water storage by comparing remotely sensed water storage anomalies and vegetative cover in an area with over 3000 sand dams to those of an area with few to no sand dams

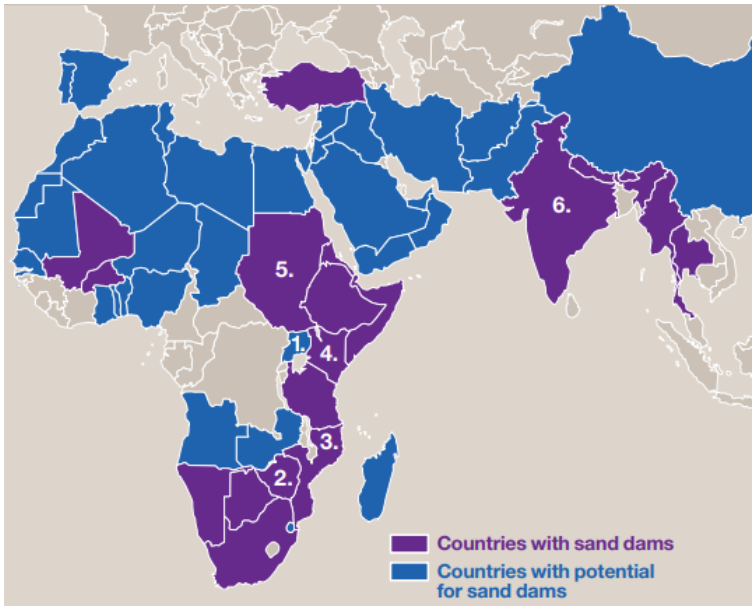

Figure 1.2. Countries around the world that have at least one sand dam. (*Pioneers of Sand Dams*, n.d.)

while accounting for various confounding factors, such as climate and time of year. This objective will primarily examine the extent to which a dense network of sand dams is capable of influencing water storage and availability on a large scale. This part of the study will reveal whether the impact of the sand dam network is greater than the local impact of each individual structure.

The second objective takes the study to the ground to discover how three different sand dams influence their local environment—including vegetative cover, water table levels, erosion, and macroinvertebrate habitat suitability in the areas in and around the sand dams. This objective will provide insights that serve as a point of comparison with sand dam anecdotal accounts and the study of the dam Kwa Ndunda to allow for a more representative understanding of sand dams to be developed. With an improved understanding of sand dams, stakeholders can begin to identify opportunities to enhance the positive aspects of sand dams and to tackle unresolved issues.

The third objective uses information collected during the field studies conducted for the second objective to create guidelines for siting new sand dams via application of the fully integrated surface and groundwater flow model, Interconnected Channel and Pond Routing Model (ICPR). This objective will explore the relative influence of hydrologic and geologic factors on the ability of a sand dam to capture and store water, focusing on factors that could be identified by sand dam stakeholders without requiring cost-prohibitive sub-surface investigations.

Meeting the aforementioned objectives will provide a more complete account of sand dams, wherein remote sensing is used to examine the regional impacts of sand dams, field studies are then used to explore the local impacts of sand dams, and finally a model is employed to identify opportunities to increase the overall performance of future sand dams.

1.4 Organization

This dissertation is organized into five parts: an introduction, three main studies, and a synthesis chapter. The first study covers the signatures, or lack thereof, of sand dams in remotely sensed datasets of water storage and vegetation. The second study explores the local environmental responses to three sand dams in Tanzania. The third study discusses the design of sand dams in an integrated surface and groundwater flow model and the insights into sand dam siting garnered from the model. The synthesis chapter ties the findings from the three main studies together and provides some further direction and recommendations.

2. A DATA-DRIVEN APPROACH TO ASSESSING THE EFFECTIVENESS OF WATER HARVESTING STRUCTURES IN EAST AFRICA

Abstract

A small-scale water harvesting structure known as a sand dam has gained popularity across East Africa in recent years, largely due to the efforts of non-governmental organizations. A sand dam is essentially a sub-surface water reservoir where the water is stored between sand grains. Stored thus, the water is filtered by the sand and protected from evaporation. This study uses remotely sensed data to investigate the impact of these structures on water storage and vegetative growth. The relationship between sand dams and water storage was modeled using a binary sand dam factor, climate data from the Famine Early Warning Systems Network Land Data Assimilation System (FLDAS), and water storage data measured by the Gravity Recovery and Climate Experiment (GRACE) twin satellites. The analysis revealed that GRACE largely fails to detect a statistically significant impact of sand dams on water storage. However, analysis of MODIS Normalized Difference Vegetation Index (NDVI) indicated that sand dams have a significant impact on the level of vegetation in the region. Vegetative growth is correlated with groundwater levels, indicating that sand dams have a positive impact on water storage albeit on a smaller scale than can regularly be detected by the GRACE satellites. In semi-arid regions that have little access to water during long dry seasons, additional water storage has a positive impact on both the food and water security of the region's inhabitants. Also, significantly, this study shows that NDVI data can be used effectively to study small-scale, regional changes in vegetation and water storage.

2.1 Introduction

One of the world's grand challenges, addressing the problem of water insecurity, is particularly problematic in developing nations where resources and infrastructure are limited. This is especially true in poorly-connected rural communities, where women and children might spend three to four hours a day collecting water (M. Henry et al., 2015). A single solution to water security in the developing world does not exist, due to variability in climatic, hydrologic, and geologic conditions. Each solution must be adapted to the specific requirements of the land and climate and to the needs of the local community. Such solutions in use today include johads, or small earthen dams, in India (Gupta, 2011), fog-harvesting meshes in Peru and Chile (Qadir, Jiménez, Farnum, Dodson, & Smakhtin, 2018), and sand dams in sub-Saharan Africa (Borst & de Haas, 2006). Despite the wide-ranging implementation of small-scale solutions to water security, very few studies have examined their effectiveness and overall ability to positively impact water availability. In many cases, the actual impact may be overstated.

Effective small-scale solutions to water security may support the maintenance of rural communities in developing countries. Rural communities are particularly vulnerable to climate change, and current projections of climate change indicate that rainfall will either decrease or be concentrated in fewer, higher intensity events in the developing world (Reyer et al., 2017). Novel, small-scale water harvesting technologies are increasingly recognized as a viable solution to rural water security and climate change. However, most efforts to spread or intensify water harvesting technologies have limited success (Bouma, Hegde, & Lasage, 2016). This is concerning, because a great deal of time, money, and human energy is often spent bringing water harvesting projects to fruition. For example, one sand dam constructed with volunteer labor can take three weeks to build and costs an average of 12,000 USD (Lasage et al., 2008; Lasage & Verburg, 2015). Despite this immense infusion of resources, approximately 50% of sand are not functioning properly (de Trincheria et al., 2018; Viducich, 2015).

The widespread issues with sand dam effectiveness are a relatively new revelation in the scientific literature (de Trincheria et al., 2015; Viducich, 2015) and similar issues may be present in other well-known water harvesting technologies.

Few studies have thoroughly assessed the effectiveness of small-scale water harvesting technologies in rural communities. Thus far, evaluation of water harvesting techniques has primarily been performed via simulation (Lasage, Aerts, Verburg, & Sileshi, 2015), field studies and surveys (Ngigi, Savenije, Thome, Rockström, & de Vries, 2005; Previati, Bevilacqua, Canone, Ferraris, & Haverkamp, 2010), meta-analysis of existing literature (Bouma et al., 2016; Lasage & Verburg, 2015), or a multi-criteria analysis aimed at potential projects rather than existing systems (Garfì, Ferrer-Martí, Bonoli, & Tondelli, 2011; Jaber & Mohsen, 2001). While the aforementioned evaluation techniques can offer valuable information regarding the effectiveness of specific water harvesting projects, their ability to provide a comprehensive perspective is limited and perhaps biased. For example, field studies and surveys are necessarily restricted in scope and likely include selection bias such that the projects studied tend to be only those that are effective. For example, sand dams are widely constructed and used as a major water harvesting structure in sub-Saharan Africa. Sand dams undoubtedly do capture and provide water to the local community for a period, but the magnitude and range of their impact on water availability may not be as reported (de Trincheria et al., 2015). No study exists that assesses the effectiveness of these structures on the overall water availability in the region. This study aims to address this issue by developing a methodology to assess the ability of sand dams in improving the overall water availability in the region. The methodology is developed and applied to study whether sand dams in south-eastern Kenya are functioning as well as reported. Considering that most of these community-based water-harvesting structures exist in developing nations with limited local data in the public domain, the methodology in this study is developed by using globally available remotely sensed data to enable broader applicability in other regions. While this study uses sand dams in Kenya as a test case, the methodology presented here can

be applied globally to assess the impact of local water harvesting schemes on regional water resources, agricultural activity and overall livelihood of the population.

A brief overview of sand dams and their history is presented below to provide the broader context for this study.

2.1.1 Sand dams

Sand dams are simple reinforced concrete dams built atop impermeable river beds in arid regions with infrequent, high-intensity rainfall (see Fig. 1.1). The high-intensity rainfall washes sand overland where it builds up behind the dam. After a few rainy seasons, the sand begins storing water, where it is naturally filtered, protected from evaporation, and helps raise the groundwater level in the surrounding area due to recharge from the increased subsurface storage (Borst & de Haas, 2006; Hut et al., 2008; Quilis et al., 2009). One sand dam can store millions of liters of water, provide clean water throughout the year to a thousand people, increase vegetation, and improve the arability of the surrounding land (Borst & de Haas, 2006).

The modern era of sand dam construction began in Kenya in 1979 through the efforts of a rural self-help group. Word spread and estimates today predict there are over 3,000 sand dams in Kenya (de Trincheria et al., 2018; Viducich, 2015). These sand dams have largely been built by myriad NGOs with private funds and volunteer labor from local communities. The de-centralized sand dam construction effort has resulted in a dearth of publicly available information, with few NGOs freely providing details of their sand dam projects. Most sand dam information comes from a handful of researchers investigating one or two "ideal" sand dams (Aerts et al., 2007; Borst & de Haas, 2006; Hut et al., 2008; Quilis et al., 2009). Researchers, however, have not yet examined whether sand dams are impacting the local environment at a regional scale.

Anecdotal evidence indicates that most of Kenya's 3,000+ sand dams are in three counties (sand dam counties). This study hypothesizes that the additional water

storage provided by the high density of sand dams in the sand dam counties leads to a higher regional groundwater table and increased vegetative cover. According to a finite element model study, a sand dam can influence the groundwater level up to 350 meters upstream and downstream of the dam (Quilis et al., 2009), but, a sand dam's area of influence is also reported to be up to two kilometers upstream of the dam and 500 meters to each side of the stream (Ryan & Elsner, 2016). Given the 3,000+ sand dams in the sand dam counties, anywhere from 3.4 to 17.2% of the sand dam counties may be impacted by sand dams. The sand dam's large area of influence should be detectable via remote sensing.

2.2 Study Area and Data

2.2.1 Study area

The south-eastern portion of Kenya is home to the majority of Kenya's sand dams. Most are concentrated in the counties of Kitui, Makueni, and Machakos (de Trincheria et al., 2015). These three counties comprise what will be hereafter referred to as the sand dam counties (see Fig. 2.1). The total land area of the sand dam counties (SDC) is 34,670 square kilometers. The average yearly rainfall within the SDC is approximately 700 mm (Fick & Hijmans, 2017). Elevation in the SDC ranges from 246 to 1803 meters above sea level with a mean elevation of 830 meters (Fischer et al., 2008). Alfisols comprise 92.4% of the soil in the SDC; the alfisols in this area of Kenya are generally well-drained sandy clay loam (Hengl et al., 2017; Ulsaker & Kilewe, 1983). Aridisols comprise 4.2% of the soil in the SDC; the aridisols are loose sandy loam underlain by an impervious sandy clay loam (Hengl et al., 2017; Makin, Schilstra, & Theisen, 1969). The SDC area is 77.0% natural and semi-natural terrestrial vegetation and 21.1% cultivated terrestrial (FAO, 2002).

This study compares water storage changes in the SDC to those in a buffer area of nearly equal land area (see Fig. 2.1). The total land area of the buffer area is 34,537 square kilometers. The average yearly rainfall in the buffer area is approximately

750mm (Fick & Hijmans, 2017). Elevation in the buffer area ranges from 180 to 1991 meters above sea level with a mean elevation of 853 meters (Fischer et al., 2008). Alfisols comprise 58.5% of the soil in the buffer area; 27.0% is aridisols (Hengl et al., 2017). The buffer area is 72.8% natural and seminatural terrestrial vegetation and 21.1% cultivated terrestrial (FAO, 2002).

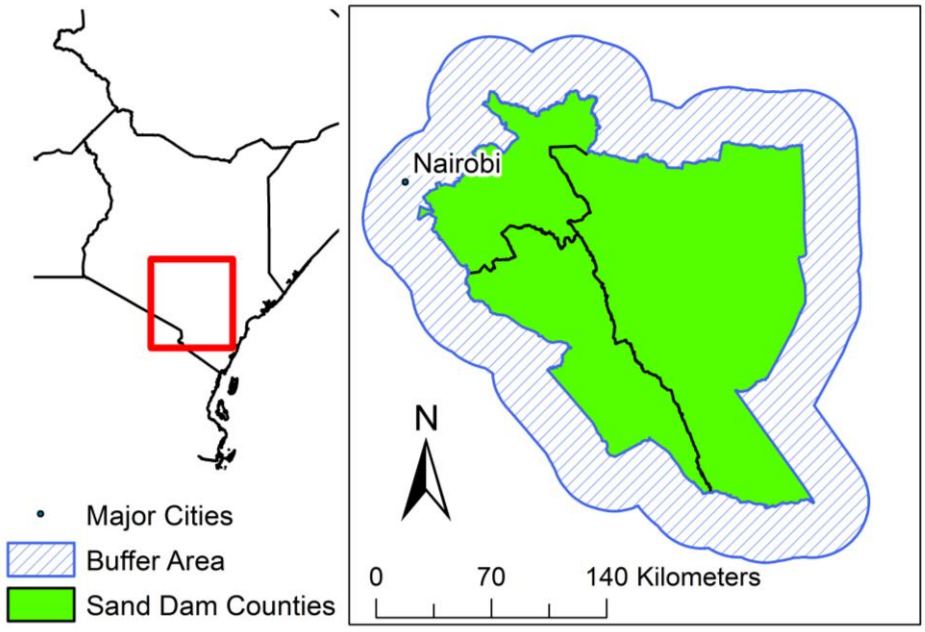

Figure 2.1. Study area in Kenya

2.2.2 Data

Gravity Recovery and Climate Experiment (GRACE)

GRACE is a joint mission between the German and American space agencies to measure Earth's gravity field via twin satellites (Tapley, Bettadpur, Watkins, & Reigber, 2004). Changes in water storage can be derived from changes in the Earth's gravity field, because most gravity field fluctuations result from shifting water vol-

umes. Therefore, the GRACE data provides an estimate of the total amount of water stored from the Earth's core out to the Earth's surface. The satellites record the gravity field at a resolution ranging from 400 km to 40,000 km every 30 days (Tapley et al., 2004). The mission began in March of 2002 and was intended to continue for five years but remained operational until October of 2017. The GRACE dataset is nearly continuous with some months missing from 2011 onwards due to battery management efforts (Herman et al., 2012). The raw data from GRACE is processed by three research centers: Center for Space Research (CSR) at the University of Texas at Austin, Jet Propulsion Laboratory (JPL) at California Institute of Technology, and GeoforschungsZentrum (GFZ) Potsdam in Germany (Tapley et al., 2004). The centers each produce monthly gridded data of the change in total water storage relative to a time mean baseline from 2004 to 2009 at a resolution of one degree, or approximately 111 kilometers. For the study area, the GRACE data has an estimated error of approximately 3.8 centimeters (Landerer & Swenson, 2012).

GRACE data has been used successfully in many academic studies to explore general trends in water storage at a variety of scales: 45,000 km^2 (Hachborn, Berg, Levison, & Ambadan, 2017), 55,000 km^2 (C. M. Henry, Allen, & Huang, 2011)), 766,000 km^2 (Huang et al., 2012), and 2,200,000 km^2 (Cao, Nan, & Cheng, 2015) up to the global scale. This study attempts to assess the consequences of man-made structures on water storage by analyzing trends in the GRACE total water storage data.

Normalized Difference Vegetation Index (NDVI)

The Moderate Resolution Imaging Spectroradiometer (MODIS) instrument aboard the Terra and Aqua satellites record every point on the Earth every one to two days in 36 spectral bands. The data stored in these spectral bands is utilized to calculate the NDVI. Vegetation absorbs most of the blue (470 nm) and red (670 nm) wavelengths while reflecting most of the near-infrared radiation. The contrast between

the absorbed and reflected wavelengths is manipulated to calculate a grid of NDVI values for the entire surface of the Earth (Didan, Barreto-Munoz, Solano, & Huete, 2015). NDVI, ranging from negative one to one, serves as an indicator of the amount of vegetation present on the land surface. Values close to one indicate the presence of thriving vegetation, whereas values from negative one to zero indicate the presence of bare ground or dead vegetation. MODIS NDVI grids are available in 16-day and monthly increments at resolutions ranging from 250 meters to one kilometer. For the purposes of this study, monthly MODIS NDVI at a resolution of one kilometer is used (Didan, 2015).

Famine Early Warning System Network Land Data Assimilation System (FLDAS)

FLDAS is a set of models designed to provide accurate climate estimates for the purpose of drought monitoring in data-sparse regions susceptible to food and water security issues (McNally et al., 2017). FLDAS currently provides daily and monthly climate data consisting of 25 different variables for Western, Eastern, and Southern Africa. FLDAS includes two different simulation schematics implementing different meteorological inputs, simulation A and simulation C. Simulation C is recommended for research purposes and is considered more accurate, so this study utilizes the data from simulation C (Anderson et al., 2012; McNally et al., 2017; Yilmaz et al., 2014). Simulation C uses the Climate Hazards group Infrared Precipitation with Stations (CHIRPS) and the Modern Era Reanalysis for Research and Applications version 2 (MERRA-2) as forcing data (McNally et al., 2017). FLDAS provides simulation C outputs for the Noah Land Surface Model (Noah) at a resolution of 0.1° (∼11.1 km) and Variable Infiltration Capacity (VIC) at a resolution of 0.25° (∼27.8 km) (NASA/GSFC/HSL, 2016).

2.3 Methods

The methodology included here outlines two techniques for quantifying the impact of sand dams: one using GRACE total water storage and one using NDVI. Both techniques are based on developing a linear model that seeks to define the relationship between the presence of sand dams and a magnitude of change in GRACE data or NDVI data. In both instances, covariates such as weather, time of year, and population are included to ensure that the observed changes in GRACE and NDVI can accurately be attributed to sand dams. A significant coefficient for the sand dam indicator variable indicates that the sand dam does impact total water storage or vegetation.

2.3.1 Relating GRACE water storage to the presence of sand dams

Processing GRACE

The monthly mass grids available for download from the GRACE database have been independently processed by CSR, JPL, and GFZ to provide three different solutions. Each research center takes the raw data, or Level-1 product, and first removes fluctuations in the mass signal due to changes in the mass of the atmosphere. The GRACE measurements of the spherical harmonic of degree two and order zero (C20), related to the principal moments of inertia, are replaced with those recorded by satellite laser ranging (SLR), because the SLR values have smaller uncertainty (Cheng, Ries, & Tapley, 2011). Then, the spherical harmonic degree one coefficients, used to pinpoint the Earth's center of mass, are estimated (Swenson, Chambers, & Wahr, 2008). The gravity field measurements are corrected using a glacial isostatic adjustment (A, Wahr, & Zhong, 2013). Next, a de-striping filter is applied to reduce correlated errors, and a 300 kilometer wide Gaussian filter is applied (Swenson & Wahr, 2006). Finally, the time-mean baseline of the gravity field from 2004 to 2009, inclusive, is subtracted from the entire dataset. The resultant product is a monthly

grid of the total water storage's equivalent water depth relative to a time-mean baseline. This processing results in a dataset whose variations are attenuated at small scales due to the aforementioned filtering. To restore the lost energy, also available for download is a grid of multiplicative scale factors that should be applied to the GRACE data before analysis proceeds. The scale factors minimize the difference between the filtered and unfiltered variations in total water storage (Landerer & Swenson, 2012).

The three available GRACE solutions (CSR, JPL, and GFZ) have slightly different error structures. Rather than select one solution to analyze, the ensemble mean of the three solutions is used. An ensemble mean of the three solutions minimizes noise in the scatter of the solutions by five to ten mm root mean square (Sakumura, Bettadpur, & Bruinsma, 2014).

The GRACE solutions were obtained for months available from the beginning of the GRACE mission to the end of 2016: April 2002 to December 2016 (TELLUS, 2012). During this time period, GRACE data is unavailable for 21 of the potential 177 months, leaving 156 months, or 88.1%, of the data available for this analysis. From 2002 to the start of 2011, only three months of data are missing. The remaining missing data months occurred during the aforementioned battery management efforts from 2011 to 2017 (Herman et al., 2012).

The Level-3 GRACE data has a resolution of 1°, while the FLDAS dataset, employed as a proxy for climate data in this research, has a resolution of 0.1°. The GRACE data was resampled using bilinear interpolation to a resolution of 0.1°, or approximately 11 km by 11 km, to allow for a one-to-one relationship between the two datasets (Cao et al., 2015). GRACE is likely highly uncertain at the scale of this study (Rodell et al., 2007). However, the study assumes that the uncertainty in the SDC and buffer areas are the same, and the comparative analysis reduces the impact of this uncertainty on the findings of the study.

Processing FLDAS for GRACE

As mentioned above, the GRACE data provides total water storage values relative to a time-mean baseline from 2004 to 2009, inclusive. To create a comparable FLDAS dataset, the gridded average value from 2004 to 2009 was calculated for each climate variable and subtracted from the raw data.

Validating FLDAS for the Study Area. The terrestrial water balance dictates that the change in water storage is equal to the difference between the inflows and outflows of the system, which can be written as:

$$\frac{dW(t)}{dt} = P(t) - R(t) - E(t), \tag{2.1}$$

where W is water storage, P is precipitation, R is runoff, E is evapotranspiration, and t is time. Each component of the right-hand side (RHS) of Eq. 2.1 can then be separated into constant, linear, and time-variable sinusoidal terms (Crowley, Mitrovica, Bailey, Tamisiea, & Davis, 2006). For example, the precipitation term can be written as:

$$P(t) = P_0 + P_1 t + P^*(t) \tag{2.2}$$

The same is true of the runoff and evaporation terms. Re-writing Eq. 2.1 to include the terms shown in Eq. 2.2 and integrating produces:

$$\begin{aligned} W(t) - (P_0 - R_0 - E_0)t - \frac{1}{2}(P_1 - R_1 - E_1)t^2 + C = \\ \int_{t_0}^{t} [P^*(t') - R^*(t') - E^*(t')]dt', \end{aligned} \tag{2.3}$$

where C is the constant of integration (Crowley et al., 2006).

Equation 2.3 can be used to test the validity of substituting FLDAS data for climate data in the SDC and buffer area. FLDAS includes the data necessary to solve Eq. 2.3 for total water storage, which can then be compared with the GRACE-provided total water storage in the region. FLDAS data includes evapotranspiration, storm surface runoff (Qs), baseflow-groundwater runoff (Qsb), and precipitation.

Linear Model for GRACE

To determine whether the 3,000+ sand dams built in the SDC have a collective impact on groundwater storage at a regional scale, monthly linear models (LM) covering the entire study area (SDC and buffer area) were developed using the GRACE data as the dependent variable. As predictor variables, the LM includes initial water storage, sand dam presence, and a suite of climate variables via principal components. The principal component analysis (PCA) was performed on 15 FLDAS climate variables: evapotranspiration, specific humidity, storm surface runoff, baseflow-groundwater runoff, total precipitation rate, soil moisture 0-10, 10-40, 40-100, and 100-200 centimeters underground, soil temperature 0-10, 10-40, 40-100, and 100-200 centimeters underground, near surface air temperature, and near surface wind speed.

Principal Component Analysis. Principal component analysis (PCA) is a statistical method employed to capture most of a multivariate dataset's variance in a few orthogonal components. Each component is a linear combination of the standardized multivariate dataset, such that a principal component takes the form:

$$PC_i = \varepsilon_{i,1} X_1^S + \varepsilon_{i,2} X_2^S + \varepsilon_{i,3} X_3^S + \cdots + \varepsilon_{i,p} X_p^S, \tag{2.4}$$

where PC_i is the ith principal component and $\varepsilon_{i,1}$ is the coefficient for the first variable in the standardized multivariate dataset, X_1^S. The first component describes most of the dataset's variance with each successive component describing most of the variance remaining after the previous component is determined. Therefore, PCA is essentially a dimension-reduction technique utilized when the original multivariate dataset contains many variables. For example, a dataset containing 15 variables may be represented by only three or four principal components without significant loss of information. PCA is conducted via eigenanalysis, with the resulting eigenvalues representative of the amount of variance captured by each principal component. For the purposes of this study, singular value decomposition PCA was employed. A complete description of the PCA computation can be found in Shlens (2014).

Many techniques exist for determining the appropriate number of principal components to retain such that information-loss is minimized. For this study, the Kaiser-Guttman criterion was utilized. The Kaiser-Guttman criterion dictates that every principal component with an eigenvalue greater than unity is retained. While this is not the most sophisticated technique available, the Kaiser-Guttman criterion is sufficient for datasets with a high communality (Yeomans & Golder, 1982).

Finalized GRACE Model. The monthly LM model developed to determine whether the presence of sand dams has a statistically significant effect on total water storage is:

$$GRACE_t = \alpha + \beta GRACE^S_{t-1} + \gamma PC_1 + \delta PC_2 + \varepsilon PC_3 + \eta PC_4 + \kappa SD + \epsilon, \tag{2.5}$$

where $GRACE_t$ is the log(GRACE$_t$ + constant) total water storage in month t, $GRACE_{t-1}$ is the standardized GRACE total water storage in month $t-1$, PC_i is the ith principal component, and SD is the sand dam indicator variable. The superscripted S indicates that the variable is standardized. The SD variable was included as a binary, categorical variable indicating whether the point is in the SDC or buffer area.

To develop a set of training and validation data for each monthly LM, 43 or 44 points were randomly sampled from each available month (e.g. 43 or 44 points from each December for a total of 564 points). The sampled points were randomly split in half, with 282 becoming training data points and 282 becoming validation data points. One point represents one square of the gridded GRACE and FLDAS datasets, and each point was sampled only once. The coefficients of Eq. 2.5 were determined through statistical analysis for every LM. One LM model was determined for every month of the year and validated via cross-validation.

2.3.2 Relating MODIS NDVI to the presence of sand dams

Processing MODIS NDVI and FLDAS

MODIS NDVI, hereafter NDVI, was obtained for the same time period as the GRACE total water storage data, April 2002 to December 2016. Invalid NDVI data were omitted (Didan et al., 2015). There are no months missing from the NDVI dataset. NDVI has a resolution of one kilometer, so the FLDAS dataset was resampled using bilinear interpolation to a resolution of one kilometer to allow for a one-to-one relationship with the NDVI data.

Linear Model for NDVI

To determine whether the 3,000+ sand dams built in the SDC have a collective impact on vegetation, a LM was developed covering the entire study area (SDC and buffer area) using NDVI data as the independent variable. As predictor variables, the LM includes sand dam presence, month of year, standardized population count, a suite of climate variables via principal components, and an auto-covariate to account for spatial autocorrelation.

Spatial Autocorrelation. Analyzing spatial data, such as the gridded GRACE or NDVI data, introduces the issue of spatial autocorrelation. Spatial autocorrelation occurs because a point is likely more similar to points nearby than distant points (Tobler, 1970). This phenomenon produces residuals of statistical analyses that violate the assumption of independently and identically distributed errors, which may cause incorrect rejection of a true null hypothesis (Anselin, 2002). Spatial autocorrelation can be detected via calculation of Moran's I and examining the resultant plot (Dormann et al., 2007). Spatial autocorrelation needs to be considered during the analysis if Moran's I is statistically significant and/or if the Moran's I plot depicts a strong trend. For large datasets, Moran's I may be statistically significant even when there is no trend evident in the Moran's I plot. When this occurs, scientific judgment

must be employed to determine the magnitude of spatial autocorrelation's impact on the results.

To address the issue of spatial autocorrelation in the residuals of the NDVI analysis, an autocovariate was added to the LM. The autocovariate is the result of a distance-weighted function that assesses how closely the response variable at one point is related to the response variable of the surrounding points (Dormann et al., 2007). The autocovariate, A_i, for point i is calculated as:

$$A_i = \sum_{j \in k_i} w_{ij} y_j, \tag{2.6}$$

where y_j is the response variable at point j, a neighbor of point i within radius k_i, and w_{ij} is the weight assigned based on a predetermined relationship between points j and i (Dormann et al., 2007). For this study, the weight is based on the inverse distance. Radius k_i was selected via trial and error to minimize the spatial autocorrelation present in the residuals. Radius k_i was determined to be three kilometers for the NDVI data.

Finalized NDVI Model. The LM model developed to determine whether the presence of sand dams has a statistically significant effect on standardized vegetative growth is:

$$\begin{aligned} NDVI^S = \alpha + \beta PC_1 + \gamma PC_2 + \delta PC_3 + \varepsilon PC_4 \\ + \eta A + \kappa_{1-12} Month + \lambda Pop^S + \mu SD + \epsilon, \end{aligned} \tag{2.7}$$

where PC_i is the ith principal component, A is the autocovariate, $Month$ is the month of year, Pop^S is the standardized population count, and SD is the sand dam indicator variable. The coefficients were determined using a set of training data and validated using a separate dataset.

The training and validation datasets for the NDVI analysis were developed similarly to the GRACE training and validation datasets. However, the higher resolution of the NDVI data provides for a much denser network of points. 457 or 458 points were randomly sampled from each month from April 2002 to December 2016. The

sampled points were randomly split in half, with 40,518 points becoming training data and 40,517 points becoming validation data points. One point represents one square of the gridded NDVI and FLDAS datasets, and each point was sampled only once.

2.4 Results

2.4.1 Sand dam impact on total water storage

Overall, GRACE water storage anomalies in the SDC and buffer area are fairly similar (see Table 2.1). The difference in average water storage anomalies from 2002 to 2016 in the SDC and buffer area is negligible, according to the GRACE data ($p=0.92$). The variation among the water storage anomalies in the SDC and in the buffer area is also insignificant ($p=0.49$). While the average total water storage and variance is insignificant, GRACE water storage anomalies show that during individual months, there is a significant difference between the SDC and buffer area stored water (see Fig. 2.2). Overall, 60 of the 156 months with GRACE data display a significant difference in the water storage anomalies of the two regions. Interestingly, the months that most often exhibit a significant difference do so right as the region is shifting from the dry season into the wet season. This may be a signature of the added storage provided by sand dams in the SDC, however additional factors must be considered.

The validity of using FLDAS data as a proxy for climate data is determined by comparing FLDAS water storage anomalies calculated via Eq. 2.3 with GRACE water storage anomalies in the SDC. The smoothed results (see Fig. 2.3) indicate that the two datasets provide similar information regarding the magnitude and direction of water storage anomalies in the SDC. The FLDAS water storage anomalies largely fall within or near the GRACE error estimated by Landerer and Swenson (2012). The most glaring exception occurs from 2013 to 2014. This, however, does not indicate that FLDAS data is inadequate climate data for the region. The data gaps

Table 2.1.
Statistics for GRACE water storage anomalies (cm) in the SDC and buffer area

	SDC	Buffer Area
Min	-16.76	-15.80
Max	22.32	20.64
Mean	3.76	3.68
Variance	59.80	53.51
Std. Dev.	7.73	7.32

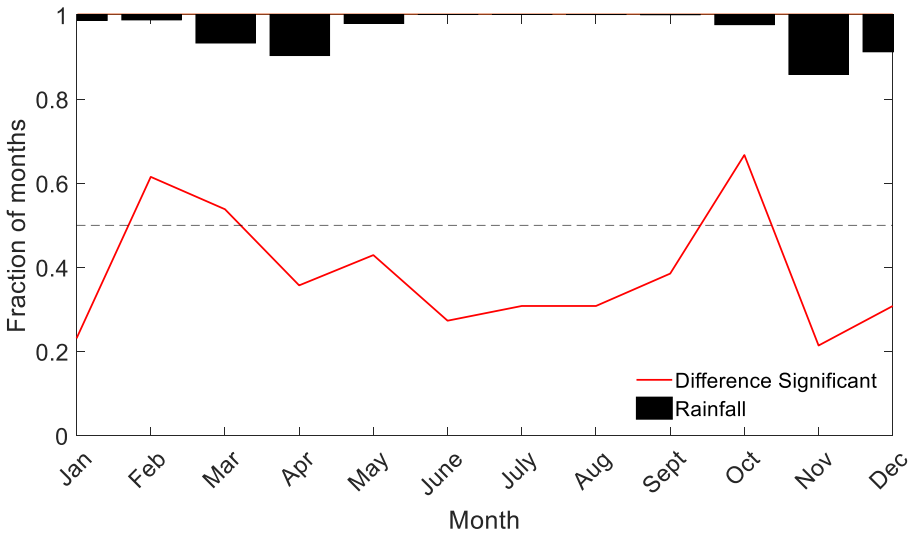

Figure 2.2. Fraction of available months indicating that there is a significant difference between the water storage anomalies observed in the SDC and buffer area.

in GRACE during the time period under scrutiny significantly skew the smoothed results, creating the impression of poor fit in some areas.

Using the Kaiser-Guttman criterion, four factors explaining, on average, 80% of the variability in the FLDAS climate data were selected from the PCA for each

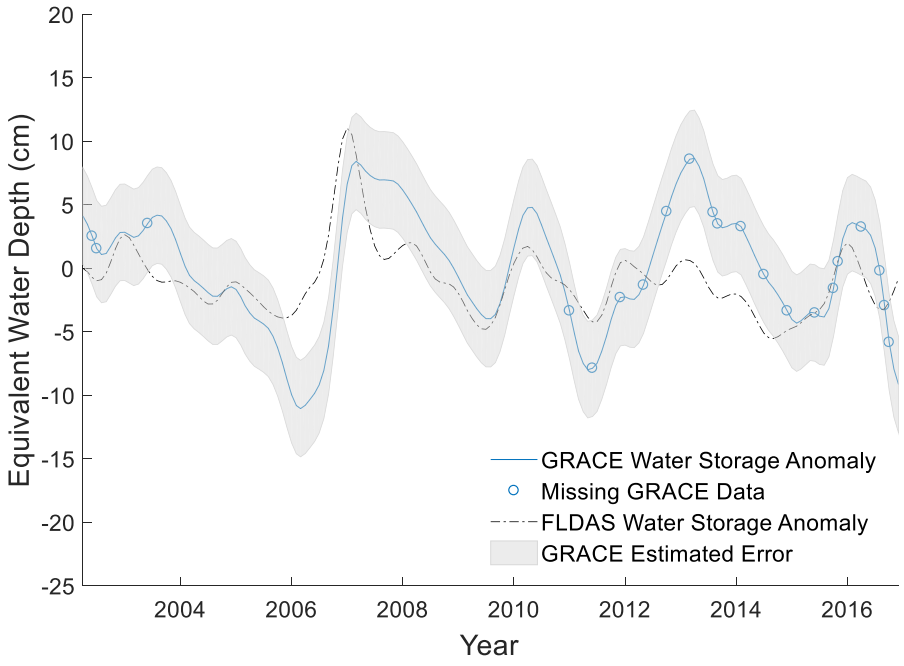

Figure 2.3. GRACE water storage anomalies compared with FLDAS-calculated water storage anomalies in the SDC. Both were smoothed with a 12-month Gaussian filter.

month. The physical interpretation of the factors varied somewhat from month to month. The first and second factors support a fairly uniform interpretation across the months. The interpretation of the third factor provides a reasonable trend across the months as well, however, the physical interpretation of the fourth factor varies greatly from month to month. The first factor (PC1) essentially represents a contrast between evapotranspiration and soil moisture and soil and air temperature. The second factor (PC2) generally represents surficial wind speed, and rainfall and surface runoff is represented by the third factor (PC3). The fourth factor (PC4), while varied greatly, does most often represent specific humidity and then baseflow-groundwater runoff. The above interpretation is based on monthly trends in the level of correlation between each factor and the initial climate data; the interpretation provided maintains the orthogonality between factors essential to PCA.

The LM designed in Eq. 2.5 indicates that sand dams do have a significant impact on water storage in the SDC during three months of the year when accounting for the confounding factors of climate and initial total water storage (see Table 2.2). The months of January (p=0.023), April (p=0.037), and November (p=0.015), all indicate that the presence of sand dams have a significant impact on total water storage in the SDC. Interestingly, these three months showed relatively low fractions of significance in Fig. 2.2, indicating that the difference between total water storage in the SDC and buffer area cannot be attributed solely to differences in climate and initial conditions. In January, the presence of a sand dam decreases the amount of total water storage by 3.6%, while in April and November, the presence of a sand dam increases the amount of total water storage by 4.6% and 3.6%, respectively. January, the first month of a dry season, may see lower levels of total water storage in the SDC than in the buffer area due to increased evapotranspiration potential resulting from added water storage during the preceding rainy season. This increased rate of evapotranspiration may reduce the amount of water stored in the SDC to levels below those of the buffer area. April and November, the wettest months of the two rainy seasons, see increased levels of water storage in the SDC commensurate with Aerts et al.'s ((2007)) estimate that sand dams store up to 3.8% of runoff.

Table 2.2.
Water storage anomaly LM summary

	Sand Dam Indicator Variable (SD)				Model
Model	Coefficient	Std. Error	t-statistic	P-value	Adj. R^2
Jan.	-0.036	0.02	-2.28	0.023*	0.67
Feb.	-0.007	0.01	-0.70	0.483	0.41
Mar.	0.013	0.01	1.37	0.171	0.60
Apr.	0.046	0.02	2.10	0.037*	0.76
May	0.027	0.01	1.85	0.066	0.79
June	-0.005	0.01	-0.31	0.754	0.75
July	0.005	0.01	0.34	0.731	0.73
Aug.	-0.011	0.01	-1.34	0.183	0.67
Sept.	-0.001	0.01	-0.08	0.937	0.76
Oct.	0.006	0.01	0.57	0.570	0.79
Nov.	0.036	0.01	2.45	0.015*	0.83
Dec.	-0.005	0.02	-0.21	0.836	0.62

* denotes significance at the 0.05 level

Overall, the monthly LM models are a good fit, with adjusted R^2 values ranging from 0.41 to 0.82 and averaging 0.70. In the SDC, inclusion of the sand dam indicator variable generally results in an improved normalized mean square error (NMSE, see Fig. 2.4). However, inclusion of the sand dam indicator variable results in a slightly higher NMSE for the southern and northeastern portions of the SDC. This is not necessarily cause for great concern though, because the increase in NMSE values is small and certainly less extreme than in the areas with improvements. Further, the sand dams known to the researchers largely fall within the areas of improved NMSE,

with only 16.2% of the known sand dams located in areas where the NMSE worsened after including the sand dam indicator variable.

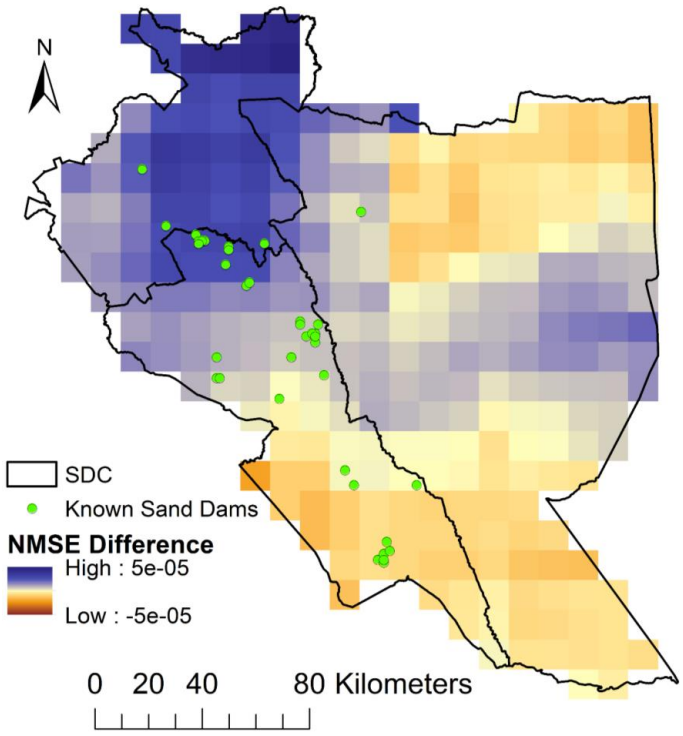

Figure 2.4. Model improvement after adding the sand dam indicator variable to the November GRACE LM. NMSE difference is the average reduction in NMSE within a five-cell range after adding the sand dam indicator variable to the model. Locations of all known sand dams are depicted, however, this represents less than 3% of all sand dams in the SDC.

2.4.2 Sand dam impact on vegetation

Overall, NDVI in the SDC and buffer area is similar in magnitude (see Table 2.3). However, the difference in average NDVI from 2002 to 2016 in the SDC and buffer area is significant (p=0.001), according to the MODIS data. The difference in variation among NDVI in the SDC and in the buffer area is also significant (p=0.001). These

results indicate that sand dams may have a significant impact on vegetation, but the relationship must be examined in conjunction with confounding factors.

Table 2.3.
Statistics for MODIS NDVI in the SDC and buffer area

	SDC	Buffer Area
Min	0.25	0.24
Max	0.70	0.64
Mean	0.43	0.40
Variance	0.01	0.01
Std. Dev.	0.11	0.09

Using the Kaiser-Guttman criterion, four factors explaining 86% of the variability in the FLDAS climate data were selected from the PCA (see Table 2.4). The first factor (PC1) represents a contrast between soil moisture and soil and air temperature. The second factor (PC2) represents the amount of water present in the atmosphere. Surficial wind speed is represented by the third factor (PC3), and runoff is represented by the fourth factor (PC4). The above interpretation is based on the level of correlation between each factor and the initial climate data; the interpretation provided maintains the orthogonality between factors essential to PCA.

Table 2.4.
Factor loadings obtained via PCA on the FLDAS climate data

	PC1	PC2	PC3	PC4
	λ=6.17	λ=4.47	λ=1.20	λ=1.04
EVAP	-0.21	0.31	-0.25	-0.27
QAIR	0.13	0.40	-0.04	-0.07
QS	-0.20	0.25	-0.12	0.53
QSB	-0.17	0.15	0.11	0.60
RAINF	-0.19	0.32	-0.32	0.27
SM00_10CM	-0.29	0.29	-0.01	-0.17
SM10_40CM	-0.24	0.32	0.29	-0.18
SM40_100CM	-0.23	0.25	0.44	-0.18
SM100_200CM	-0.22	0.07	0.47	-0.07
ST00_10CM	0.35	0.20	0.04	0.01
ST10_40CM	0.35	0.22	0.05	0.03
ST40_100CM	0.35	0.24	0.07	0.04
ST100_200CM	0.33	0.24	0.11	0.04
TAIR	0.32	0.26	0.01	-0.04
WIND	0.12	-0.17	0.53	0.33

Abbreviations : λ, eigenvalue; EVAP, evapotranspiration; QAIR, specific humidity; QS, storm surface runoff; QSB, baseflow-groundwater runoff; RAINF, total precipitation rate; SM00_10CM, soil moisture at 0-10 cm underground; SM10_40CM, soil moisture at 10-40 cm; SM40_100CM, soil moisture at 40-100 cm; SM100_200CM, soil moisture at 100-200 cm; ST00_10CM, soil temperature at 0-10 cm; ST10_40CM, soil temperature at 10-40 cm; ST40_100CM, soil temperature at 40-100 cm; ST100_200CM, soil temperature at 100-200 cm; TAIR, near surface air temperature; WIND, near surface wind speed.

The spatial autocorrelation inherent in the NDVI data could cause issues with model validity and interpretability. The autocovariate function included in Eq. 2.6 accounts for most of the spatial autocorrelation in the NDVI data (see Fig. 2.5). Moran's I for the residuals of the model without the autocovariate function is 0.4559; Moran's I with the autocovariate function is 0.0419. This represents a more than 90% decrease in the amount of spatial autocorrelation present in the model residuals. Moran's I is the slope of the best-fit line through the points, and is used as a measure of how much spatial autocorrelation is present in the data. A Monte Carlo simulation performed to determine the significance of Moran's I for the model with an autocovariate indicated that spatial autocorrelation may still be an issue (p=0.01). However, this result is likely due to the number of points used in the analysis (16,000+) rather than crippling spatial autocorrelation.

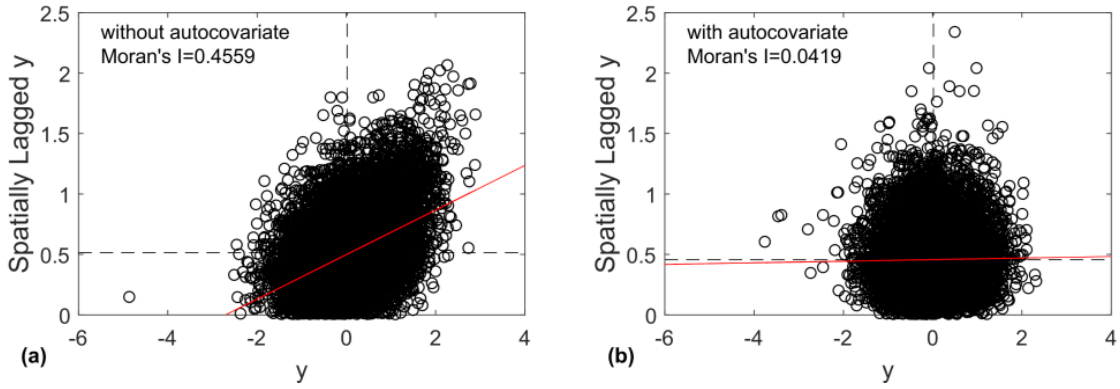

Figure 2.5. Moran scatter plot for LM validation residuals (a) without an autocovariate function in the LM and (b) with an autocovariate function. The red line is the line of best fit through the points.

The LM designed in Eq. 2.7 indicates that sand dams do have a significant impact (p<0.001) on vegetation in the SDC when accounting for the confounding factors of climate, time of year, and population (see Table 2.5). The presence of a sand dam increases NDVI by 0.07 standard deviations. All the other confounding factors included in the LM also significantly impact NDVI. The amount of water present

Table 2.5.
Vegetation LM Summary

	Coefficient	Std. Error	t-statistic	P-value
Intercept	0.32	0.01	30.45	<0.001*
PC1	-0.11	0.00	-77.66	<0.001*
PC2	0.19	0.00	83.64	<0.001*
PC3	-0.13	0.00	-41.02	<0.001*
PC4	-0.14	0.00	-48.55	<0.001*
A	0.08	0.00	138.13	<0.001*
January	0.00	-	-	-
February	-0.28	0.01	-20.16	<0.001*
March	-0.55	0.01	-38.94	<0.001*
April	-0.42	0.01	-28.92	<0.001*
May	-0.06	0.01	-4.08	<0.001*
June	-0.11	0.01	-7.63	<0.001*
July	-0.27	0.02	-17.44	<0.001*
August	-0.46	0.02	-29.10	<0.001*
September	-0.57	0.02	-36.99	<0.001*
October	-0.87	0.01	-61.57	<0.001*
November	-0.61	0.01	-41.03	<0.001*
December	-0.03	0.01	-2.21	0.027*
Pop.	-0.01	0.00	-2.03	0.042*
SD no (0)	0.00	-	-	-
SD yes (1)	0.07	0.01	12.18	<0.001*

* denotes significance at the 0.05 level

in the atmosphere (PC2) has the greatest positive impact on NDVI; for every unit increase in PC2, NDVI increases by 0.19 standard deviations. The month of October

has the greatest negative impact on NDVI—NDVI is 0.87 standard deviations lower in October than in January. October falls right at the end of the dry season and the beginning of the rainy season, so one would expect the vegetation to be in poor condition in October.

The vegetation LM simulates the standardized NDVI based on climate, time of year, population, spatial autocorrelation, and sand dam presence very well. The validation data results in an adjusted R^2 of 0.69. Throughout the SDC, inclusion of the sand dam indicator variable results in an improved NMSE (see Fig. 2.6). The overall model fit is very good and establishes confidence that the model structure can provide valuable insight into the relationship between sand dams and NDVI.

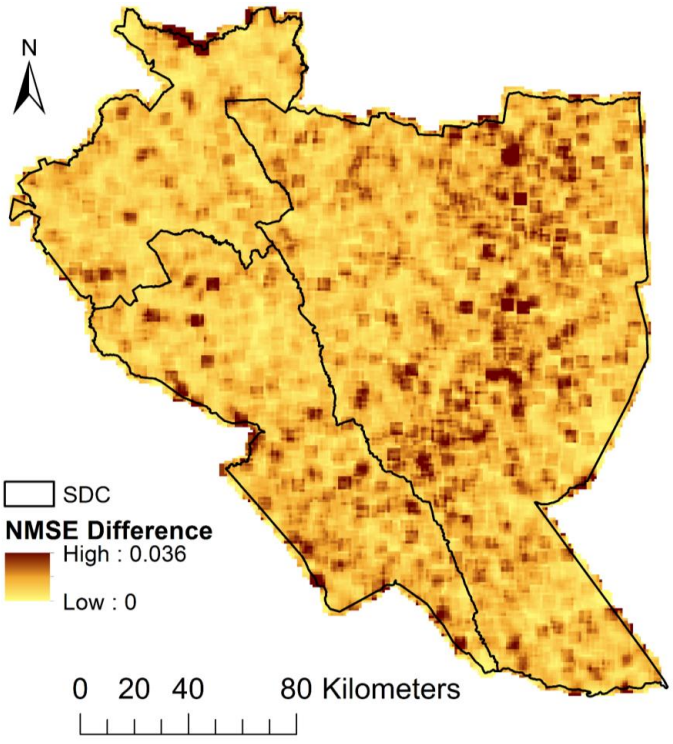

Figure 2.6. Model improvement after adding the sand dam indicator variable to the NDVI LM. NMSE difference is the average reduction in NMSE within a five-cell range after adding the sand dam indicator variable to the model. Adjusted R^2 is 0.69.

2.5 Discussion

2.5.1 Role of GRACE Data in Capturing Sand Dams Impact

The authors hypothesized that the sand dam's large area of influence coupled with the 3,000+ sand dams in the SDC would lead to substantial groundwater recharge that could be detected via GRACE. A monthly test of means revealed that some months of the year are more likely to produce differences in water storage in the SDC and buffer area. When accounting for climate factors and initial conditions, the GRACE LMs indicated that GRACE total water storage data is only sufficient for detecting a significant impact of sand dams on water storage in the SDC during three months of the year. The sand dams have a positive impact on total water storage during the months that experience the highest rainfall during each rainy season, April and November. However, the months following April and November do not exhibit a significant increase in SDC total water storage compared to the buffer area. This pattern indicates that sand dams do indeed capture more water, but they do not necessarily store significantly more water in their local watershed for long periods. The inability to store water long-term can be attributed to issues with seepage under the sand dam and high rates of evapotranspiration during the rainy seasons. A study of 30 sand dams in Kenya found that up to 37% of sand dams have severe seepage issues, and up to 87% of sand dams lose over half of their stored water to evaporation (de Trincheria et al., 2015). Sand dams may not be as effective at storing water as previously thought.

Most of the rainfall in the SDC is lost either to baseflow-groundwater runoff or evapotranspiration (Fig. 2.7). A properly sited and constructed sand dam will minimize the amount of stored water lost to baseflow-groundwater runoff, because the dam will be built atop a near-impermeable streambed such as bedrock or consolidated clay. Nevertheless, sand dams are most often located in rural communities with limited or no access to subsurface surveying technology. Thus, many sand dams are likely constructed upon fractured bedrock, which could lead to significant water

loss from the sand dam via rainwater infiltration into the bedrock (Kosugi, Katsura, Katsuyama, & Mizuyama, 2006). Furthermore, farmers grow many crops at the edge of sand dams and use water from the sand dam to irrigate their crops at least once a week. These healthy crops contribute greatly to the community's food security, but they also increase the amount of water lost from the sand dam via evapotranspiration. Water loss through baseflow-groundwater runoff and/or evapotranspiration could be further contributing to the failure of GRACE total water storage data to confirm the positive impact of sand dams on water storage throughout the year.

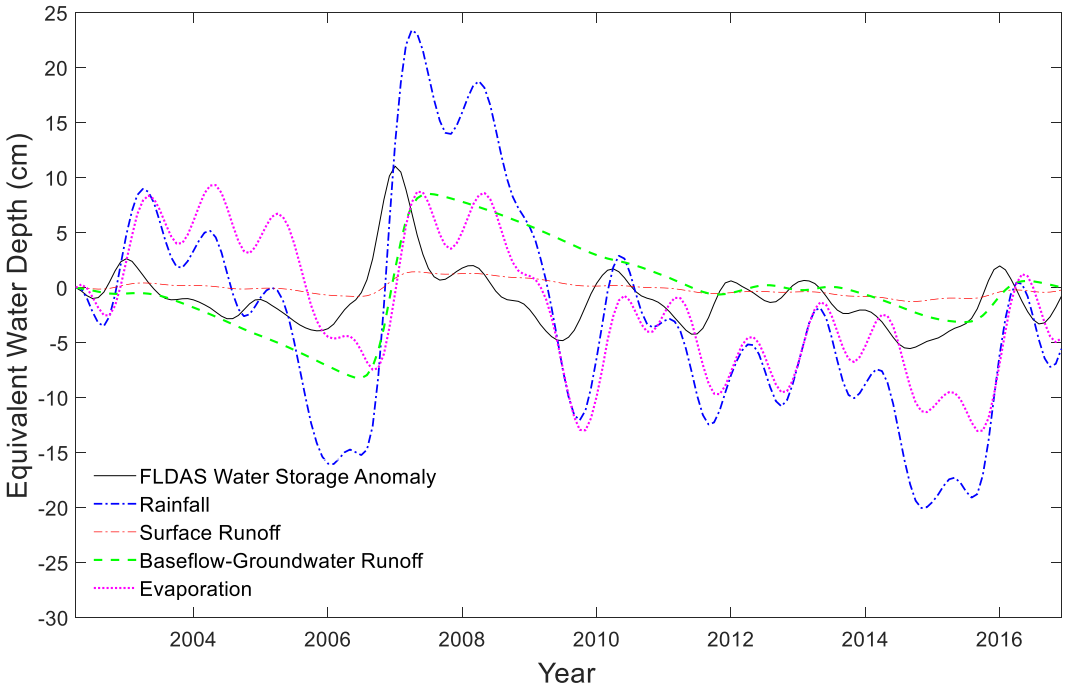

Figure 2.7. Influence of FLDAS climate factors on the calculation of FLDAS water storage anomaly. Precipitation is a forcing variable for the FLDAS models; surface runoff, baseflow-groundwater runoff, and evapotranspiration are simulated.

Further complicating the ability of GRACE to detect a year-round, significant impact of sand dams on total water storage is the 1° resolution of the GRACE data. Anecdotal evidence suggests that sand dams do have a positive impact on their local

environment, but these impacts could be occurring at too small of a scale to be regularly observed via GRACE. The sand dams in the SDC may be constructed too far from each other to have any overlap in their area of influence, decreasing the magnitude of their water storage signal. Unfortunately, a complete database of sand dam locations has never been created, because the many different NGOs involved in building sand dams often do not make information about their specific projects publicly available. Further clouding the issue is the approximately 50% of sand dams that are not functioning properly due to issues of siltation and/or seepage (Viducich, 2015). If half of the sand dams in the SDC are not storing the expected amount of water, the issue of GRACE's low resolution is exacerbated.

As a note, the FLDAS climate data employed for this study is largely simulated. There may be some concern that the impact of sand dams is already captured by increased evapotranspiration, increased baseflow-groundwater runoff, etc. in the FLDAS climate data. However, the FLDAS models likely do not account for sand dams, because sand dams cover only a small portion of the FLDAS study area, sub-Saharan Africa, and are relatively undocumented.

2.5.2 Link between Increased Vegetation and Sand Dams in the SDC

While the water storage anomaly LM was unable to discern a significant impact of sand dams on GRACE total water storage throughout the entire year, the vegetation LM indicated that sand dams have a small, positive impact on the health and density of vegetative cover. Interestingly, there is a direct connection between vegetative cover and groundwater—a connection that allows conclusions to be drawn about the small-scale impact of sand dams on water storage. This impact is restricted to the influence area of the sand dams, and thus occurs at a smaller scale than can be detected by GRACE each month.

The types of vegetation present in an area are directly linked to the depth of the groundwater (Le Maitre, Scott, & Colvin, 1999). Vegetation undergoes a marked

decrease in height and structural complexity as groundwater retreats from the land surface (Le Maitre et al., 1999). Sand dams store water just below the land surface, resulting in pseudo-perched groundwater. The pseudo-perched groundwater seeps through the stream banks and has the potential to raise the local groundwater table, supporting increased vegetative growth. In addition to the vegetation that naturally results from a higher local groundwater table, farmers also grow crops near the sand dam. The crops are often irrigated using water from the sand dam and thus further contribute to the increased NDVI. Unfortunately, the increased natural vegetation and cultivated crops results in increased transpiration, thereby lowering the groundwater table and reducing the length of time that the sand dam will store water in the dry season.

The interaction between the sand dam's influence on the local groundwater table and local vegetation creates a boom-bust dynamic for the vegetation (see Fig. 2.8). During the rainy season, rainfall is stored in the sand dam and raises the local groundwater table; vegetation springs up as a result. The vegetation transpires water from the sand dam, drawing down the levels of stored water. When the rainy season ends and the sand dam dries up, the vegetation senesces and NDVI decreases. The cycle is repeated each rainy season. Fig. 2.8 depicts this cycle very well, with the LM coefficient for the month categorical variable being the lowest for the month right at the beginning of the rainy season and the highest at the end of a rainy season.

The NDVI LM revealed that sand dams do indeed positively impact NDVI and, therefore, the amount of available water. This increase in available water leads to improved food and water security for the local communities, which is important from a human rights perspective. However, what could this mean from an engineering international development standpoint? Currently, many sand dams are ineffective (Viducich, 2015). Given the limited availability of information about individual sand dam projects, measuring the overall effectiveness of a sand dam and identifying hydrologic, geologic, and geographic features that significantly impact this effectiveness is extremely challenging. However, examining the impact of an individual sand dam on

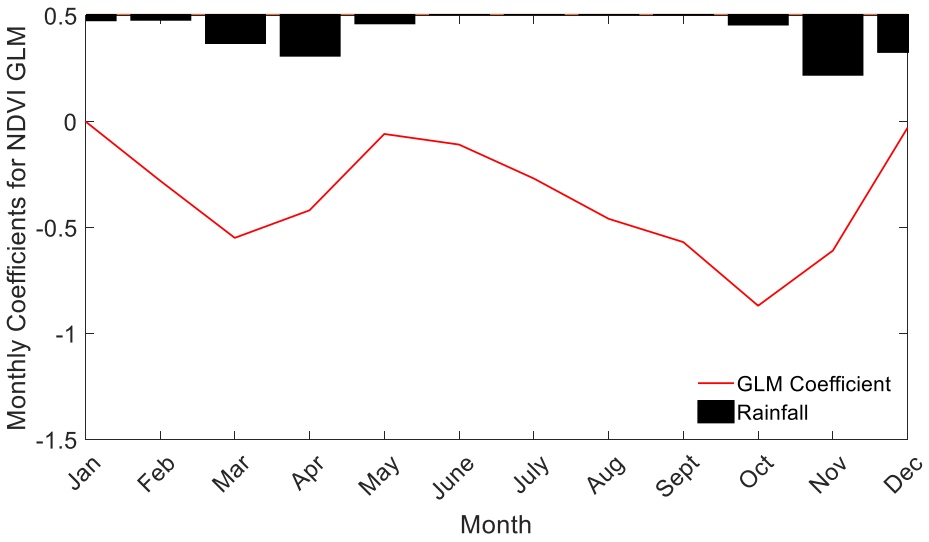

Figure 2.8. Coefficients for the Month categorical variable in the NDVI LM are directly correlated to the rainy and dry seasons in the SDC.

the local NDVI might be a promising method for quantifying the overall effectiveness of the sand dam. For example, a relatively greater increase in local NDVI during the rainy season would signify that a sand dam is storing more water than a sand dam with a smaller increase in local NDVI. This concept is supported by Manzi and Kuria (2011), who found that stream banks near sand dams were likely to convert from bare land to vegetative cover over time. Further, there may be potential for using NDVI, coupled with the Normalized Difference Moisture Index and stream network maps, to identify the locations of functioning sand dams. With a database of functioning sand dams, a plethora of studies could be performed to further improve the site selection and design for sand dams.

2.6 Conclusions

A methodology was developed and tested using two different remote sensing products. The methodology capably detected and quantified the effectiveness of a water

harvesting technology common in south-eastern Kenya. The study revealed that despite a sand dam's numerous positive effects on the food and water security of a local community, a sand dam likely does not significantly affect long-term regional groundwater levels. Any impact on groundwater levels is temporary and limited to the area directly surrounding the sand dam. The community near the sand dam draws water from the dam for domestic and agricultural purposes, and the increased vegetation near the sand dam transpires the stored water. These two factors largely contribute to the temporary nature of the increased groundwater levels. The GRACE total water storage data indicates that sand dams capture and store additional water during the rainy season, but that this additional storage is not significantly greater than water storage in an area without sand dams outside of the two months of the year with the most rainfall. GRACE's spatial resolution may limit the detection of increased water storage provided by sand dams, even when there are thousands of said structures in an area. MODIS NDVI, however, can detect the impact of sand dams on vegetative cover throughout the year. NDVI indicates that there is a heightened level of vegetation in an area with a high density of sand dams. This increased vegetation suggests increased groundwater levels resulting from the water storage added by sand dams. The water stored by sand dams may be only a seasonal resource, but the increased access to water can have a lasting, positive influence on the food and water security of the community. Future work will focus on leveraging the knowledge that sand dams cause a quantifiable change in NDVI to identify the locations of other sand dams and to assess the effectiveness of individual sand dams.

3. INVESTIGATING THE ENVIRONMENTAL RESPONSE TO WATER HARVESTING STRUCTURES: A FIELD STUDY IN TANZANIA

Abstract

Sand dams, a popular water harvesting structure employed by rural communities, capture and store water for use during the dry season in arid and semi-arid regions. Most sand dam research has been performed on the "ideal" sand dam, despite approximately fifty percent of sand dams not functioning as intended. This research involves a year-long, in-depth field study of three sand dams in Tanzania, one of which is essentially non-functioning. The study investigated a sand dam's impact on macroinvertebrate habitat, vegetation, and streambank erosion and explored a sand dam's water loss mechanisms. Surveys of macroinvertebrate assemblage were performed each season. Vegetation surveys were performed every other month, and erosion was recorded semi-monthly. Water table monitoring wells were installed at each sand dam, and measurements were taken twice a day. The study found that sand dams are too homogeneous to provide the sustenance and refugia macroinvertebrates need at different life stages. The non-functioning sand dam has a thick layer of silt preventing infiltration of rainwater. The functioning sand dams store a significant amount of water, but most is lost to evapotranspiration within a few months of the last rainfall. Unlike the non-functioning sand dam, the functioning sand dams have a positive impact on local vegetation and minimal impact on erosion. Sand dams can increase the water security of a community, but site characteristics and construction methods must be considered to maximize the sand dam's positive impact.

3.1 Introduction

International development projects in the Global South are managed by either a national department, private company, non-governmental organization (NGO), or a group of international development agencies (Ika, 2012). Success metrics for international development projects are typically defined by the funding organization, which are most often multilateral or bilateral organizations (e.g. the World Bank, United States Agency for International Development, etc.) or individual donors (Ika, 2012). Unfortunately, project success metrics frequently tell only one side of the story, focusing on financial and technical management rather than the social, cultural, and environmental impacts (Ika, 2012; Julian, 2016). Such a narrow definition of success omits both positive and negative unexpected consequences of international development work (Julian, 2016). Underreporting of project outcomes results in an inadequate understanding of the impact of international development work. Failure to consider whether intended long-term goals are met wastes time, money, and resources.

One example of international development projects with a questionable record of success are water harvesting structures in sub-Saharan Africa. When a specific technology's ability to improve water security is not honestly communicated along with the technology's other long-term impacts, outside organizations may embrace the technology without understanding the associated risks. Misunderstood risks lead to situations where a water harvesting technology proliferates without consideration of project pitfalls. This has been the case with sand dams in sub-Saharan Africa. Sub-Saharan Africa is home to over 3000 sand dams, yet approximately 50% of sand dams are essentially non-functioning (de Trincheria et al., 2018; Viducich, 2015).

Sand dams are small, reinforced concrete dams built atop impermeable streambeds in arid regions with infrequent, high-intensity rainfall (see Fig. 1.1). The high-intensity rainfall erodes soil from the land surface and deposits the coarser particles, usually sand, upstream of the dam. The sand stores primarily flash flood-water, where

it is naturally filtered, protected from evaporation, and helps raise the groundwater level in the surrounding area due to recharge from the increased subsurface storage (Borst & de Haas, 2006; Hut et al., 2008; Quilis et al., 2009). The extent of a sand dam's impact on the groundwater level, however, is limited by the geologic connectivity between the sand dam and the riparian zone and by the community's water use rate (Hut et al., 2008; Quinn, Rushton, & Parker, 2019). While a sand dam does filter water in a process similar to a slow sand filter, water abstracted from sand dams via scoopholes and covered wells exceeds World Health Organization recommendations for turbidity (73% exceedance), conductivity (24% exceedance), and thermotolerant coliform concentration (55% exceedance) (Quinn, Avis, Decker, Parker, & Cairncross, 2018).

Most information about sand dams comes from NGOs painting a rosy picture of the innumerable positive impacts of sand dams. Other information on sand dams comes from studies published on one or two ideal sand dams or from sand dam models. One in-depth sand dam study examined the hydrology of a Kenyan sand dam and performed a water balance assessment of the sand dam (Borst & de Haas, 2006). Results from this study were used to develop sand dam models that explored how sand dams impact the local water table (Hoogmoed, 2007; Quilis et al., 2009). A comprehensive study of three Kenyan sand dams explored their hydrology and bare soil evaporation, while a survey of at least 50 sand dams analysed their water quality (Quinn, Parker, & Rushton, 2018; Quinn, Avis, et al., 2018; Quinn et al., 2019). Other studies used modelling to further explore the seepage of sand dam water through streambanks (Hut et al., 2008) and the potential of sand dams to increase water security in Ethiopia (Lasage & Verburg, 2015). The socio-economic benefits of sand dams have also been explored (Lasage et al., 2008) along with the negative effects of sand dam siltation and/or seepage due to poor construction and or siting (Nissen-Petersen, 2006; de Trincheria et al., 2015; Viducich, 2015). Except for the Borst and de Haas (2006) study and the Quinn, Parker, and Rushton (2018) and Quinn et al. (2019) studies on high-functioning sand dams, most published sand

dam studies are based on survey data or modelling efforts. Published studies do not tell the whole story of sand dam impacts, and this has created a false perception of the risks involved with sand dam construction.

This study examines claims made by non-scientific bodies about sand dam impacts by investigating how diverse sand dams influence macroinvertebrate habitat, vegetation, erosion, and local water availability. Specifically, the study will investigate the following questions: (1) Are sand dams able to support macroinvertebrates? (2) What factors determine a sand dam's impact on vegetative growth? (3) How is streambank erosion affected by sand dams? (4) What are the dominant mechanisms driving water loss from the sand dams and riparian zone? Answering these questions will provide some insight into the validity of the claim that sand dams revitalize the entire ecosystem (*Reversing Land Degradation and Desertification*, n.d.; *Sand Dams*, n.d.). These questions will be explored through an in-depth field study of three sand dams in Tanzania. The sand dams are selected based on community interest in the study and diversity of dam features, such as stream width, dam effectiveness, stream valley slope, and local vegetation. This diversity of features provides a broad representation of the sand dams found throughout the region, and this study will therefore create a better understanding of how a sand dam interacts with the local environment. The study is limited to only three sand dams, because the study design relies on the active participation of local community water groups. Only three of the community water groups formed during sand dam construction remained active at the time of this study. The breadth of the study was further limited by long travel times between sites and difficulties related to equipment access.

3.2 Study Area

Tanzania is home to 55.5 million people, 70% of whom reside in rural areas (United Republic of Tanzania National Bureau of Statistics, 2015). The climate of Tanzania varies regionally, but most of the country experiences a tropical savannah or a warm

semi-arid climate (Peel, Finlayson, & McMahon, 2007). The northern part of the country experiences annual bimodal rainfall, with rainy seasons occurring March to May and October to December. The central and southern part of the country experiences annual unimodal rainfall, with the rainy season occurring from October to April (see Fig. 3.1a; Luhunga and Djolov, (2017)). Tanzania is fairly flat, with the exception of the highlands on the southern border and, of course, Mount Kilimanjaro to the east of Arusha. There are at least 15 sand dams in Tanzania, three of which will serve as study sites for this research (see Fig. 3.1a). Most of the sand dams were funded by the Mennonite Central Committee of Tanzania (MCC) and designed by Kenya-based NGOs. Dodoma has nine sand dams; Longido, a small town near the Kimokouwa sand dam (see Fig. 3.1a), has four sand dams, and there are a few sand dams elsewhere in the country. The average annual rainfall for Dodoma is 601 mm, and the potential evapotranspiration is 1800 mm. The average annual temperature in Dodoma is 23.0°C. The average annual rainfall for Longido is 696 mm, and the potential evapotranspiration is 1640 mm. The average annual temperature in Longido is 20.7°C (Platts, Omeny, & Marchant, 2015).

The sand dams selected for inclusion in this study all have an active community water group that was willing and able to participate in the study. The community water groups have formal ownership of the land surrounding the sand dams, and the research activities were generally limited to this land. One of the sand dams selected, Kimokouwa, was known to store very little water outside of a few days after a rain event. The other two sand dams, Soweto and Chididimo, store water for a couple of months into the dry season. The Soweto and Chididimo sites have different site geology, and therefore provide different insights into the potential of sand dams

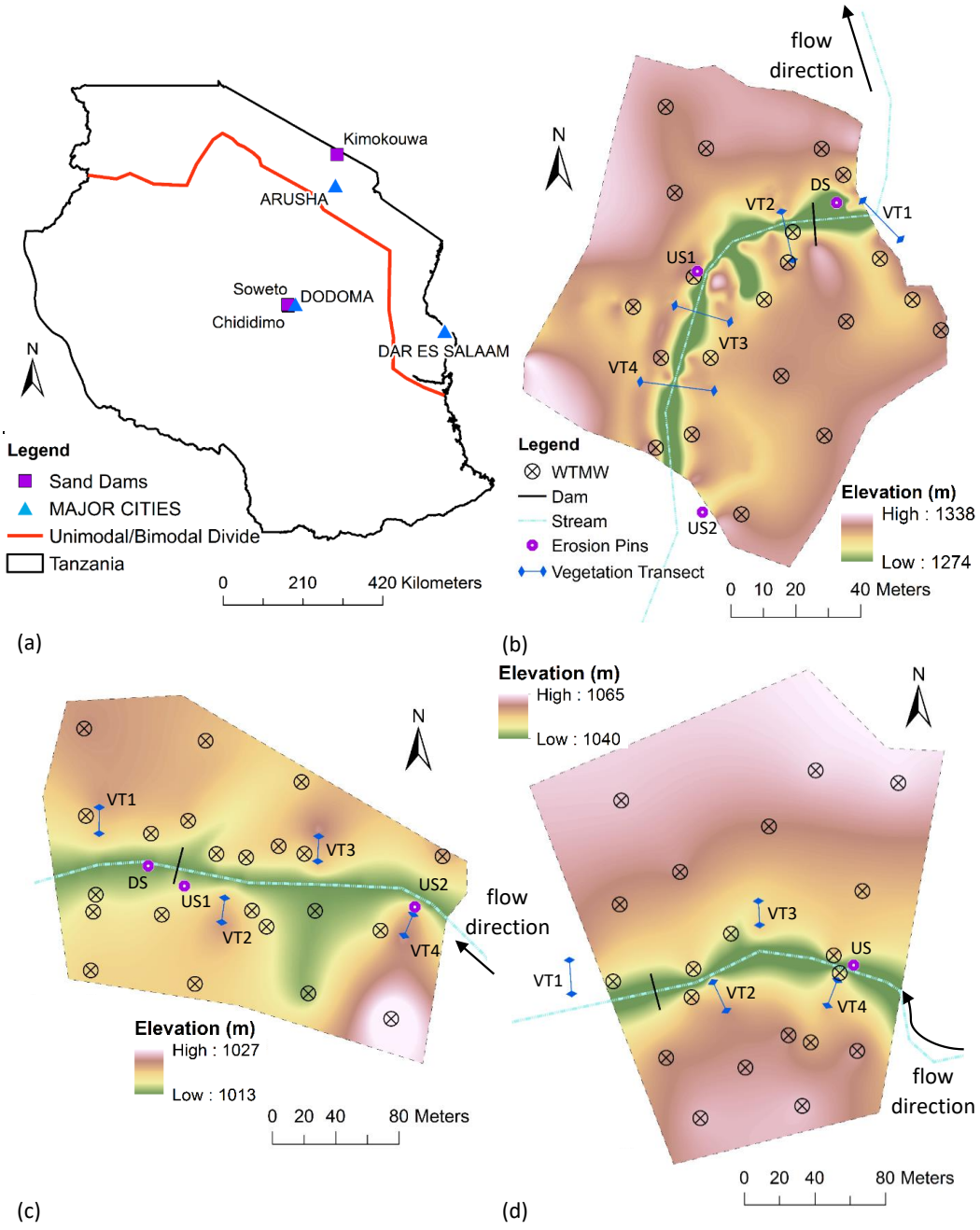

Figure 3.1. (a) Study Area. The bimodal rainfall region is north of the red line; the unimodal rainfall region is south of the red line (Luhunga & Djolov, 2017); (b) Kimokouwa study area; (c) Soweto study area; (d) Chididimo study area. Elevations are interpolated from GPS points taken during study. The elevation map includes only the area controlled by the community water groups.

to impact their local environment. All three sand dams vary in their construction specifications, length, and storage capacity (see Table 3.1). The width of the spillway is essentially equal to the width of the stream at each site.

Table 3.1.
Physical parameters of the three sand dams

Sand Dam	Total width (m)	Total length (m)	Spillway (m)	Estimated storage volume* (m^3)	Wing walls (m)	Spillway height (m)
Kimokouwa	28.78	150	8.74	1,310	20.04	2.06
Soweto	23.96	350	16.95	5,930	7.01	1.27
Chididimo	22.71	300	9.60	2,880	13.11	1.30

**Note* : Storage volume estimated using an average sand dam depth of 2.5 m and porosity of 0.40. The spillway is approximately equal to the width of the stream channel.

3.2.1 Kimokouwa sand dam

The Kimokouwa sand dam (see Fig. 3.1b) is located approximately 11.5 km south of the Kenya border. Construction of the sand dam was completed in November 2011 with funding provided by MCC and design and construction expertise provided by the Utooni Development Organization of Kenya. The soil deposited behind the Kimokouwa sand dam is largely silty sand with thick silt layers interspersed. In the riparian zone, the soil is primarily reddish sandy clay. A hand pump was installed in the right bank, 30 m upstream of the sand dam in April 2016. MCC requested this site be included in the study, because the sand dam proved ineffective at capturing and storing water for the community's use. MCC hoped that the research could help identify the factors contributing to the sand dam's failings and inform their future work.

3.2.2 Soweto sand dam

The Soweto sand dam (see Fig. 3.1c) is located approximately 20 km west of Dodoma, Tanzania's capital city. Construction of the sand dam was completed in June 2011 with funding provided by MCC and design and construction expertise provided by the Sahelian Solutions Foundation of Kenya. The soil deposited behind the Soweto sand dam is moderately sorted sand, and the riparian zone is predominantly silty sand. A hand pump was installed in the left bank, 85 m upstream of the sand dam at the time of dam construction. The Soweto site is the flattest of the three sand dam sites, with an elevation change of only 14 m across the site. The streambanks are quite flat near the dam, and the community is able to grow many crops on the banks, using water from the sand dam for irrigation. At 17 m wide, the stream at Soweto is also the widest of the three sand dam sites.

3.2.3 Chididimo sand dam

The Chididimo sand dam (see Fig. 3.1d) is located approximately 3.2 km south of the Soweto sand dam. Construction of the sand dam was completed in June 2011 with funding provided by MCC and design and construction expertise provided by the Sahelian Solutions Foundation of Kenya. The soil deposited behind the Chididimo sand dam is moderately sorted sand. The riparian zone contains primarily silty sandy gravel. A hand pump was installed within the stream channel 150 m upstream of the sand dam at the time of dam construction. The community selected this site for the hand pump, because they were able to extract water from the sandy streambed at that location before the sand dam was constructed. The Chididimo sand dam is constructed in a fairly uniform stream valley, with relatively steep slopes covered with long grasses and large trees. The abundant vegetation is expected to reduce erosion at the site, but the steep stream valley likely means that the sand dam will have a less pronounced impact on the local water table.

3.3 Data Collection and Analysis

3.3.1 Community water groups

Each sand dam selected for this study has an active, officially registered, community water group responsible for managing the sand dam. The community water groups were involved in the field work for this study from the first day. In addition to meeting with the researchers regularly, each group provided three to six volunteers to take twice daily and bi-weekly measurements. The volunteers were trained in proper data collection and recording procedures and were provided all materials necessary to complete the work.

3.3.2 Macroinvertebrate survey

Macroinvertebrate surveys performed at each site were intended to serve as an indication of water quality and overall habitat health. At each sand dam, samples were extracted at two locations upstream of the dam and one location downstream of the dam. All samples were taken from the middle of the streambed. During the dry season, a 25 cm x 25 cm by 10 cm-deep hole was dug in the streambed with a small shovel, and the extracted bed material was transferred to a plastic bucket (Verdonschot, van Oosten-Siedlecka, ter Braak, & Verdonschot, 2015). Holes drilled in the bucket's lid were plugged with cotton to prevent transfer of macroinvertebrates into or out of the sample (Stubbington et al., 2009). The samples were transported to the research base and rehydrated with de-chlorinated water to encourage re-emergence of desiccation-tolerant life stages (Boulton, Stanley, Fisher, & Lake, 1992; Stubbington et al., 2009). For a 28-day period, the samples were checked daily for macroinvertebrates. During the rainy season and at the start of the dry season when the streambed was still fairly wet, a 25 cm x 25 cm by 10 cm-deep hole was dug in the streambed with a small shovel, and the extracted bed material was sieved through a 2 mm mesh sieve at the

site. Any macroinvertebrates found would have been stored in a 10% formaldehyde solution for later identification (Stubbington et al., 2009).

3.3.3 Vegetation survey

Vegetation surveys were performed approximately every two months to capture the seasonal change in vegetative cover near the sand dams. The surveys were done in accordance with the line intercept method (Lutes et al., 2006). At each site, four 20 m-long transects were laid perpendicular to the stream flow and marked with wooden stakes. One transect was sampled downstream of each sand dam and three transects were sampled upstream of each dam with a 50 cm x 50 cm quadrat (Lutes et al., 2006). During each survey, the quadrat was placed consecutively along the transect, and the percent of vegetative cover was estimated visually (Lutes et al., 2006; Mallik & Richardson, 2009). At Soweto and Chididimo, quadrat 1 was placed at the stream edge and the transect extended away from the stream. Two transects were laid on the left-hand side of the stream, and two were laid on the right (see Fig. 3.1b,c). At Kimokouwa, where the stream is narrow, the centre of each transect lay at the middle of the stream (see Fig. 3.1d).

3.3.4 Erosion study

Erosion pins were installed at each site to track the amount of streambank erosion occurring upstream and downstream of the sand dams. Welding rods 300 mm in length and 4 mm in diameter were used as erosion pins when the bank material was soft enough to insert the rods without deforming them (Lawler, Grove, Couperthwaite, & Leeks, 1999; Saynor & Erskine, 2006). The welding rods were painted to prevent rusting (Saynor & Erskine, 2006). Stainless steel rods 300 mm in length and 6 mm in diameter were used as erosion pins elsewhere (Stott, 1997). The pins were inserted into the streambank leaving 75 mm of the pin exposed at a vertical spacing of 1/4, 1/2, and 3/4 of the bank height and at a horizontal spacing of one meter

(Palmer, Schilling, Isenhart, Schultz, & Tomer, 2014). At Kimokouwa and Soweto, erosion pins were placed at two locations upstream of the dam and one location downstream of the dam. At Chididimo, pins were placed at one location upstream of the dam (see Table 3.2). Pins were installed at fewer locations at Chididimo, because the stream did not have a clearly defined bank, and, where present, the streambank was often too rocky to permit insertion of the pins.

Volunteers from the community water groups took erosion measurements approximately every two weeks using a 150 mm rule depth gauge. The length of pin exposed was recorded to the nearest mm for each pin. If more than 100 mm of the pin was exposed, the pin was reset so only 75 mm was exposed. In the event that the pin was missing due to extraordinary erosion, the researchers assumed that 240 mm, or 80% of the pin's length, of erosion occurred at the pin's location (Palmer et al., 2014). When a pin could not be found and appeared to be buried in the streambank, 300 mm deposition was assumed, and a new pin was installed with 75 mm exposed.

3.3.5 Water table monitoring

Water table monitoring wells (WTMW) were installed at each sand dam to track changes in the water table over time. A drilling team hand-augured boreholes 10 cm in diameter at 63 locations across the three sites (see Table 3.3). For each WTMW, the drilling team continued drilling until the team encountered hard rock or another material prohibiting the progress of the auger. A WTMW was installed only if a hole deeper than 0.5 m was achieved. A soil log was completed for each WTMW noting the soil depth, texture, colour, wetness, and cohesion for each horizon. See Fig. 3.1b-d for WTMW layout at the sand dams. Fig. 3.2 provides a schematic of the WTMWs. The WTMWs installed were schedule 40 polyvinyl chloride pipe 32 mm in diameter. To create a well screen, four 6.35 mm holes were drilled around the circumference of the pipe every 2.5 cm, leaving the top 60 cm of the pipe undrilled (Sprecher, 2008). Geotextile filter fabric was unavailable, so the well screen was covered with women's

Table 3.2.
Site characteristics of each erosion pin section

Sand Dam	Site Name	Bank	Length of bank pinned (m)	Bank height (m)	Bank morphology	Floodplain vegetation	Bank material	No. of pins	Pin spacing (m) V	Pin spacing (m) H	Date installed
Kimokouwa	US1	left	5	3.7	gently sloping	sparse trees and long grasses	silty sand	13	0.9	1	10/14/16
	US2	right	6	5.2	composite		silty sand and gravel	18	1.3	1	12/8/16
	DS	left	5	1.0	concave		clayey sand	15	0.2	1	11/24/16
Soweto	US1	left	4	2.4	vertical	large bushes and trees	silty sand	12	0.6	1	12/11/16
	US2	left	4	2.7	steeply sloping	long grasses, small bushes and trees	clayey sand and gravel	12	0.7	1	12/11/16
	DS	left	6	3.7	composite	long grasses and bushes	sand	18	0.9	1	12/11/16
Chididimo	US	right	9	3.7	composite	long grasses and bushes	sand	26	0.9	1	12/13/16

Note : US is upstream; DS is downstream; V is vertical pin spacing); H is horizontal pin spacing.

hosiery instead (Borst & de Haas, 2006). The well caps at the top and bottom of the WTMWs were vented to prevent pressure from building up inside the pipe resulting in incorrect measurements. At the ground surface, a mounded concrete pad was built to secure the WTMW in place and to encourage rainfall to drain away from the structure (see Fig. 3.2). The elevation of the top of the WTMW pipes was measured relative to the ground surface with a tape measure, accurate to the nearest cm. The ground elevation at the WTMWs was determined with a calibrated GARMIN GPSMAP 64s.

Table 3.3.
Water table monitoring well installations at the three sand dams

Sand Dam	Number installed	Range of depths (m)	Average (m)	Standard deviation (m)
Kimokouwa	21	0.6–2.6	1.4	0.6
Soweto	22	0.5–3.7	1.5	0.8
Chididimo	20	0.5–1.9	1.0	0.4

Volunteers from the community water groups took measurements of the water table every morning and evening during the rainy season after the WTMWs were installed. After the wells dried up, measurements were taken less frequently—approximately once per week. The water table measurements were taken by slowly lowering a Solinst Model 101B Basic Water Level Meter into the WTMW until the buzzer was activated indicating water had been reached. At this point, the distance from the top of the WTMW pipe to the sensor was recorded to the nearest cm in a notebook along with the date and time of day.

At Kimokouwa, the community water group volunteers took measurements of the water depth for a few weeks after the WTMWs were installed, but water was only detected in the well closest to the sand dam up to two days following even a large rainfall event. The sand dam was clearly not storing much water. The volunteers and the researchers agreed to cease WTMW measurements at Kimokouwa so as to not

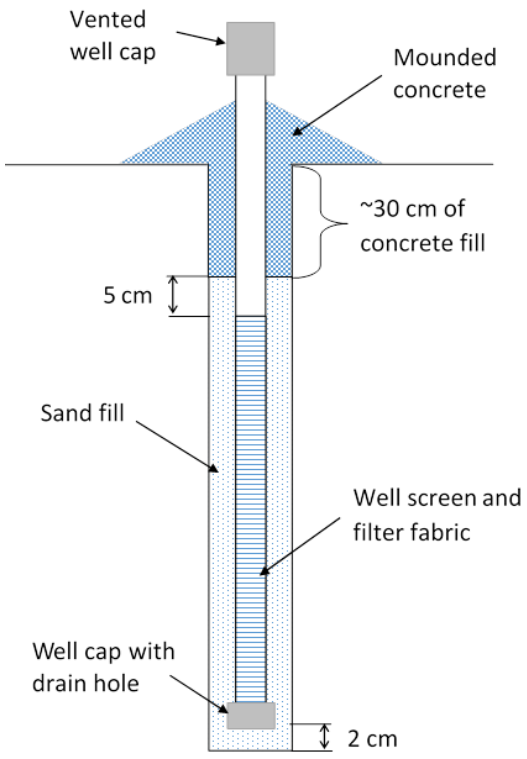

Figure 3.2. Schematic of the water table monitoring wells installed (adapted from Sprecher (2008)).

waste the volunteers' time. At Soweto, the frequency and regularity of the WTMW measurements varied somewhat, with the measurements being more consistent later in the project timeline. The Chididimo community water group volunteers were very dedicated to the task of recording water table depths every morning and evening. Of the three sand dams studied, the Chididimo data provides the most complete understanding of how water storage in the sand dam changed over time.

The water table measurements were used to determine the volume of water in the sand dam and riparian zone over time. The weekly average height of subsurface water in each WTMW was calculated from the field data, accounting for the difference in soil porosity between the sand dam and the riparian zone. A value of 0.42 was used for the porosity in the sand dam; 0.40 was used for the porosity in the riparian zone

(Rawls, Brakensiek, & Saxton, 1982). Inverse distance weighting interpolation was applied to create uniformly spaced grids of average water height at a weekly time step. The weekly average water volume was then calculated by multiplying the water height grids by the grid spacing and summing across the control area. The control area is the portion of the study area enclosed by the installed WTMWs (see Fig. 3.1c,d). For Chididimo, this area is 32,274 m^2, while it is 41,995 m^2 for Soweto. The weekly average control area water volume calculated from the field data is compared to a theoretical weekly average water volume, described below.

To determine the various causes of water loss from the sand dam and their relative magnitude, a theoretical water balance was calculated using data from Famine Early Warning Systems Network Land Data Assimilation System (FLDAS). FLDAS is a set of models designed to provide accurate climate estimates for the purpose of drought monitoring in data-sparse regions susceptible to food and water security issues (McNally et al., 2017). FLDAS provides daily and monthly climate data consisting of 25 different variables for Western, Eastern, and Southern Africa. In this study, FLDAS data was used as a proxy for climate data, because there is not a reliable source of climate data freely available for Dodoma, Tanzania. The theoretical water loss from the sand dam is:

$$Q_{out,dryseason}(t) = -\alpha \times E(t) - Q_{sb}(t) - Q_{com}(t), \tag{3.1}$$

where $Q_{out,dryseason}$ is the rate of water loss from the sand dam after the end of the rainy season, E is total evapotranspiration modified by α, which is 0.85, Q_{sb} is baseflow-groundwater runoff, and Q_{com} is the community's water use. E and Q_{sb} are taken directly from the FLDAS dataset (McNally et al., 2017), while Q_{com} was calculated based on each community's accounting of their water use. Equation 3.1 is integrated over time, t, and subtracted from the field data-determined volume of water in the control area at the end of the rainy season to create a theoretical volume of water curve for the sand dam area (see Fig. 3.8). The control area to which Eq. 3.1 is applied is that used for the field data water volume calculations: the portion of the study area enclosed by the installed WTMWs (see Fig. 3.1c,d). The theoretical

volume of water resulting from Eq. 3.1 has a high degree of uncertainty, because it is a simplified representation of water loss that utilizes modelled FLDAS data. However, the relative magnitude of the loss terms is likely reliable, and this is the primary focus of the conclusions that will be drawn from the model.

Total evapotranspiration, E, is the sum of canopy-intercepted evaporation, transpiration from vegetation canopies, and evaporation from bare soil (McNally et al., 2017). Equation 3.1 is only applied during the dry season, and therefore the control volume will not lose water due to evaporation of canopy-intercepted rainfall. Including this portion of E in the water balance is inappropriate. Kumar, Holmes, Mocko, Wang, and Peters-Lidard (2018) found that canopy-intercepted evaporation accounts for approximately 15% of the total evapotranspiration simulated in the Noah Land Surface Models, which are incorporated into FLDAS (McNally et al., 2017). Therefore, total evapotranspiration is reduced by 15% in Eq. 3.1, resulting in an α of 0.85. FLDAS calculates transpiration by scaling potential evapotranspiration in proportion to solar radiation, vapor pressure deficit, air temperature, and soil moisture. Evaporation from bare soil in the FLDAS dataset is calculated by scaling potential evapotranspiration based on current soil moisture (McNally et al., 2017). Therefore, the rates of transpiration and evaporation in the FLDAS dataset will decrease as the water table retreats from the ground surface and soil moisture declines.

The community's water use was calculated using estimates provided by the community water groups, and thus has an unknown degree of uncertainty. At least one sand dam researcher has noted that unsanctioned machine pumping of water from sand dams can cause rapid drawdown of stored water (Hut et al., 2008). However, no evidence was present at either Dodoma site to indicate the community was drawing significantly more water from the sand dams than they indicated.

3.4 Results and Discussion

3.4.1 Macroinvertebrates

The various macroinvertebrate survey trials produced only one specimen—at Kimokouwa during the dry season. This failure to produce macroinvertebrates indicates that sand dams are not a suitable habitat for macroinvertebrates during any season of the year. The absence of macroinvertebrates in the sand dams might suggest that sand dams have a negative impact on macroinvertebrate habitat, but it is also likely that sandy streambeds in semi-arid regions are simply inhospitable to macroinvertebrates. To make this distinction, further studies are needed to compare macroinvertebrate assemblages in undammed sandy streambeds with those in sand dams. Of all substrates studied, Duan, Wang, and Tian (2008) identified sandy substrate to have the lowest taxa richness and to be the least suitable for macroinvertebrates and benthic fauna, causing sandy substrates to be fairly homogeneous. Sandy substrate also has small interstice dimensions that provide only very small living spaces for macroinvertebrates (Duan et al., 2008). Homogeneous bed material suggests that there are few, or no, structures available for macroinvertebrates to use as refugia during high streamflow (Taniguchi & Tokeshi, 2004) and few niches for different species to utilize during various stages of their life cycle (Salant, Schmidt, Budy, & Wilcock, 2012). Furthermore, macroinvertebrates feed on bacteria, algae, and other organic matter, which may be scarce in sandy substrate (Taniguchi & Tokeshi, 2004).

In the case of the sand dams studied, there were very few plants, cobbles, or larger rocks present in the stream channel. The sand within the sand dam, with the exception of Kimokouwa, was largely a mixture of fine- and coarse-grained sand, as determined by a visual and tactile assessment of the material. This environment precluded macroinvertebrates from inhabiting the sand dam. Macroinvertebrates are often used as an indicator of water quality, but the lack of macroinvertebrates in the sand dams here should not be assumed to signify the water was of low qual-

ity. The aforementioned compounding factors likely largely explain the absence of macroinvertebrates in the sand dams.

3.4.2 Vegetation

The vegetative cover at the three sand dams differed greatly throughout the study (see Fig. 3.3). Kimokouwa had the lowest level of vegetative cover overall and did not exhibit much increase in vegetative cover during the rainy season. Soweto, the flattest site, showed the greatest improvement in vegetative cover between the dry season and the rainy season. Each Soweto transect exhibits a significant increase in vegetation. Interestingly, Chididimo only had significantly more vegetation at the two transects farthest upstream from the sand dam (VT3 and VT4). The slope of the Chididimo stream valley became gentler farther upstream of the dam (see Fig. 3.1d), which created favourable conditions for increased vegetation during the rainy season. Of the three sand dams, Chididimo has the highest level of vegetation during the dry season, and therefore had the least opportunity for significant increases in vegetation during the rainy season.

That Soweto, the flattest site, and the two transects located in the flattest part of Chididimo display significant increases in vegetation between the dry and rainy seasons suggest that the average percent vegetative cover at a sand dam is correlated to the land slope near the sand dam. The Pearson Correlation Coefficient, ρ, corroborates this observation. The change in vegetative cover between the dry and rainy seasons is negatively correlated (ρ=-0.73) to increasing land slope at the two functioning sand dams, Soweto and Chididimo, indicating that as the land slope increases, the improvement in vegetative cover decreases. The same correlation is not observed at the non-functioning Kimokouwa sand dam (ρ=0.04), which is expected because the sand dam is not contributing to a locally raised water table.

As the elevation above the streambed increases, the percent vegetative cover generally decreases during both the rainy season and the dry season (see Fig. 3.4a). The

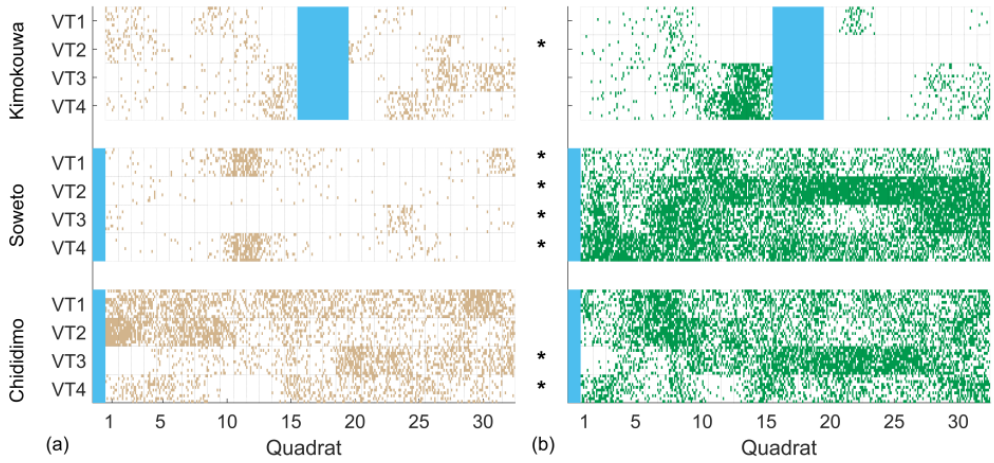

Figure 3.3. Representation of percent vegetative cover for each transect at each sand dam during the (a) dry season and (b) rainy season. The stars indicate a significant difference ($p<0.05$) between the wet and dry season vegetative cover for that transect. The solid colour indicates the location of the stream relative to the transect. VT1 is downstream of the dam; VT2–4 are upstream.

trend of decreasing vegetative cover with increasing elevation above the streambed is more consistent during the dry season but is also evident during the rainy season. Two conditions may combine to create the trend seen in Fig. 3.4a. First, at low elevations above the streambed, groundwater seepage through the streambanks creates a raised water table that is close to the land surface (see Fig. 3.5). The raised water table has a positive impact on the soil moisture of the unsaturated soil layer, and this additional moisture supports vegetation growth. Second, a lower elevation above the streambed implies a gentler land slope. Gentle slopes give rainwater more time to infiltrate into the soil, because storm surface runoff travels slower over a gentle slope. Increased infiltration results in increased soil moisture and increased recharge of the water table. As Fig. 3.4a indicates, there is low vegetative cover right at the stream edge (lowest elevation), which signifies streamflow frequently rising above this point and inhibiting vegetation growth.

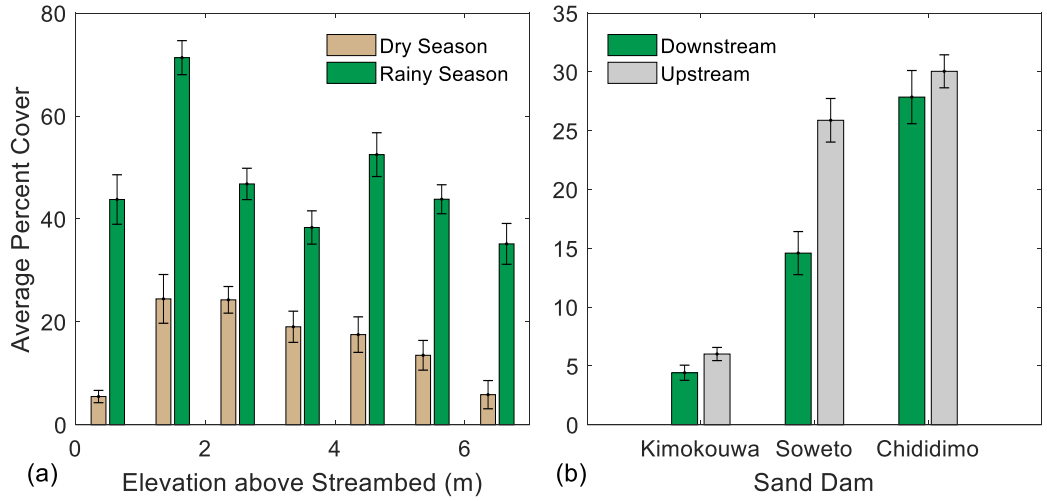

Figure 3.4. (a) Average percent cover at different elevations above the streambed for the dry and rainy seasons at the Soweto and Chididimo dams. Kimokouwa sand dam was excluded, because the sand dam is not functioning. Standard error bars are shown; (b) Average upstream and downstream vegetative cover at the three sand dams. Standard error bars are shown.

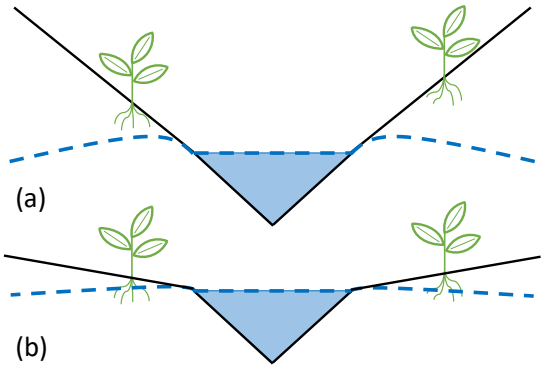

Figure 3.5. The roots of plants growing on a (a) steep slope will be farther from the locally raised water table created by a sand dam, and therefore have less access to soil water, than vegetation growing on a (b) gentle slope.

That the dry season shows a consistent relationship between elevation above the streambed and vegetative cover indicates that the vegetation at Soweto and Chididimo has at least some level of groundwater dependence (see Fig. 3.4a). The dependence of vegetation on groundwater in arid and semi-arid regions has been well-documented (Elmore, Kaste, Okin, & Fantle, 2008; Mata-González, McLendon, Martin, Trlica, & Pearce, 2012; Naumburg, Mata-gonzalez, Hunter, Mclendon, & Martin, 2005; Seeyan, Merkel, & Abo, 2014; Stromberg, Tiller, & Richter, 1996; Wang, Zhang, Yu, Fu, & Ao, 2011). In arid and semi-arid regions where rainfall is minimal, vegetation often relies on groundwater to supply the additional water needed for plant growth and transpiration (Naumburg et al., 2005). In semi-arid Dodoma, local communities use their knowledge of the relationship between vegetation and groundwater to inform their decisions on where to dig shallow wells (Shemsanga, Muzuka, Martz, Komakech, & Mcharo, 2018). Therefore, it is reasonable to expect that the vegetative cover at the Soweto and Chididimo sand dams is improved, in part, by a locally raised water table near the ground surface.

The upstream and downstream vegetative cover trends differ at the three sand dams. At each sand dam, there is more vegetation upstream of the sand dam than downstream (see Fig. 3.4b). However, this difference is most significant at Soweto, where the change in elevation across the site is small relative to the Kimokouwa and Chididimo sand dams. Of the three sand dams studied, only the sand dam located in a flat area exhibited a large increase in vegetation upstream of dam, indicating that a sand dam's impact on vegetation may be limited by the slope of the surrounding land. Nevertheless, additional studies are needed to verify this relationship. Also, the vegetative cover at the two functioning sand dams, Chididimo and Soweto, is high compared to the non-functioning Kimokouwa sand dam. This may be due solely to the impact of the sand dams, but it is equally likely that the steeper slopes and finer soils at Kimokouwa impact its vegetative cover. A functioning sand dam has the potential to support more vegetation, because of the additional stored water that is

available to vegetation for use in transpiration. Land slope and soil, however, must also be considered.

3.4.3 Streambank erosion

The temporal changes in the bank soil varied somewhat across the three sand dams (see Fig. 3.6). Kimokouwa and Soweto exhibited little change in bank volume at the upstream locations, and Chididimo experienced a high rate of soil deposition. Interestingly, bank erosion increased at Kimokouwa during the rainy season, while bank deposition increased at Chididimo during the rainy season. The differences in bank morphology and floodplain vegetation between the two sites impact their respective erosion/deposition dynamics. At the downstream location, Soweto did not exhibit much change in bank soil, while the Kimokouwa site showed severe erosion, particularly during the long rain season (mid-February to April). The Kimokouwa downstream bank lost a total of nearly 300 mm of soil throughout the course of the study due to mass bank failure. The heavy rainfall during the long rain season led to a pre-wetted bank with heightened pore water pressures. Eventually, the pore water pressures exceeded the structural integrity of the bank, and the bank material fell into the stream channel in large volumes (Hooke, 1979; Lawler et al., 1999). The downstream Kimokouwa bank experienced multiple mass failures throughout the long rain season (see Fig. 3.6).

The spatial changes in bank soil also vary between the three sand dam sites (see Fig. 3.7). The Kimokouwa streambanks exhibit a consistently high rate of erosion across the entire bank height. The high rate of erosion is likely due to the relatively steep and/or vertical banks and minimal vegetative cover. At Chididimo, the streambank generally experiences deposition across the bank height, but does experience lower rates of deposition at the foot of the bank with some periods of erosion occurring. This is clear from the high standard error for 1/4 bank height at Chididimo. Erosion at the foot of the Chididimo streambank is caused by high streamflow during

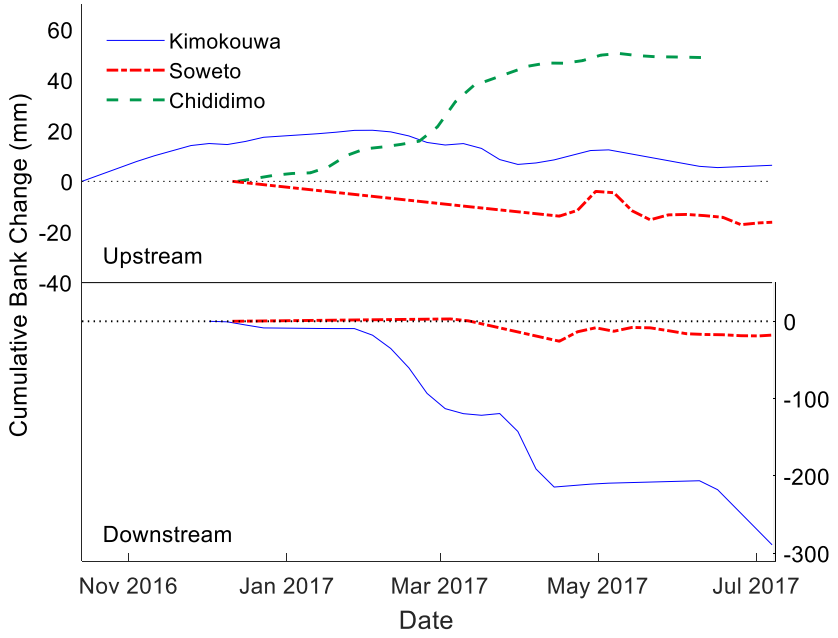

Figure 3.6. Cumulative bank change over the duration of measurement at each sand dam for the upstream and downstream pinned banks. A positive value signifies deposition, a negative value indicates erosion.

the rainy seasons. At Soweto, soil eroded from the top of the bank is deposited at the middle and foot of the bank. However, the extremely long standard error bars for Soweto erosion measurements at all bank heights challenge the validity of the Soweto erosion data. The community volunteers at Soweto may have erroneously recorded the erosion measurements, despite repeated training and practice sessions with the primary field researcher. The Soweto erosion data should be considered sceptically. However, based on Soweto erosion data taken solely by the primary field researcher, the overall trend of little erosion and deposition occurring at Soweto can be confirmed.

The Kimokouwa sand dam was constructed in an unstable reach. The stream channel is actively migrating, which causes the stream to flow into the left wing wall of the sand dam, rather than flow over the spillway. A strong eddy develops, eroding

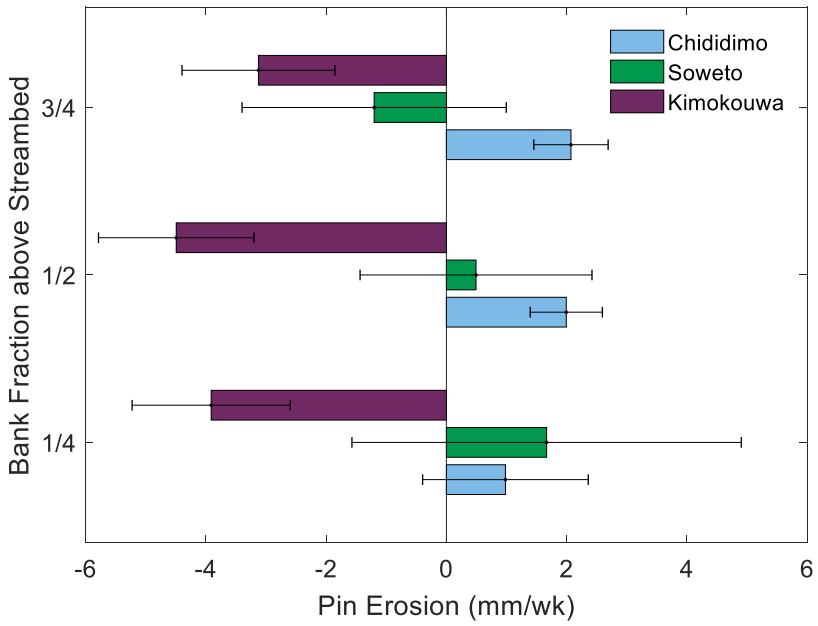

Figure 3.7. Average weekly change in the bank soil at 1/4, 1/2, and 3/4 bank height. Positive values represent deposition; negative values represent erosion. Standard error bars are shown.

the soil directly behind the dam. This erosion threatens the stability of the dam, because the dam's design depends on the weight of the soil to help hold the dam in place. The migration of the stream channel likely contributes to the mass erosion of the bank downstream of the sand dam (see Fig. 3.6).

3.4.4 Water storage and loss

The sand dam at Kimokouwa has a 1.2 m thick silt layer beginning at a depth of 0.5 m that acts as a capillary barrier, inhibiting the infiltration and, therefore, storage of water in the sand dam. Kimokouwa sand dam's water storage is also likely limited by the poor connectivity between the silty sand in the channel and the reddish clay that dominates the riparian zone. Groundwater is unable to travel freely between the sand dam and the riparian zone, as evidenced by the absence of water in all but

one WTMW. As a result of limited storage, the community is unable to use the sand dam as a source of domestic water. Silt layers formed at the Kimokouwa sand dam, because the dam was improperly constructed for the type of topsoil present in the area (Nissen-Petersen, 2006; de Trincheria et al., 2015). While the literature on this topic is not well-developed, the soil composition of the streambed before a sand dam is constructed can likely be helpful in determining the distribution of grain sizes a sand dam is expected to capture. This information, coupled with knowledge of the sediment load typically carried by the stream, can inform the need to construct a sand dam's spillway in stages to prevent siltation. Siltation of a sand dam occurs during rainfall events prior to the sand dam's maturation, or before the sand reservoir has naturally reached the height of the spillway (see Fig. 1.1). Sand dams in areas with silty sand should be constructed in thirty cm stages to ensure that the portion of the water column with suspended silt flows over the spillway instead of settling behind an immature sand dam (Nissen-Petersen, 2006).

A functioning sand dam typically fills with water after one high intensity rainfall event and remains essentially full throughout the rainy season (Ertsen & Hut, 2009). The stored water seeps into the banks, raising the water table in the riparian zone. The last rainfall of the season at Chididimo and Soweto occurred around early to mid-April, approximately the fourteenth or fifteenth week of the year. Fig. 3.8a shows that within just ten weeks of the last rainfall, the Chididimo sand dam had dried significantly, leaving very little abstractable water available to the community. The Soweto sand dam has a much greater storage capacity and retains abstractable water for approximately fifteen weeks after the last rainfall (Fig. 3.8b). Soweto's greater storage is due to the wider and deeper sand reservoir. The sand dams at Chididimo and Soweto only store water for community use during the first few months of the dry season.

In Chididimo, there are three sources of water: the sand dam and two boreholes drilled by an international non-profit organization. When there is water in the sand dam, the community draws all water for agricultural use from the dam and about

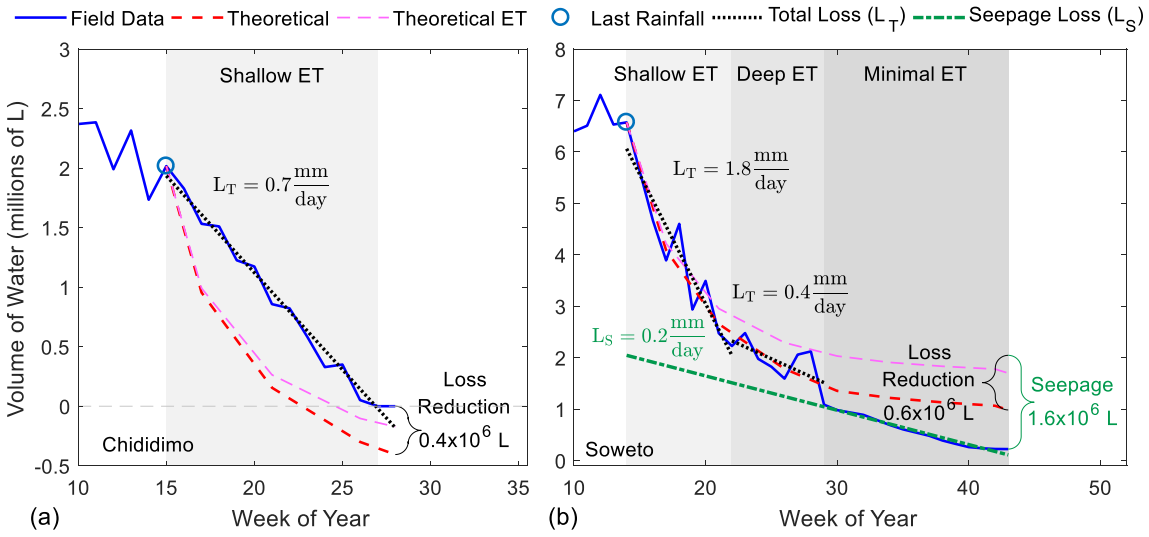

Figure 3.8. Volume of water in the area enclosed by the WTMWs of the (a) Chididimo and (b) Soweto sand dams. The field data line shows the volume of water in the study area during the specified week. The theoretical line, initiated at the end of the rainy season, shows the theoretical volume of water in the study area, calculated by integrating Eq. 3.1 and subtracting from the field-determined volume of water at the end of the rainy season. The theoretical line accounts for losses due to evapotranspiration, baseflow-groundwater runoff, and community use. The theoretical ET line shows the portion of total theoretical loss attributed to ET in the FLDAS dataset.

half of the domestic water from the dam, totalling 15,000 litres of water per week (Chijendelele na Mlimo Group, personal communication, May 30, 2017). However, their total water use accounts for only about 10% of the water stored by the sand dam at the end of the rainy season. Unsurprisingly, most of the water in the sand dam is lost to evapotranspiration (ET). With only 2% of the total water lost during the dry season attributed to baseflow-groundwater runoff, ET was responsible for the remaining 88% of the water lost from the Chididimo sand dam according to FLDAS data and Eq. 3.1 (see Fig. 3.8a). Equation 3.1 predicted the sand dam would lose its stored water by week 23. The measured data indicates the sand dam retained

water until week 27. Furthermore, Fig. 3.8a shows that the sand dam experienced a loss reduction of 400,000 litres during the first twelve weeks of the dry season. This suggests the dam effectively reduced ET by 19% compared to the ET simulated by FLDAS.

The nearly constant decrease in water volume, or total loss rate (LT), after the end of the rainy season at the Chididimo sand dam indicates that most water is lost due to ET (see Fig. 3.8a). Chididimo's relatively shallow sand reservoir results in all ET occurring at a shallow ET rate. When ET occurs from a sub-surface water table, the rate of ET is lower than would be expected if the water table was at the ground surface (Hellwig, 1973). The rate of sub-surface ET decreases as the water table retreats farther underground, and the rate of decrease is dependent upon depth and grain size (Hellwig, 1973; Quinn, Parker, & Rushton, 2018). Seepage could contribute to the total loss rate at Chididimo. While there was no evidence of seepage under the dam wall, downward seepage through the streambed could impact the total loss rate at Chididimo.

In Soweto, the sand dam is the only nearby source of water. When the sand dam is dry, community members must travel seven km to draw water from a well in a nearby village. When able, the community draws approximately 39,000 litres of water from the sand dam per week for both agricultural and domestic use (Vumilia Group, personal communication, June 1, 2017). Their total water use accounts for only about 10% of the water stored by the sand dam at the end of the rainy season. With only 1% of the total water lost attributed to baseflow-groundwater runoff and 16% of loss unaccounted by FLDAS, ET was responsible for 65% of the water lost from the Soweto sand dam according to Eq. 3.1 (see Fig. 3.8b). The unaccounted water loss could be due to seepage under the sand dam wall, through the streambanks, or streambed combined with a lower rate of ET than simulated by FLDAS.

The Soweto dam exhibits three distinct phases of water loss: shallow ET, deep ET, and minimal ET (see Fig. 3.8b; Quinn et al., 2018b). The minimal ET phase occurs during the period in which the community water group indicated they were no

longer able to abstract water from the sand dam. At this point, the water table has retreated too far underground for the community to draw water and, at this depth, the rate of ET is likely negligible (Hellwig, 1973; Quinn, Parker, & Rushton, 2018). Therefore, most of the water lost during the minimal ET phase is lost due to seepage under the dam wall and/or through the streambed. Unlike Chididimo, the Soweto sand dam does exhibit evidence of seepage—the community members collect water from scoopholes they dig just downstream of the dam. The seepage loss at Soweto occurs at a rate of approximately 0.2 mm/day and accounts for 24% of the water stored by the sand dam at the end of the rainy season. The seepage rate is assumed to remain essentially constant throughout the shallow, deep, and minimal ET phases (see Fig. 3.8b). Having accounted for seepage, Fig. 3.8b shows that the sand dam experienced a loss reduction of 600,000 litres during the first 29 weeks of the dry season. This suggests the dam effectively reduced ET by 11% compared to the ET simulated by FLDAS.

Figure 3.8 shows that the sand dams lost water at a slower rate than predicted by Eq. 3.1 during the dry season. The FLDAS dataset calculates evaporation from bare soil based on simulated soil moisture content (McNally et al., 2017). However, the dataset does not account for the depth at which the sand dam water is stored or for unique features, such as wind speed, topography, vegetation, and shading, that impact ET rates (Hellwig, 1973; Quinn, Parker, & Rushton, 2018). The lines fit to the field data after the end of the rainy season indicate that the Chididimo and Soweto sand dams are losing water primarily via ET at a nearly constant rate of 0.7 mm/day and 1.6 mm/day, respectively. Due to ET and other major losses, the sand dams can no longer provide water to the community after the months of July or August in most years.

The Soweto sand dam is losing water during the shallow ET phase at more than twice the rate of the Chididimo sand dam. The combination of stream width and vegetative cover contribute to Soweto's higher rate of water loss. The width of the Soweto sand dam is nearly twice that of Chididimo, providing a greater surface area of

sand from which evaporation occurs (see Table 3.1). For an equivalent water content, sub-surface evaporation rates from sand in the sand dam are higher than from the loamy soils in the riparian zone due to the differences in soil suction (Wilson, Fredlund, & Barbour, 1997). Also, different types of vegetation transpire water at different rates (Lautz, 2008). The banks of Chididimo are generally covered with natural vegetation, whereas the Soweto community intensively cultivates the banks. Natural vegetation in a semi-arid climate requires less water than cultivated crops, therefore the rate at which the Soweto vegetation transpires water contributes to Soweto's rapid water loss.

One of the most common reasons given for building sand dams is that they provide water to communities throughout the dry season. At Chididimo and Soweto, this is simply not the case. Chididimo and Soweto experience approximately 100 mm lower annual rainfall in one, four-month rainy season and higher rates of ET than a typical sand dam in Kenya experiences during two rainy seasons (NASA/GSFC/HSL, 2016). Therefore, the Dodoma sand dams have lower potential for storing water than their Kenyan counterparts. Sand dams are intended to protect the stored water from evaporation and they do to some extent, but the ground surface is inadequate protection against the high temperatures and dry air at the Chididimo and Soweto sand dams.

3.5 General Discussion and Considerations

The impact of a sand dam depends not only on its dimensions and construction but also on features of the surrounding land and the management of the dam's water resource by the local community. The field study revealed that a non-functioning sand dam might significantly influence streambank erosion but has little impact on the local water storage and vegetation. The functioning sand dams, however, had little impact on streambank erosion, significant impact on local water storage and in reducing ET losses, and varied impact on vegetation. Regardless of a sand dam's

functionality, none of the sand dams in the study were a suitable habitat for macroinvertebrates. The absence of macroinvertebrates in sand dams may limit the value of ecosystem services, such as nutrient cycling, decomposition of organic matter, or primary productivity. The lack of these services, however, may be outweighed by the increased water security.

The two functioning sand dams support more vegetation than the non-functioning sand dam. The increase in vegetation caused by the sand dam's additional stored water is much more apparent when the surrounding land is relatively flat (i.e. at Soweto). A locally raised water table in a flat area results in soil water that is closer to the land surface than if the sand dam were surrounded by steep slopes, like at Chididimo (see Fig. 3.5). The increased soil water near the land surface is available to support vegetative growth and transpiration, leading to higher vegetative cover. Holding all other variables constant, building a sand dam in a flat area would likely maximize the positive impact of the sand dam on local vegetation. However, this needs to be further explored to see if the trend holds when more sand dams are examined.

The two functioning sand dams have stable streambanks compared to the non-functioning Kimokouwa sand dam. The streambanks at Kimokouwa exhibit severe erosion, particularly at the site downstream of the sand dam. The Kimokouwa sand dam was constructed between two sharp bends in the stream, and the flow of water over the sand dam adds energy to the water in the stream. With this added energy, the water erodes more of the streambanks and likely contributes to the migrating of the Kimokouwa stream channel. Severe streambank erosion and/or stream migration can lead directly to sand dam failure by weakening the soil supporting the structure. When this happens, the dam may break or be washed downstream. Sand dams should probably be built in stable, straight reaches to minimize the chance that the construction of a sand dam will negatively impact the course of the stream.

While the non-functioning Kimokouwa sand dam does not increase the availability of water in the local community, the functioning sand dams provide a local water

resource for at least the first few months of the dry season. However, the two functioning Dodoma sand dams do not store water throughout the entire dry season, as is an often-stated benefit of sand dams. Dodoma lies in the unimodal rainfall region of Tanzania, whereas Kenyan sand dams experience bimodal rainfall. With only one period of rainfall refilling the sand dams every year, the Dodoma sand dams are unable to supply water throughout the eight-month dry season. In addition, the Dodoma sand dams receive approximately 100 fewer mm of rainfall every year and average higher rates of ET than the annual rainfall and average ET at the Kenyan sand dams. Less rainfall limited to one rainy season of the year and higher ET result in sand dams that function at a lower level than those in Kenya.

A frequently cited benefit of sand dams is that they protect the stored water from ET. While the Chididimo and Soweto sand dams helped slow the rate of ET by 19% and 11%, respectively, ET is still the greatest loss factor for the stored water. Chididimo has a shallower sand dam and lost 88% of its stored water to ET, while Soweto is deeper and lost 65% of its stored water to ET. The deeper Soweto sand dam lost less water to ET than the shallower Chididimo sand dam, because the rate at which sub-surface water can be evaporated depends, in part, on the depth of the water below the ground surface (Hellwig, 1973; Quinn, Parker, & Rushton, 2018). To help reduce the amount of water lost from sand dams due to ET, sand dams should likely be constructed in locations where a deep sand reservoir can develop. At least one other study, de Trincheria et al. (2015), also recognised the impact of shallow sand reservoirs on water lost to ET.

3.6 Future Work

Future analysis of the collected dataset will focus on exploring the spatial variability in the local geology and its interactions with groundwater in the vicinity of the sand dam. Groundwater dynamics will be investigated in conjunction with the variability of evapotranspiration in and around the sand dams. In addition, the change

in vegetative cover relative to groundwater depth will be studied using both the field measurements detailed here and Normalized Difference Vegetation Index. Future sand dam research should also investigate water quality in the sand dams in the context of increasing salinity as evidence for or against high rates of evapotranspiration.

4. MODEL-BASED GUIDELINES FOR IMPROVING SITE SELECTION OF SMALL-SCALE WATER HARVESTING STRUCTURES

Abstract

Sand dams, a water-harvesting structure commonly employed by rural communities, capture and store water for use during the dry season in arid and semi-arid regions. Non-governmental organizations (NGOs) in sub-Saharan Africa construct new sand dams every year at a cost of $12,000 per sand dam and three months of construction time. Sand dams sometimes rejuvenate the surrounding area by raising the local water table and supplying domestic and agricultural water to the community throughout the dry season. However, the NGO and community often invest their time and money only to construct a poorly functioning sand dam. These sand dams are low-functioning due to improper siting, siltation, seepage, and high rates of evaporation from shallow sand reservoirs. These issues can be addressed through the development and implementation of better site-selection guidelines for new sand dams. This study aims to develop such guidelines through analysis of an integrated surface and subsurface flow model created using data gathered during a field study in Tanzania. The model analysis considers the effect of geomorphological factors such as channel width, land slope, and channel/riparian zone connectivity in addition to riparian zone vegetative cover and rainfall patterns. The impact of seasonal rainfall patterns on sand dam performance is also considered. The results of this study are a set of guidelines on selecting sites to construct a sand dam with high potential for capturing and storing water throughout the dry season. By utilizing such guidelines in the sand dam planning process, NGOs and community groups can maximize a sand dam's positive impact on local water security.

4.1 Introduction

Billions of dollars are invested into international development projects in Africa every year (Moyo, 2009), and yet 64% of donor-funded projects fail (Hekala, 2012). Recent project management studies have identified a wide range of reasons why international development projects in Africa have such a high failure rate (Ika, 2012). Commonly cited reasons are: geography, poor management, insufficient resources, unforeseen conflict, ineffective design, and corruption (Ika, 2012). Such issues are rarely easy to solve; some are nearly impossible to fix at the project level. However, at least one or two of the common traps in international development are relatively solvable: ineffective design and possibly geography. The primary issue regarding ineffective design as it relates to geography is that the selection of appropriate projects is often based on the donor's wishes rather than the demonstrated needs and wishes of the target country (Youker, 2003). Even more, the donors or funding agency not only select the project, but also decide the objectives of the project (Youker, 2003). Unsurprisingly, this leads to projects that are "for the donor" rather than for the local community (Ika, 2012) and are ill-suited to the local condition. Better site selection for international development projects could significantly reduce their chance of failure.

Unfortunately, water resources projects are not immune to high rates of failure. Only 50-66% of evaluated water supply and sanitation projects were considered satisfactory by the World Bank (McConville & Mihelcic, 2007). This failure rate is consistent with estimates for one water supply international development initiative in sub-Saharan Africa: the construction of sand dams (de Trincheria et al., 2015; Viducich, 2015). Sand dams are small concrete dams built across an ephemeral stream with an impermeable streambed in an arid or semi-arid region. Over time, sand builds up behind the dam wall, creating a sand reservoir. The sand reservoir fills with water during subsequent high-intensity rains and flash floods (Borst & de Haas, 2006; Hut et al., 2008). Rural communities draw water from the sand dam

for domestic and agricultural use. Because the water is stored underground, it is protected from evaporation, and communities are able to use the stored water well into the dry season.

Sand dams can be highly effective and have provided many communities with the means to thrive (*Sand Dams*, n.d.). However, 50% of sand dams are essentially non-functioning (de Trincheria et al., 2015; Viducich, 2015). Sand dams fail, due to poor siting, poor construction, and unexpectedly high water loss due to seepage and evapotranspiration (ET) from the sand reservoir. Of these issues, site selection and construction issues can be addressed, but this study will only focus on site selection. Site selection can be improved through implementation of better guidelines for selecting optimal sites where a sand dam can thrive. Current sand dam site selection guidelines are based on field experience, but there are obviously issues with this practice, as evidenced by the high failure rate. This study aims to create guidelines for siting new sand dams based on a fully integrated surface and groundwater flow model.

Previous studies have developed three sand dam models, but they have not been implemented towards the goal of improving siting. The three sand dam models developed have all used finite-difference methods to simulate groundwater hydrology at the same sand dam, Dam Kwa Ndunda in Kitui County, Kenya (Hoogmoed, 2007; Hut et al., 2008; Quilis et al., 2009). One of the three models was also applied to another nearby dam, Voi (Hut et al., 2008). Some work has been done to improve siting of sand dams, but it was inconclusive (Beswetherick et al., 2018). Beswetherick et al. (2018) examined various catchment characteristics of nine sand dams in Kenya and Zimbabwe in an attempt to find consistent relationships between watershed characteristics and sand dam success, but were unsuccessful. Other studies have looked at improving the functioning of sand dams, but they have focused more on the physical characteristics of the structures themselves, as in Viducich (2015).

The study presented here constructs a model of the Chididimo watershed, home to three cascading sand dams using the integrated surface flow and groundwater model,

Interconnected Channel and Pond Routing (ICPR). Four 6-month simulations are run: a control, with heightened cropland, with increased rainfall and reduced ET, and finally with sandier soils. Trends in local groundwater elevation and in surface and groundwater flow parameters are analyzed to determine which simulation produces the most beneficial conditions for sand dam success. The study concludes with a discussion of site characteristics that will likely support a successful sand dam.

4.1.1 Interconnected Channel and Pond Routing (ICPR)

ICPR connects 1D and/or 2D surface water flow with 2D groundwater flow using variable-resolution meshes that allow areas of interest to be simulated at a higher resolution than less critical parts of the study area, saving computational time and power. This capability is ideal for simulating sand dams, because, while a model of the entire watershed is simulated in ICPR, sand dams have a relatively small area of influence. The area of influence for a sand dam is at most 2 km^2 in the channel and riparian zone upstream of the dam structure (Ryan & Elsner, 2016) but is oftentimes much smaller (Quilis et al., 2009). Furthermore, as a sub-surface sand reservoir in an ephemeral stream, both surface and groundwater flows are vital for sand dams. Until now, ICPR has primarily been used for studies of urban flooding in the conterminous United States. The application of this modelling software to a rural, ungauged watershed with a semi-arid climate is unique. As a physics-based modeling system with options for specifying ET that varies according to crop types and growing seasons, rainfall, and a highly discretized vadose zone, ICPR is appropriate for rural and semi-arid applications. Published research on ICPR has largely been completed by Saksena et al. (2019) and Saksena, Dey, Merwade, and Singhofen (2020), where they studied the performance of difference ICPR model compositions and applied ICPR to an unprecedented flood event in Hurricane Harvey, respectively.

4.2 Study Area

Simulations of three cascading sand dams near Chididimo, a village 20 km west of Dodoma, were included in this study (see Fig. 4.1). The Chididimo sand dams were constructed by the Mennonite Central Committee of Tanzania. The most upstream sand dam, Umoja Ni Nguvu (hereafter, Umoja), was constructed in 2010 and is the smallest with a spillway of approximately 4.5 m. Next in the system is the Seje Seje dam, also constructed in 2010. The Seje Seje dam has a spillway width of 7.5 m and is the most productive of the three dams. Community members near the Seje Seje dam are still able to access water from the hand pump six months into the dry season. The most downstream dam in the system, the Chijendelele Na Mlimo (hereafter, Chijendelele) sand dam, was constructed in 2011 with a spillway width of 9.6 m.

The three sand dams are in the Chididimo watershed. The Chididimo watershed is 7.5 km^2 and is sparsely populated. The dominant land use in the watershed is shrub cover at 60% land cover, followed by cropland at 39% land cover (ESA CCI land cover). The Chididimo watershed has a hot semi-arid climate, receiving only 601 mm of rainfall during the year in one rainy season lasting from October to April (Luhunga and Djolov, 2017; Peet et al., 2007; Platts et al., 2015). The potential ET in Dodoma is 1800 mm, and the average annual temperature 23°C (Platts et al., 2015).

4.3 Data

Initially designed for applications in United States urban areas, where high resolution, high quality data is widely available, ICPR is data intensive. ICPR requires the following data: elevation, soil, land cover, bedrock depth, water table depth, ET, and rainfall. High resolution data is rarely freely available for sub-Saharan Africa, so the best data available was used to construct the model. Elevation data at a resolution of 30 m was obtained from the Shuttle Radar Tomography Mission (SRTM) (NASA JPL, 2013). Soil texture and drainage properties were obtained from the Harmonized

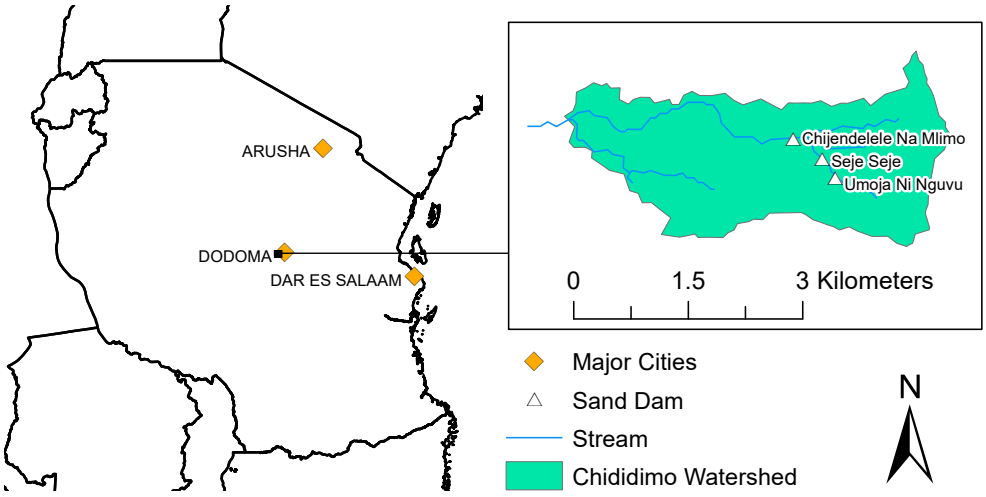

Figure 4.1. Chididimo watershed near Dodoma, Tanzania with three cascading sand dams.

World Soil Database (HWSD) (Fischer et al., 2008). Elevation and land use data together inform the 1D/2D surface water model. The depth of the water table below the ground surface was obtained from the British Geological Survey (BGS) (MacDonald, Bonsor, Dochartaigh, & Taylor, 2012). Finally, the depth of bedrock below the ground surface was obtained from research conducted by the Land-Atmosphere Interaction Research Group (L-AIRG) at Sun Yat-Sen University (Shangguan, Hengl, Mendes de Jesus, Yuan, & Dai, 2017). The soil data, water table elevation, and bedrock elevation data were used to design the 2D groundwater portion of the model. As forcing data for the model, 3 hourly, 1.0° resolution ET and rainfall data from the Global Land Data Assimilation System (GLDAS) was used (Beaudoing & Rodell, 2016; Rodell et al., 2004) While 1.0° resolution forcing data is course relative to the study site, the event patterns and magnitude are consistent with what is expected.

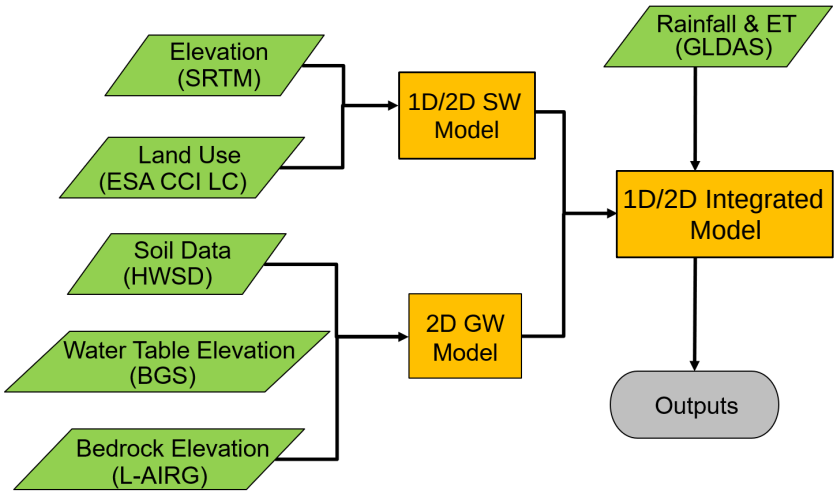

Figure 4.2. ICPR model process with input data specified (adapted from Saksena et al., (2019))

4.4 ICPR Model Description

An overview of the ICPR model framework is presented here. See Saksena et al. (2019) and Saksena et al. (2020) for a detailed model description and related equations and capabilities. An ICPR model consists of overland flow elements and saturated groundwater elements that are connected by flow through the vadose zone (Saksena et al., 2019).

4.4.1 Overland flow region

The structure of the overland flow region determines how the model routes surface flow and transfers excess rainfall to the vadose zone. Elements of the overland flow region are derived from the gridded DEM and gridded land cover (see Fig. 4.2), but can be manipulated and refined by the user to ensure that unique features and areas of particular interest are represented in the model.

Overland flow computational mesh generation

The basis of all flow routing in ICPR is the flexible mesh that defines individual control volumes and linkages between the control volumes. The flexible mesh is unique, because it allows the user to specify variable resolution of model calculations based on the objectives of the model. For example, in this study, high-resolution mesh is described in the areas near sand dams but low-resolution mesh is maintained elsewhere, reserving computational power for the most important model features. To define the resolution of the mesh, the user places a pattern of breakpoints throughout the overland flow region. Using the Delaunay method of triangulation, ICPR then automatically generates a flexible triangular mesh where each breakpoint is a triangle vertex, as seen in Fig. 4.3a (Streamline Technologies, 2018). Flow directions are then assigned to each edge of the triangular mesh based on DEM-derived land slopes.

The triangular mesh is the foundational mesh of the overland flow region. Once the triangular mesh has been generated, the honeycomb mesh is generated. Each vertex of the triangular mesh serves as the center of a honeycomb polygon. The vertices of the honeycomb polygon are then the centroids and midpoints of the adjacent triangles in the triangular mesh, as represented in Fig. 4.3b. The honeycomb mesh is intersected with the soil, land cover, rainfall, and ET zones, further refining the mesh where a honeycomb polygon crosses different zones. The honeycomb polygons serve as the control volumes, or catchments, of the ICPR calculations. ICPR calculates a mass balance for each honeycomb catchment polygon to determine the amount of excess rainfall, after accounting for losses due to infiltration and ET. Excess rainfall results in ponded surface water that first satisfies potential ET, and then may flow to an adjacent surface node along the triangular mesh or be infiltrated to the vadose zone.

The last mesh ICPR generates for the overland flow region is the diamond mesh. The diamond mesh is created along the edge of each triangle with the centroids of the two adjacent triangles serving as the remaining two vertices (see Fig. 4.3c). The diamonds in the diamond mesh serve as the links between each catchment polygon,

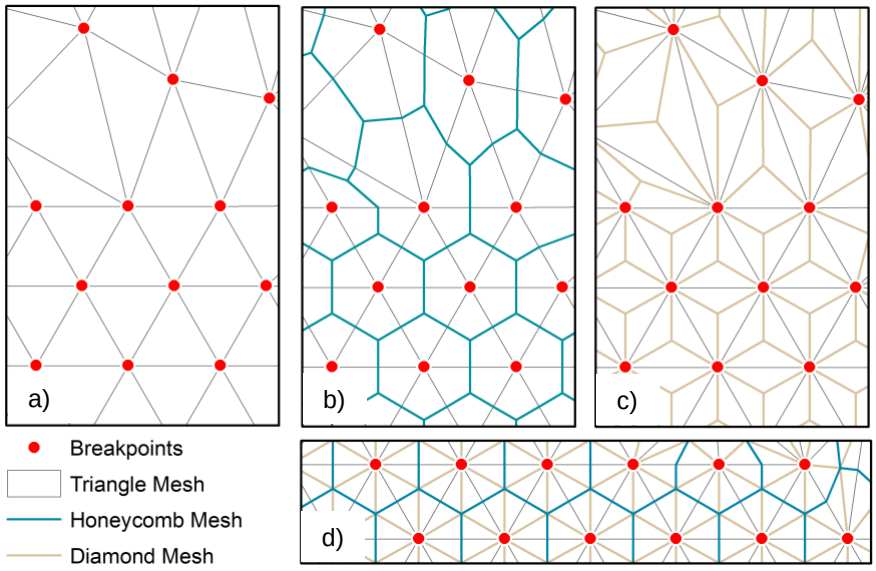

Figure 4.3. (a) Triangular mesh. Note the variability in breakpoint spacing; (b) Triangular mesh with honeycomb mesh overlain; (c) Triangular mesh with diamond mesh overlain; (d) All three overland flow meshes.

transferring flow from one catchment to the next. The diamond mesh is intersected with, and further refined by, surface roughness zones.

Overland flow calculations

Surface flow calculations are performed via the finite volume method for each catchment, and the transfer of flow from one catchment to the next is defined by the St. Venant, or momentum, equations (Streamline Technologies, 2018). The momentum equation employed by ICPR is:

$$\frac{\partial Q}{\partial t} + \frac{\partial (Q^2/A)}{\partial x} + gA\frac{\partial Z}{\partial x} + gAS_f = 0, \tag{4.1}$$

where Q is the flow rate during time, t, over surface area, A, x is the flow distance, S_f is the energy slope, and g is acceleration due to gravity.

Roughness zones. Roughness zones define Manning's n value for different land cover types. ICPR further delineates this variable Manning's n value into shallow and deep conditions, where Manning's n is decreased when water is ponded on the land surface. Manning's n decays exponentially from the shallow Manning's n to the deep Manning's n based on the surface depth, as explained in the following equation:

$$n_d = n_{shallow} \exp\left[\ln\left(\frac{n_{deep}}{n_{shallow}}\right)\frac{d}{d_{max}}\right], \tag{4.2}$$

where n_d is Manning's roughness at flow depth, d, $n_{shallow}$ is Manning's n at the ground surface, n_{deep} is Manning's n at depth d_{max}, and d_{max} is the user specified depth at which n_{deep} occurs, usually 1 m (Streamline Technologies, 2018).

4.4.2 Vadose zone

The vadose zone is the unsaturated zone in the soil column between the ground surface and the water table. As the water table falls and rises, it exposes more or less of the vadose zone. ICPR has three options for soil moisture accounting and tracking vadose zone water movement/rainfall excess computations: (1) an unrefined Green-Ampt method that has homogeneous soil with root zone and transmission zone layers for use in shallow water table conditions, (2) a refined Green-Ampt method that has homogeneous soil with user-defined layers for use in deep water table conditions, and (3) a vertical layers method that allows the user to specify the properties of variable soil layers. The vadose zone interacts with the groundwater region via recharge from the last soil layer (Streamline Technologies, 2018).

Vadose zone polygon soil cylinders are created by intersecting overland flow and groundwater honeycomb meshes along with soil and land cover grids. Rainfall excess from the surface honeycomb is transferred to the soil cylinder, and groundwater recharge from the soil cylinder is transferred to the associated groundwater honeycomb. The transfer of water from one layer to the next occurs at the rate of saturated hydraulic conductivity, as defined by the Brooks-Corey soil water retention-hydraulic conductivity relationship (Rawls et al., 1982; Rawls & Brakensiek, 1982):

$$\frac{K(\theta)}{K_s} = \left(\frac{\theta - \theta_r}{\phi - \theta_r}\right)^{\left(3+\frac{2}{\lambda}\right)}, \tag{4.3}$$

where K is the unsaturated vertical conductivity at the current moisture content, θ, K_s is the saturated vertical conductivity, θ_r is the residual moisture content, ϕ is the saturated moisture content, and λ is the pore size index. The recharge rate delivered to the groundwater is the area-weighted sum of the unsaturated hydraulic conductivity for all soil cylinders in a single groundwater honeycomb polygon, accounting for the available fillable porosity (Streamline Technologies, 2018).

When the vadose zone is discretized into multiple layers with multiple cells, as with the refined Green-Ampt and vertical layers methods, fluxes between cells are calculated based on the moisture content and unsaturated vertical conductivity of each cell. The groundwater recharge rate is equal to the calculated flux across the cell just above the saturated water table. As the water table rises and falls, cells in the vadose zone are merged and unmerged with the water table. If the groundwater table inundates 75% of a cell, that cell is merged with the saturated groundwater surface. As the water table falls, cells are unmerged from the saturated groundwater surface when more than 25% of the cell is exposed and again become part of the vadose zone (Streamline Technologies, 2018).

Infiltration and ET. Rainfall and ponded water in excess of potential ET are available for infiltration from the overland flow region to the vadose zone. The infiltration rate is determined from the Green-Ampt equation and cannot exceed the saturated vertical conductivity. While calculating infiltration, ICPR conducts two passes over each cell. The first pass transfers water from the surface down to the last cell above the saturated groundwater level, calculating mass balances at each cell. The flux through the last cell is added to the groundwater surface. The second pass rebalances the moisture content of each cell to ensure that the saturation level is not exceeded. Water in excess of saturation is transferred upward through the soil

cylinder, until no cells have water in excess of saturation or until the excess water reaches the overland flow surface (Saksena et al., 2019).

Potential ET in ICPR is calculated from reference ET, which is either supplied to ICPR directly by the user or calculated using the Penman-Montieth equation. The potential ET is modified by crop coefficients unique to crop-types, soil-types, and time of year (Allen, Pereira, Raes, Smith, et al., 1998; Saksena et al., 2019). When rainfall and ponded water are insufficient to meet the potential ET, the deficit is extracted from the soil moisture in the polygon soil cylinders above the root depth.

4.4.3 Saturated groundwater region

The groundwater region consists of a saturated surficial aquifer underlain by a confining layer. If the user wishes, leakage through the confining layer can be defined. The groundwater region is connected to the vadose zone by recharge from the last active cell of the associated soil cylinder.

The groundwater region in ICPR uses a flexible triangular mesh as the computational framework, like that used in the overland flow region. However, unlike in the overland flow region, the groundwater triangular mesh has vertices at the midpoints of the triangle sides, and these additional vertices also serve as centers of the associated honeycomb mesh. The groundwater triangular mesh is refined by soil zones to determine the average weighted porosity and conductivity for each triangle. Nodes in the triangular mesh are assigned elevation values for the ground surface, confining layer, initial water table. The groundwater honeycomb mesh can be refined with leakage zones when leakage through the confining layer is allowed (Streamline Technologies, 2018).

The groundwater region calculates saturated horizontal flow in the surficial aquifer above the confining layer. Water table elevations are calculated at the triangle vertices and midpoint nodes. Calculations for horizontal flow are based on finite element anal-

ysis and use the Martínez (1989) approach to solve the continuity equation (Saksena et al., 2019; Streamline Technologies, 2018).

4.4.4 Time-marching scheme

ICPR contains two options for defining the time marching of simulations: the Successive Approximation technique with Over-Relaxation (SAOR) method and the "FIREBALL" method. The SAOR method is commonly used in water resources applications and allows time steps that vary in time but are uniform spatially. This can result in long runtimes due to small mesh elements (Saksena et al., 2020). This study employs the unique FIREBALL method that allows time marching to be variable in both space and time. In the FIREBALL application used here, groundwater calculations are at 1 hour time steps (3,600 s), hydrologic time steps are 5 minutes (300 s), and the surface hydraulics calculations are performed at 10 times steps varying between 0.01 to 5.121 s (Saksena et al., 2020; Streamline Technologies, 2018).

4.5 Methodology

4.5.1 Sand-dam specific assumptions

The three sand dams in the Chididimo watershed were modeled using the integrated 1D/2D surface and groundwater model, ICPR. Pre-construction survey information is not available for the sand dams, requiring many assumptions to be made about the sand dam subsurface. The primary assumptions defining the representation of sand dams in the model are:

1. The length of each sand reservoir upstream of a sand dam can be determined through site knowledge coupled with visual analysis of aerial imagery. The terminus of a sand reservoir can be identified in aerial imagery by the re-surfacing of bedrock and/or the narrowing of the visible stream bed.

2. The depth of each sand reservoir is assumed to be a maximum of two meters above the SRTM land surface plus one meter below the SRTM land surface.

3. The surface slope of the upstream sand reservoir is assumed to be uniform, at a rate of two meters divided by the length of the sand reservoir.

4. The sand reservoir is underlain by a nearly impervious layer, adequately represented by a 2-meter thick clay layer.

5. The sand dam structure blocks most subsurface flow within the stream valley at the location of the sand dam. The sand dam structure allows some throughflow as seepage, represented by a hydraulic conductivity value of 0.05 m/day, a value equivalent to that of the clay layer underlying the sand reservoir.

4.5.2 Building the Chididimo ICPR model

A description of the basic methodology for creating an ICPR model of the Chididimo watershed follows. The Chididimo model contains an overland flow region and a groundwater region (see Fig. 4.4). The overland flow region contains 2D elements outside of the stream channels, 2D elements within the stream channels in the vicinity of the sand dams, and 1D elements elsewhere in the stream channels. The groundwater region contains only 2D flow elements, as is the case for all ICPR groundwater regions (see Fig. 4.4b).

Overland flow region

The overland flow region consists of a DEM-defined channel network and spatially varied land use and soil zones. The overland flow region also includes forcing parameters: rainfall and ET. The Chididimo watershed and stream network were defined from 30-m resolution DEM using hydrology geoprocessing tools. An up-catchment flow aggregation limit of 0.45 km^2 was used in stream delineation, because the sand dam streams were defined at this aggregation limit. The width of the streams was

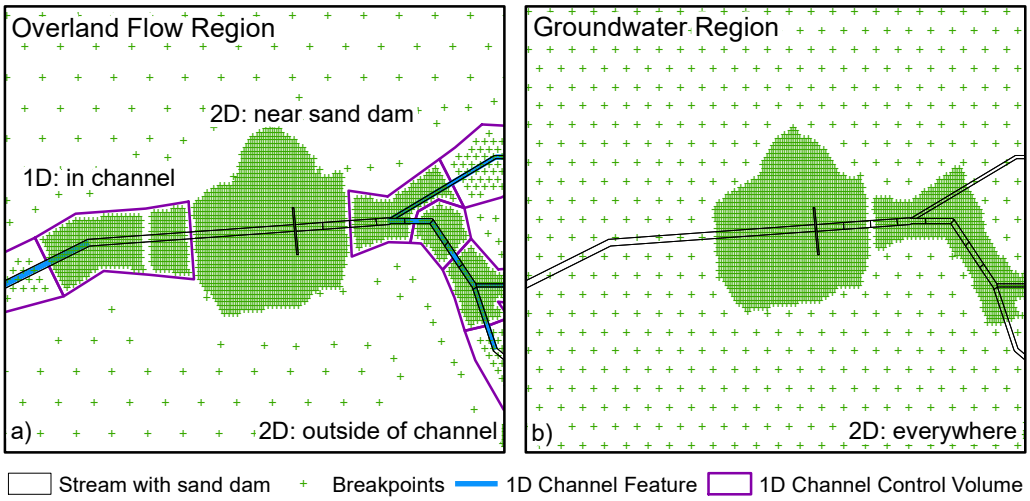

Figure 4.4. (a) Overland flow region and (b) groundwater region in ICPR near the Chijendelele sand dam. Note the high density of breakpoints near the sand dam.

determined by manual measurement of aerial imagery. Surface runoff is influenced by the roughness of the land surface through the application of Manning's n. Manning's n is set to 0.048 in the channels and 0.08 on the land surface (Chow, 1959; Liu, Merwade, & Jafarzadegan, 2019). A value of 0.08 for Manning's n on the land surface was calculated by an area-weighted average of the primary land cover types: shrubs and cropland (Liu et al., 2019; Saksena et al., 2019).

The rate of ET is modified by crop coefficients that vary with land cover. Crop coefficients can be set to account for the different water needs of crops in the overland flow region during the different phases of the growing season. Maize, millet, and sorghum are the most common crop in Dodoma (Msongaleli, Tumbo, Kihupi, & Rwehumbiza, 2017; Yohan, Oteng'i, & Lukorito, 2006), so therefore, all cropland was assigned crop coefficients that represented an average of the dominant three crop types. Crop coefficients were set to 1.00 for natural land cover. Crop coefficients for natural ecosystems have not been widely studied (Corbari, Ravazzani, Galvagno, Cremonese, & Mancini, 2017), so there is little evidence to support crop coefficients

other than 1.00. The crop coefficients and growing season can be seen in Table 4.1. While ICPR allows for gridded rainfall, the model incorporates uniform rainfall across the study area. The amount of rainfall that infiltrates into the ground is determined by the vertical layers method. The vertical layers method in ICPR uses the Green-Ampt infiltration parameters and equation but allows the user to define multiple soil horizons, as described below.

Table 4.1.
Crop coefficients and growing season in the Chididimo watershed

Crop	K_{ini} (time (d))	K_{mid} (time (d))	K_{end} (time (d))	Growing season begins	Root depth (m)
Sorghum	1.00 (55)	1.00-1.10 (45)	0.55 (30)	Dec./Jan.	1.5
Maize	1.00 (65)	1.20 (45)	0.35-0.60 (30)	Dec./Jan.	2.0
Millet	1.00 (50)	1.00-1.10 (55)	0.30 (35)	Dec./Jan.	2.0
ICPR	1.00 (55)	1.20 (45)	0.48 (30)	Dec. 1	2.0

The vadose zone in the Chididimo model was described by three soil types: sand, clay, and loam (see Table 4.2). The watershed beyond the streambanks was entirely represented by a thick layer of loam per HWSD (Fischer et al., 2008). Within the stream channel, the vadose zone is described by a 1-m thick layer of sand, underlain by 2 m of clay, and a thick layer of loam. The vadose zone within the sand reservoir upstream of the sand dam required a detailed representation to capture the varying depth of the sand reservoir (see Fig. 4.6 and Table 4.4).

Table 4.2.
ICPR vadose zone soil parameters

Parameter*	Sand	Clay	Loam
Saturated vertical conductivity (mm/h)	134.90	1.90	3.90
Moisture content at saturation	0.42	0.44	0.47
Residual moisture content	0.02	0.02	0.027
Initial moisture content	0.08	0.38	0.30
Moisture content at field capacity	0.08	0.38	0.30
Moisture content at wilting point	0.03	0.30	0.15
Pore size index	0.70	0.17	0.25
Soil matric potential (cm)	15.98	85.60	40.12

* Values taken from Rawls et al. (1982) and Rawls, Gimenez, and Grossman (1998).

Incorporation of sand dams in overland flow region and vadose zone The sand dams were simulated within the ICPR framework by building the sand dams into the DEM and by assigning the soil parameters in the vertical layers loss method to describe the physical structure of a sand dam. To build the sand dam into the DEM, the surface of each sand dam was assumed to be at most two meters above the SRTM land surface. Furthermore, the DEM was smoothed at a constant slope in the sand reservoir upstream of the sand dam for the length of the sand dam, as determined via aerial imagery (see Table 4.3). Figure 4.5 provides a profile view of the final smoothed DEM at the Seje Seje sand dam. Building the sand dam into the DEM ensured that the model would accurately account for flow over and through the sand dam and sand reservoir.

In addition to building the sand dams into the DEM, the vertical layers infiltration parameters were designed to account for the unique structure of sand dams (see Fig. 4.6). Each sand reservoir was split into eight segments, and different vertical layer

Table 4.3.
Length of the sand reservoir upstream of each sand dam

Sand Dam	Reservoir length (m)
Umoja	200
Seje Seje	200
Chijendelele	300

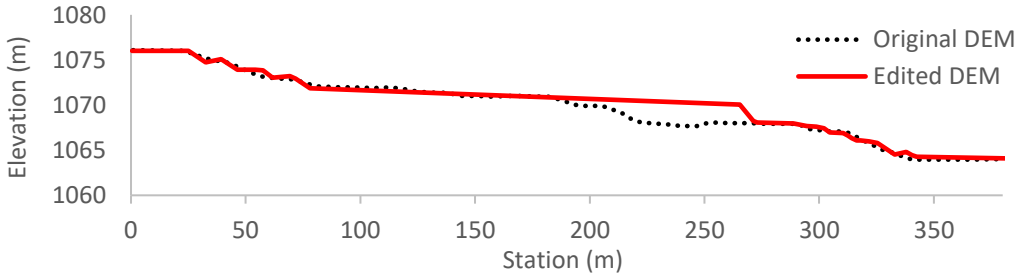

Figure 4.5. Original elevation profile down the centerline of the stream at the location of the Seje Seje sand dam from the SRTM DEM compared to the edited elevation profile with the sand dam and sand reservoir "built" into the DEM.

infiltration parameters were assigned to each segment to account for the gradually tapered sand reservoir depth (see Table 4.4).

Groundwater region

The groundwater region connects to the bottom of the vadose zone and, depending on the elevation of the water table, may merge with cells of the vadose zone. The overland flow and the groundwater regions are connected at mesh nodes by recharge from the overland flow region to the vadose zone and then to the groundwater region. The groundwater region also includes the depth of the bedrock beneath the land surface and an initial depth of the water table below the land surface. To determine

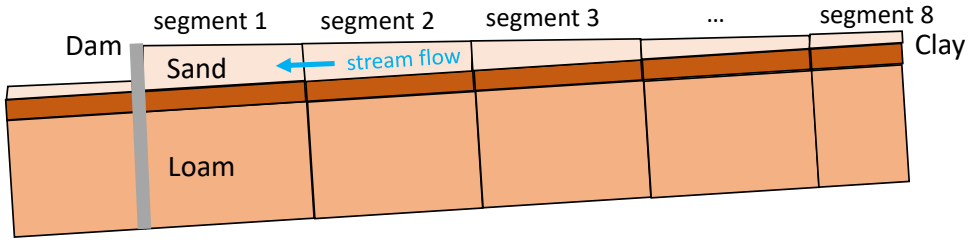

Figure 4.6. Representation of the vertical layers design for sand dams. The sand reservoir upstream of the dam structure was represented by sand underlain by a thick clay layer and loam, the primary soil type of the Chididimo watershed. The dam structures are represented by a deep, nearly impervious soil layer.

Table 4.4.
Sand dam design in the vadose zone

Section	Sand	Clay	Loam
	Layer thickness (m) | No. of cells		
segment 1	3 | 21	2 | 3	20 | 21
segment 2	2.75 | 18	2 | 3	20.25 | 21
segment 3	2.5 | 18	2 | 3	20.5 | 21
segment 4	2.25 | 15	2 | 3	20.75 | 21
segment 5	2 | 15	2 | 3	21 | 21
segment 6	1.75 | 12	2 | 3	21.25 | 21
segment 7	1.5 | 9	2 | 3	21.5 | 21
segment 8	1.25 | 9	2 | 3	21.75 | 21
stream	1 | 6	2 | 3	21.75 | 21

Note : See Fig. 4.6 for depiction of seg. 1 - 8.

the depth of the water table below the land surface, the BGS water table was set as the initial water table elevation, and a one-month simulation was performed. The water

table was assumed to be essentially at equilibrium after a one-month simulation with no rainfall. The water table elevation grid at the end of the simulation was exported, compared with the DEM, and set to a minimum of 1.5 m below the land surface. Enforcing a minimum depth to the water table ensures that there is not excessive seepage from the water table to the overland flow region given the semi-arid climate of the Chididimo watershed. The depth of the bedrock was then set to at least 30 m below the water table elevation. Finally, the fillable porosity and conductivities of the groundwater region were set to the porosity and vertical hydraulic conductivity, respectively, of the associated soil types, as described in Table 4.2.

4.5.3 Model Simulations

A total of four, six-month simulations were performed to identify the impact of different rainfall patterns, vegetation, and soils on the ability of sand dams to capture and store rainwater throughout the dry season. The rainfall, vegetation, and soils in southeastern Kenya were used for alternative scenarios. Southeastern Kenya is home to thousands of sand dams, many of which store water throughout the entire dry season. All simulations were performed using rainfall and ET data from 2/13/2017 to 8/13/2017. This six-month time period was chosen, because it provides a one-month spin up period and one month of heavy rainfall before the dry season begins. The middle of August was selected as the end of the simulation time, because the Dodoma sand dams have usually lost their abstractable water by then (Chijendelele Na Mlimo Group, personal communication, November 14, 2016; Vumilia Group, personal communication, November 15, 2016).

The model was not calibrated prior to performing simulations. The Chididimo watershed is ungauged, and physically-based ICPR has been shown to perform well with minimal calibration in various watersheds (Saksena et al., 2019, 2020), albeit not yet in an arid or semi-arid watershed. Short test simulations were performed to

verify surface and groundwater flow patterns in and around the sand dam reservoirs match literature and experience-based expectations.

Simulation 1 (S1) – The base case

The first simulation (S1) is the base case for comparison with the other three simulations. S1 utilizes Dodoma rainfall and ET and the actual soil texture and land cover in the Chididimo watershed.

Simulation 2 (S2) – Heavily cultivated

The second simulation (S2) maintains Dodoma rainfall and ET as the forcing data and uses the Chididimo watershed soil texture. However, the land cover types have been replaced with those representative of southeastern Kenya (see Fig. 4.7). Southeastern Kenya is much more heavily cultivated than the Chididimo watershed. The sample of land cover from southeastern Kenya is 94% cropland compared to Chididimo watershed's 39% cropland, as seen in Fig. 4.7. However, both the Dodoma region and southeastern Kenya have maize, millet, and sorghum as their primary crops, so the same crop coefficients are used in both S1 and S2. Only the area where the crop coefficients are applied has been changed for S2 compared to S1. S2 was performed to determine the magnitude of impact that land cover has on the performance of sand dams.

Simulation 3 (S3) – Different rainfall pattern

The third simulation (S3) maintains the Chididimo soil textures and land cover, while using southeastern Kenya rainfall and ET as forcing data. Southeastern Kenya, where most sand dams have been built experiences a bi-modal rainfall regime that provides approximately 100 mm more annual rainfall than the unimodal rainfall in Dodoma. In addition, annual potential ET is lower in southeastern Kenya compared

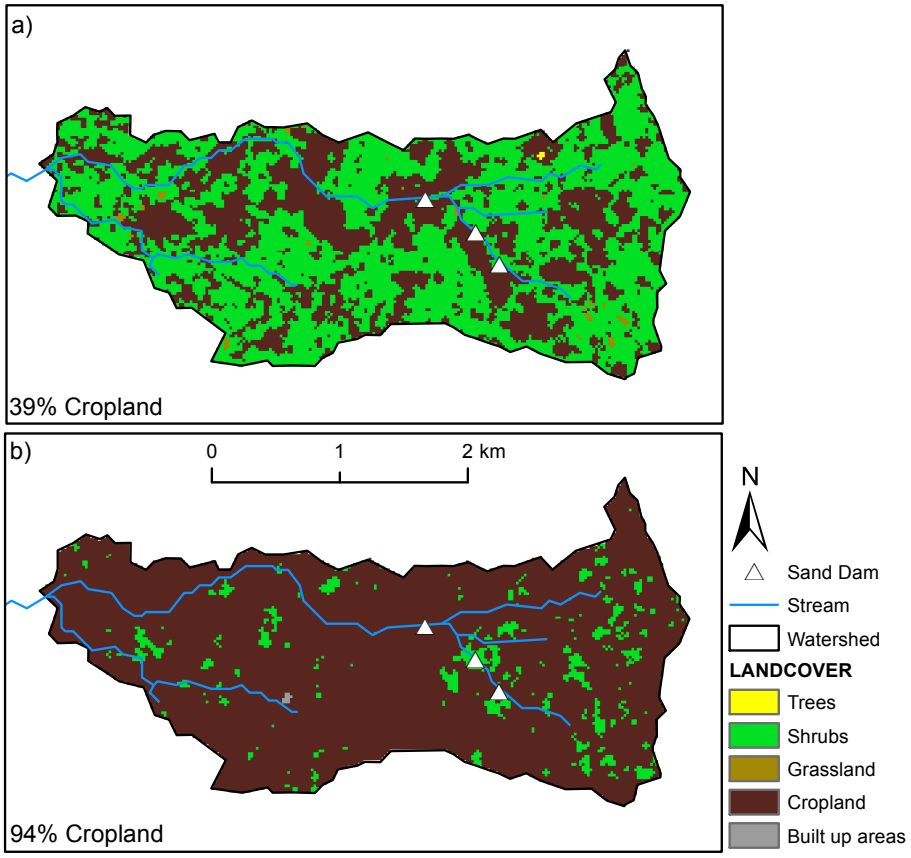

Figure 4.7. (a) Land cover for the Chididimo watershed that is used in S1; (b) Land cover pattern from southeastern Kenya that is used in S2.

to Dodoma. During the six-month study duration, Kenya's rainy season not only provides 58 mm more rainfall, but the rainy season lasts about three weeks longer than in Dodoma (see Fig. 4.8). In addition, Fig. 4.8 shows that the Kenya rainfall pattern tends to provide larger, more infrequent rain events compared to frequent, smaller magnitude rain events in Dodoma. S3 was performed to determine the degree of impact that rainfall and ET patterns have on the performance of sand dams.

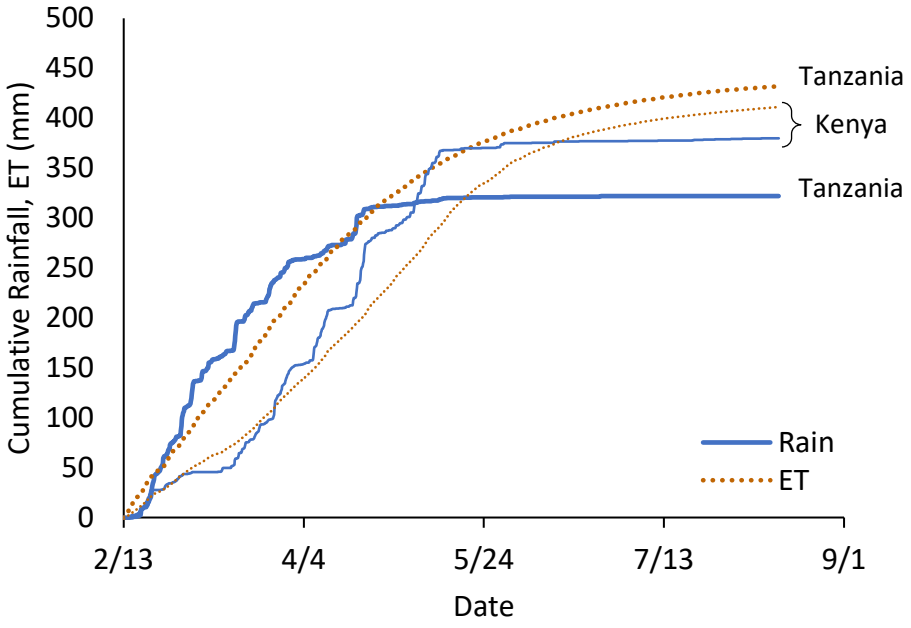

Figure 4.8. Kenya receives more rainfall in two rainy seasons each year and experiences less ET throughout the year than Dodoma. For the study duration, Kenya receives an additional 58 mm of rainfall and experiences 21 mm less ET. Also, note that Kenya's rainy seasons ends about 3 weeks after the end of Tanzania's rainy season. Kenya's rainfall pattern involves high-volume rain events spaced out, whereas Dodoma is likely to have more frequent, smaller volume rain events.

Simulation 4 (S4) – Sandier soils

The fourth simulation utilized Dodoma rainfall and ET with land cover from the Chididimo watershed. However, S4 replaced Chididimo's loam soil with sandy clay loams, which have a higher sand content (see Table 4.5). The sandy clay loams allow greater connectivity between the sand dam and the stream margins. This has the effect of allowing more water to seep from the sand dam into the streambanks and riparian zone. Furthermore, the sandy clay loams have a higher conductivity and lower moisture content at saturation, or porosity (see Table 4.5), affecting the maximum

infiltration rate. S4 was performed to determine the extent to which watershed soil types may influence sand dam performance.

Table 4.5.
Comparison of soil types for S1 and S4

Parameter	S1 (Loam)	S4 (Sandy clay loam)
Saturated vertical conductivity (mm/h)	3.90	7.70
Moisture content at saturation	0.47	0.40
Residual moisture content	0.027	0.068
Initial moisture content	0.30	0.29
Moisture content at field capacity	0.30	0.31
Moisture content at wilting point	0.15	0.20
Pore size index	0.25	0.32
Soil matric potential (cm)	40.12	59.41
Sand (%)	31	66
Clay (%)	24	27

4.5.4 Site selection criteria

The difference between S1 and S2-S4 overland flow and groundwater parameters will be examined to determine which simulation arrangement produces preferable conditions for sand dam performance. The performance of sand dams will primarily be assessed based on the following four parameters:

1. High recharge: A high performing sand dam will help raise the local groundwater table, as indicated by the transfer of water from the vadose zone to the surficial aquifer.

2. Low ET: A high performing sand dam will store water long into the dry season. To do so, the actual amount of water lost to ET should be minimized.

3. High vadose zone storage: Minimizing ET and maximizing recharge will be achieved through high levels of vadose zone storage. When the vadose zone has a high moisture content, the infiltration rate will be reduced. However, ET will occur from the existing water in the vadose zone before suctioning water from the surficial aquifer to the vadose zone to then be lost to ET. Further, recharge occurs from the vadose zone. Therefore, high vadose zone storage will result in more recharge flowing to the surficial aquifer. Vadose zone storage essentially protects groundwater from ET while also increasing the rate of recharge to the groundwater.

4. High rainfall excess: Most sand dams are filled by flash floods. High levels of rainfall excess will result in more surficial ponding and inundation that can fill a sand dam. For each honeycomb polygon at each time step, ICPR calculates rainfall excess as:

$$\sum Q_{excess} = Rainfall + Irrigation - Infiltration - ET, \qquad (4.4)$$

Therefore, if infiltration and ET are greater than the rainfall for the time step, the rainfall excess amount will be negative. As shown in Fig. 4.8, the ET rate is generally greater than the rainfall rate in both Tanzania and Kenya. Therefore, negative rainfall excess values are expected. Note that the irrigation value for this model is zero.

Some consideration will also be given to lateral seepage. Lateral seepage represents a loss of stored water from the surficial aquifer. A highly performing sand dam will exhibit low levels of seepage.

4.6 Results and Discussion

4.6.1 Insights from the base case

The base case, S1, provides a starting point for exploring how overland flow parameters influence water capture and storage in sand dams. Here, the modelled Chididimo watershed simulates reality as closely as possible, given data and model framework limitations.

Over the course of the study, the Chididimo watershed loses almost 300 mm of water to ET, vadose zone water is added to the groundwater via recharge, contributing to significant drying of the vadose zone, and infiltration and ET rates consistently outpace rainfall rates, resulting in negative rainfall excess (see Fig. 4.9). The rainfall rate and available vadose zone water are sufficient to meet and exceed potential ET in the watershed. The actual rate of ET is slightly higher than the potential ET, due to the transpiration of maize, sorghum, and millet cultivated on the Chididimo watershed cropland. Water that remains in the vadose zone after ET requirements are met, is percolated to the groundwater as recharge at a rate based on the moisture content, suction head, and depth of the vadose zone (Saksena et al., 2019; Streamline Technologies, 2018). As expected, vadose zone storage steadily declines during the end of the rainy season and throughout the dry season (see Fig. 4.9). Further simulations identify overland flow features relative to this base case that are likely to either improve or reduce the performance of sand dams in the Chididimo watershed.

Impact of stream characteristics

Stream characteristics, such as sinuosity and width seem to have little impact on the ability of a sand dam to capture and store water in the Chididimo watershed (see Fig. 4.10). The Chijendelele sand dam is on the most sinuous and widest stretch of stream. Conversely, the Seje Seje and Umoja sand dams are in nearly straight, relatively narrow reaches. The Seje Seje sand dam has the largest area of impact on

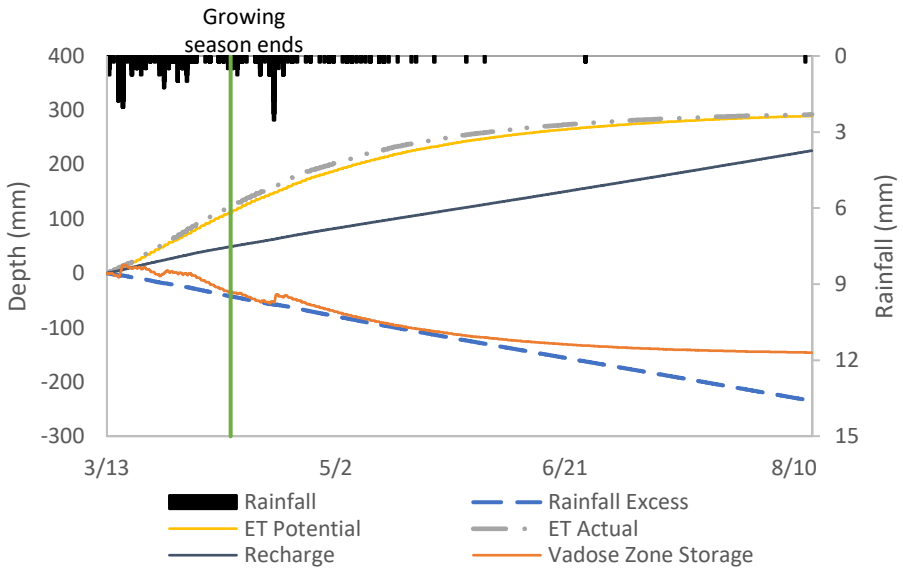

Figure 4.9. Cumulative overland flow quantities for the Chididimo watershed during S1, the base case.

the groundwater table, and the Umoja sand dam has the smallest area of impact. However, the impact area discrepancy is only 1,650 m^2 between the sand dams. Despite differences in sinuosity, stream width, and area of maximum groundwater table impact, all three modelled sand dams produce similar changes to local groundwater elevation, as seen in Fig. 4.10.

While stream characteristics do not significantly impact local groundwater elevations in the Chididimo watershed, a few caveats must be noted. As mentioned in Section 4.5.1, all three sand dams were modelled with a maximum sand reservoir depth of 3 m. A lack of pre-construction information necessitated this assumption; however, it is unlikely that all three sand dams have the same sand reservoir depth. The Chijendelele sand dam is in a steeper stream valley than found at Seje Seje and Umoja. This likely means that the channel at Chijendelele is deeper, and therefore would result in development of a deeper sand reservoir than at Seje Seje and Umoja. Furthermore, while the 120° bend in the middle of the Chijendelele sand dam does not negatively impact water storage, the bend may contribute to increased erosion and

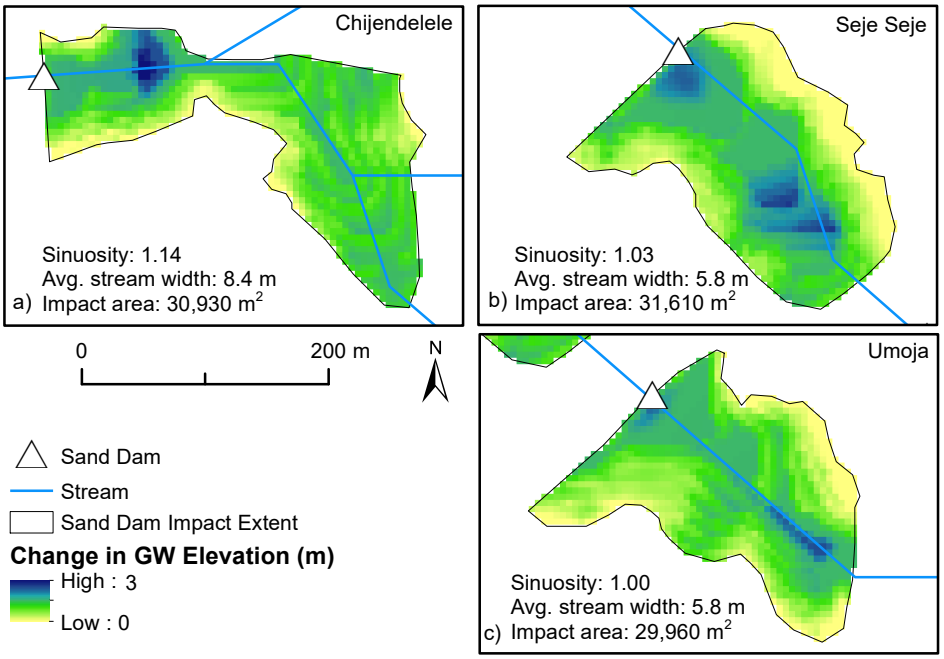

Figure 4.10. The change in GW elevation at the end of the dry season over the maximum area of groundwater table impact at the a) Chijendelele, b) Seje Seje, and c) Umoja sand dams.

deposition in the sand reservoir. Sand dams in meandering reaches are susceptible to increased channel instability that may threaten the longevity of the sand dam (Shen, Schumm, & Doehring, 1979).

Lastly, the impact of stream width on sand dam performance depends heavily on the connectivity between the sand dam and stream margins. If there is low connectivity between the sand dam and stream margins, the storage capacity and sand dam area of impact would be limited to the sand reservoir developed within the stream channel itself. Lateral seepage from the sand dam to the banks and recharge from the sand dam to the groundwater would be negligible. Conversely, a well-connected sand dam and riparian zone will allow two-way lateral seepage between the sand dam and the streambanks and will permit the water stored in the sand dam to recharge

the groundwater. Stream width minimally impacts sand dam storage in a sand dam that is well-connected to the stream margins.

Impact of land slope

Areas prone to surface ponding are likely good locations to build a sand dam, because most sand dam reservoirs are filled by flash floods (Hut et al., 2008). The 25% depth exceedance grid constructed from S1 shows areas within the Chididimo watershed susceptible to surface ponding (see Fig. 4.11). A similar land elevation pattern is seen around most of the areas with ponded water, that of a small u-shaped valley: a low area surrounded on three sides by relatively steep slopes, as in Fig. 4.11b. This geomorphology collects and directs overland flow to one centrally located low spot on the land surface, resulting in localized inundation during the rainy season. There would likely be ample water available to fill a sand dam reservoir several times during the rainy season were a sand dam constructed in or just downstream of such a landscape.

If, however, the stream typically carries a high suspended load of silt and/or clay, construction of a sand dam in an area prone to flooding should be reconsidered. Frequent floodwater with suspended silt and clay behind an immature sand dam may produce a sand reservoir with multiple low conductivity layers interspersed (Hut et al., 2008; Nissen-Petersen, 2006). These low conductivity layers create a capillary barrier, reducing both the infiltration rate and storage capacity of the sand dam. A capillary barrier also makes abstracting water from the sand dam more difficult. A sand dam built in a small u-shaped valley reach that does not typically carry a high suspended load of silt and clay would likely collect and store water.

4.6.2 Impact of land cover on sand dam performance

Increasing the cropland cover in the Chididimo watershed results in significant changes for all overland flow and groundwater region quantities considered. Fig. 4.12

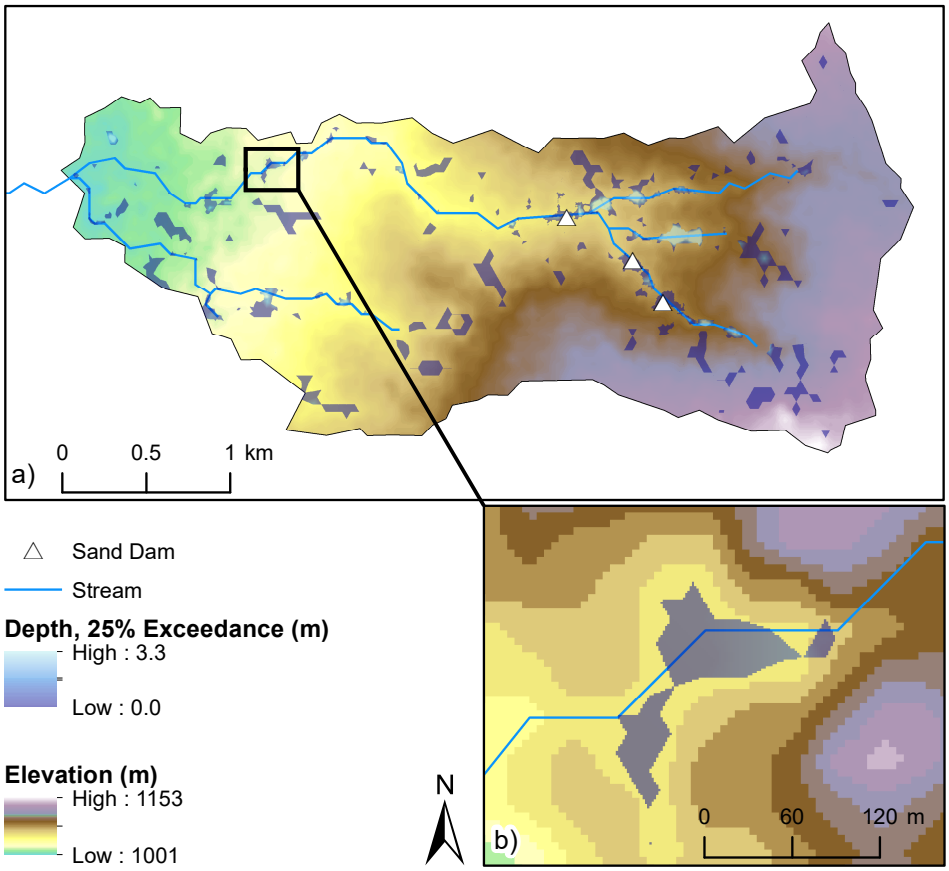

Figure 4.11. a) Areas of the Chididimo watershed that have ponded water for more than 25% of the simulation duration; b) Focused view of typical ponded water. Note that here, the elevation colormap has been set to a viewable range.

provides an overview of which simulation produces overland flow parameter values that are beneficial to sand dam performance. Specifically, Fig. 4.12 depicts the difference between S1 and S2 results for various parameters. Based on the commentary in Section 4.5.4, the line is above $y = 0$ if the S1 result is more beneficial for sand dams than the S2 result. Fig. 4.13 provides a similar depiction for groundwater parameters.

Interestingly, during the growing season, the high cultivation simulation, S2, provides a greater increase in vadose zone storage than the base simulation, S1, but this trend begins to reverse after the growing season ends (see Fig. 4.12). Within a few

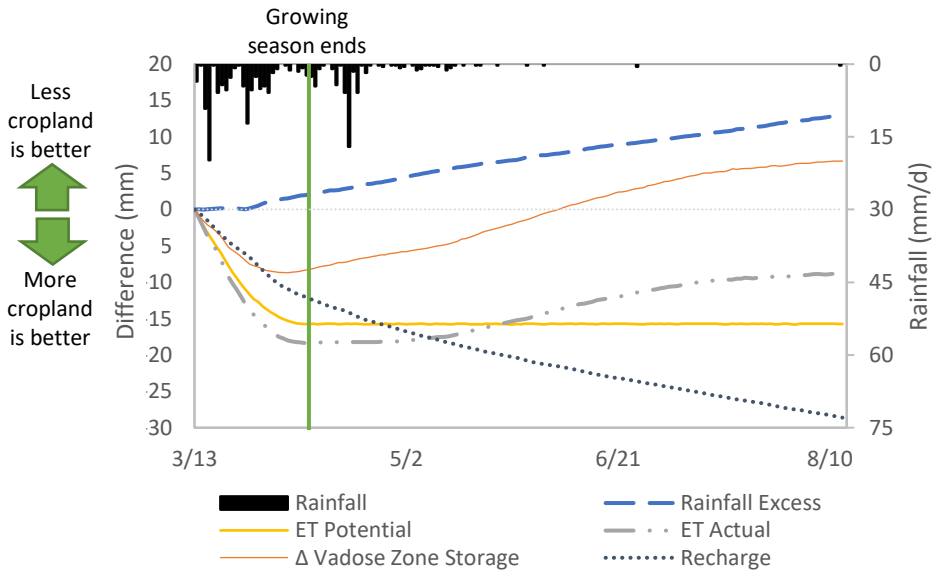

Figure 4.12. Comparative trends in aggregate overland flow quantities for the Chididimo watershed after increasing cropland. A quantity above the $y = 0$ line indicates that S1 (less cropland) produced values more beneficial to water storage in sand dams than S2. The converse also applies with quantities below the $y = 0$ line indicating S2 is more beneficial.

weeks after the end of the rainy season, more water is stored in the vadose zone in S1 compared with S2. Despite these differences in vadose zone storage, S1 consistently provides more excess rainfall to satisfy potential ET and infiltration compared with S2. It follows then, that S1 results in greater potential and actual ET than S2, which is seen in Fig. 4.12. Lower ET is desirable for a sustainable sand dam, and therefore Fig. 4.12 shows the potential and actual ET lines in the "more cropland is better" portion of the plot. Overall, higher rates of cultivation are better for sand dam success for ET and rainy season vadose zone storage. Conversely, lower rates of cultivation are better for sand dam success when examining rainfall excess and dry season vadose zone storage.

In S1, land cover is dominated by natural vegetation, which is simulated with a constant crop coefficient of 1.00 (see Table 4.1). Conversely, most of the land cover in S2 is cropland, which has a 55-day period of increased ET followed by a 30-day period

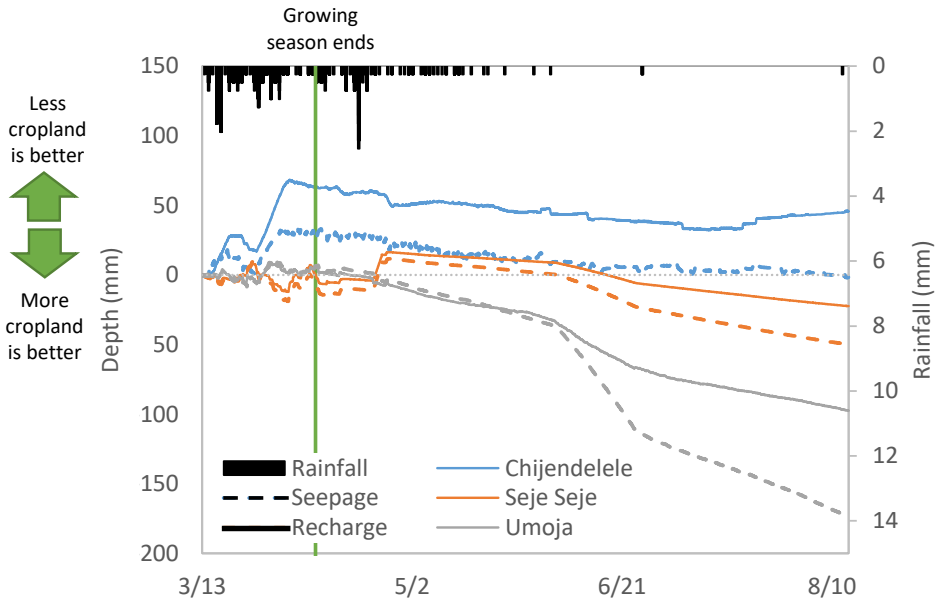

Figure 4.13. Comparative trends in groundwater flow parameters for each of the three sand dams after increasing cropland. Like Fig. 4.12, quantities above the $y = 0$ line indicate S1 is better for sand dams and vice versa.

of reduced ET before the growing season ends on 4/9 (see Table 4.1). The vadose zone is drier in S2 at the start of the study period, because its large area of cropland experiences increased ET during the simulation spin up. The drier S2 vadose zone can then infiltrate more rainfall, resulting in a greater increase in vadose zone storage and less rainfall excess than occurs in S1. Furthermore, S2's larger area of reduced ET during the end of the growing season results in more water retained by the vadose zone. Due to variable ET during the growing season, S2 is more beneficial for vadose zone storage than S1 during the rainy season. However, this trend reverses at the end of the growing season, when all landcover has the same crop coefficient of 1.00.

Actual ET and vadose zone storage are linked. Actual ET results from potential ET that is limited by rainfall excess and vadose zone moisture content. ET in S1 is initially higher than S2, because higher rainfall excess increases the water available for ET. However, as the rainy season ends and S2 has higher vadose zone storage,

the rate of actual ET in S2 increases. This increased ET begins to deplete S2 vadose zone storage faster than in S1. Thus, S1 has a greater positive change in vadose zone storage at the end of the simulation time than S2.

Recharge of the groundwater occurs as a direct result of percolation from vadose zone storage. S1 has less vadose zone storage, thus it is unsurprising that S1 also has less recharge than S2 overall (see Fig. 4.12 and 4.13). While this is true for the entire Chididimo watershed, the trend varies somewhat for the individual sand dams. S2 produces greater recharge at the Umoja sand dam for the entire study and at the Seje Seje sand dam until the end of the rainy season. The Chijendelele sand dam always has greater recharge in S1 compared with S2. Chijendelele likely does not follow the overall recharge trend, because it is immediately downstream of two confluences that are near locations of frequent inundation (see Fig. 4.11). The frequent local flooding likely contributes to greater vadose zone storage and thus greater recharge at the Chijendelele sand dam compared to the rest of the Chididimo watershed.

4.6.3 Impact of rainfall patterns on sand dam performance

Changing the rainfall volume and pattern and ET occurring in the Chididimo watershed significantly impacted most of the overland flow and groundwater parameters studied (see Figs. 4.14 and 4.15). However, the increased rainfall volume, higher frequency of large rainfall events, and lower ET in S3 did not significantly affect the amount of rainfall excess or recharge for the entire watershed (see Fig. 4.14). Also, recharge and seepage at the Chijendele sand dam were largely unaffected by the change in rainfall and ET (see Fig. 4.15).

S3 results in lower potential and actual ET during the rainy season when compared with S1, as is expected based on Fig. 4.8. However, the S1 potential and actual ET rates fall below the those of S3 when the S1 rainy season ends. This lasts for approximately one month before the S3 rainy season also ends (see Fig. 4.14). The extended rainy season in S3 results in higher S3 ET for a short period, but the

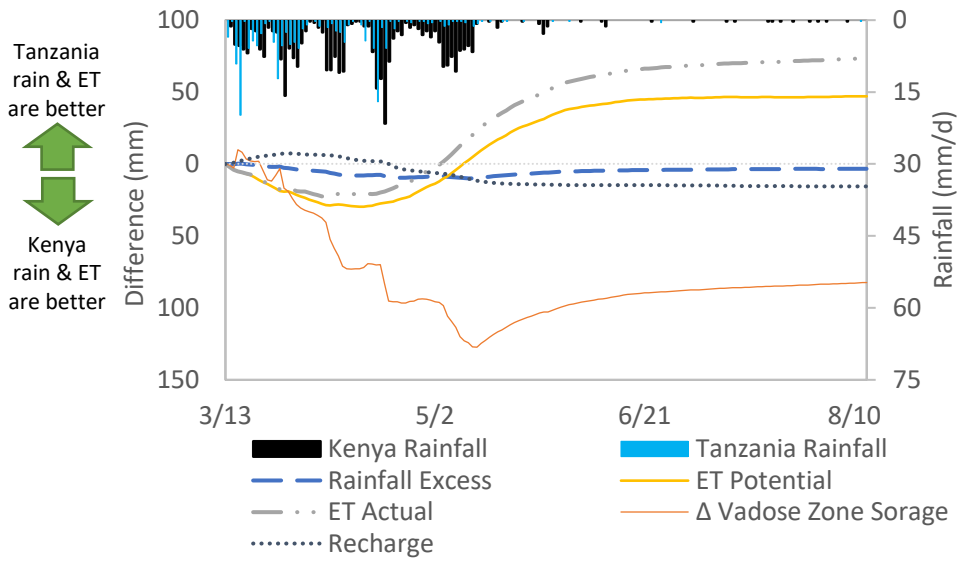

Figure 4.14. Comparative trends in aggregate overland flow quantities for the Chididimo watershed after changing the rainfall pattern and ET. A quantity above the $y = 0$ line indicates that S1 (Tanzania climate) produced values more beneficial to water storage in sand dams than S3 (Kenya climate). The converse also applies with quantities below the $y = 0$ line indicating S4 is more beneficial.

benefits of the additional rain and the shorter dry season that follows likely outweigh any potential negative impacts. For example, Fig. 4.14 shows that the vadose zone in S3 stores nearly 100 mm more water compared with S1 at the end of the rainy season. This additional vadose zone storage can be used to support vegetation or for groundwater recharge. Most of S3's increased rainfall immediately fulfills ET requirements or infiltrates into the vadose zone, as evidenced by the minimal difference between S1 and S3 rainfall excess and recharge. Vadose zone water is just as unlikely to recharge the groundwater in S3 compared with S1. While S3 results in greater vadose zone storage than S1, the additional water is not enough to saturate the vadose zone and drive increased groundwater recharge.

The difference in S1 and S3 recharge is minimal over the entire Chididimo watershed, but the trends in groundwater recharge vary somewhat at the three sand

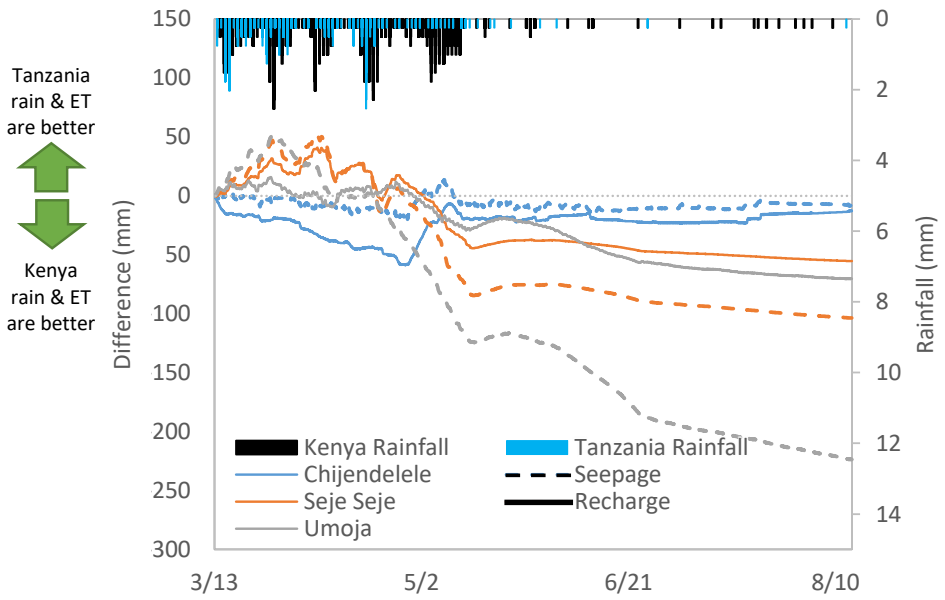

Figure 4.15. Comparative trends in groundwater flow parameters for each of the three sand dams after changing the rainfall pattern and ET. Like Fig. 4.14, quantities above the $y = 0$ line indicate S1 is better for sand dams and vice versa.

dams (see Fig. 4.15). While there is some difference in Chijendelele recharge and seepage during the rainy season for S1 and S3, this difference is minimized during the subsequent dry season. The additional rain that falls at Chijendelele in S3 is likely just rainfall excess that ends up as surface runoff. As mentioned previously, the Chijendelele sand dam is immediately downstream of two small confluences, which transport up-catchment excess rainfall to Chijendelele. Therefore, the maximum infiltration rate at Chijendelele is likely already met by S1-levels of rainfall. The Seje Seje and Umoja sand dams provide slightly more recharge than the Chijendelele sand dam during S3, indicating that the vadose zone storage at these sand dams are benefitting from the additional rainfall.

The most striking result of the S3 groundwater analysis is the significantly lower seepage at the Umoja sand dam compared with S1, especially after the end of the S1 rainy season (see Fig. 4.15). Analysis of S2 also indicated that the Umoja sand

dam has significantly less seepage than both Chijendelele and Seje Seje relative to S1 seepage rates (See Fig. 4.13). S2 produced 175 mm less lateral seepage compared to S1, while S3 produced about 225 mm less lateral seepage. It is also important to note that seepage at the Umoja sand dam generally occurs from the surficial aquifer to the overland flow system. Taken together, these trends indicate that groundwater elevation at the Umoja sand dam is highly responsive to changes in the overland flow region. The groundwater at Umoja is likely to release water to the surface due to topography that produces small surface reservoirs just upstream of the sand dam. These reservoirs capture and store surface runoff until it is lost via ET or to groundwater recharge. Lateral flow within the surficial aquifer from these reservoirs resurfaces at the Umoja sand dam in the form of seepage.

4.6.4 Impact of catchment soil texture on sand dam performance

Simulating the Chididimo watershed with sandier soils significantly impacted most of the overland flow and groundwater parameters studied (see Figs. 4.16 and 4.17). However, the sandier soils of S4 did not significantly affect the rate of potential ET or vadose zone storage (see Fig. 4.16). Also, seepage at the Chijendele sand dam was largely unaffected by the change in soils (see Fig. 4.17).

S4 results in less rainfall excess, and more groundwater recharge than S1. The rate of rainfall excess is greater in S1, because once the soil becomes saturated, infiltration occurs at the saturated vertical conductivity of the soil. The saturated vertical conductivity of S1 (3.90 mm/h) is less than that of S4 (7.70 mm/h), which means that not only is the minimum rate of infiltration higher in S4 but the rate of recharge from the vadose zone to the groundwater is higher. S4 infiltrates more rainwater than S1, and this infiltrated water percolates through the vadose zone to the groundwater as recharge. Some of this additional infiltrated water remains in the vadose zone as storage. More water is retained in the S4 vadose zone, because S4 has a higher residual moisture content than S1 (see Table 4.5).

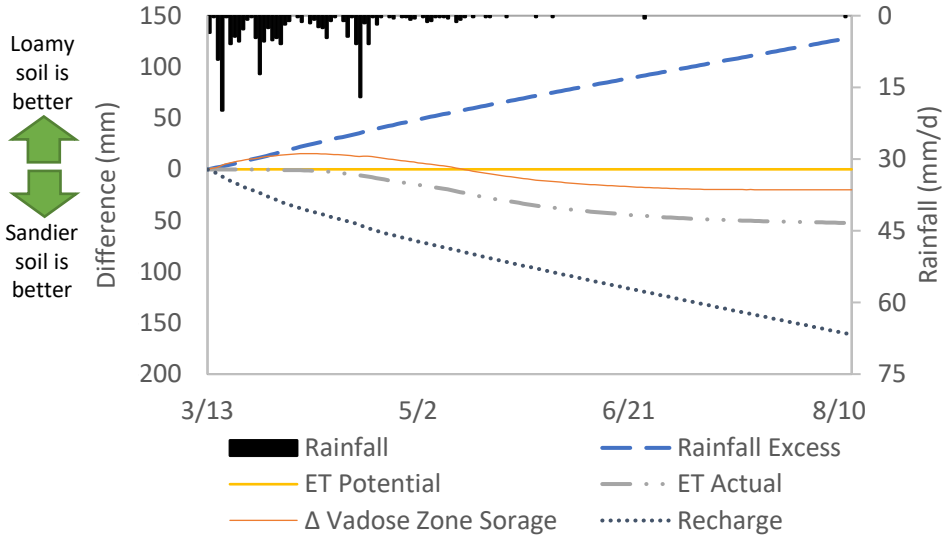

Figure 4.16. Comparative trends in aggregate overland flow quantities for the Chididimo watershed after increasing the sand fraction. A quantity above the $y = 0$ line indicates that S1 (loam) produced values more beneficial to water storage in sand dams than S4 (sandy clay loam). The converse also applies with quantities below the $y = 0$ line indicating S4 is more beneficial.

S4 has a lower rate of actual ET than S1, due to the differences in soil matric potential and the moisture content at wilting point. The soil matric potential of S4 (59.41 cm) is greater than that of S1 (40.12 cm). Soils with a higher matric potential hold onto water with greater force, making it harder for plants to remove the water during transpiration. In semi-arid regions where transpiration accounts for 85% of ET (Nagler et al., 2007), matric potential can greatly influence overall ET. The relative rates of ET are also influenced by the difference in plant available water between the two simulations. Plant available water is defined as water stored between the moisture contents at field capacity and at wilting point. The plant available water for S1 is 0.15 and is 0.11 for S4 (see Table 4.5). S1 has more plant available water, and therefore will lose more water to ET.

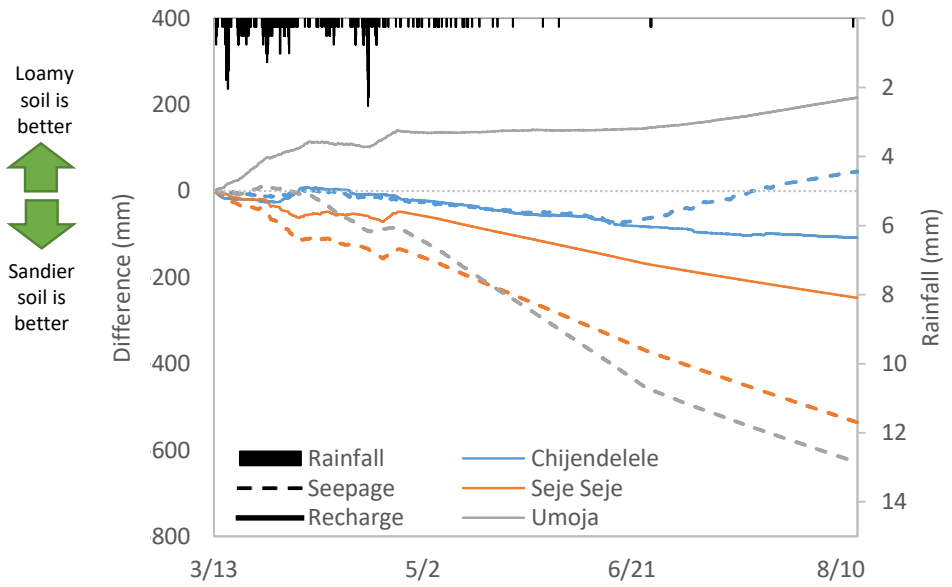

Figure 4.17. Comparative trends in groundwater flow parameters for each of the three sand dams after increasing sand fraction. Like Fig. 4.16, quantities above the $y = 0$ line indicate S1 is better for sand dams and vice versa.

When considering the entire Chididimo watershed, S4 always produces greater cumulative recharge than S1. However, this is not always the case when considering the sand dams individually. Unlike the Chijendelele and Seje Seje sand dams, the Umoja sand dam produces more recharge in S1 compared with S4. This may be due to the topography near the Umoja sand dam that creates small surface reservoirs, as mentioned in the previous section. S1 has a lower minimum rate of infiltration, but a higher saturated moisture content. If given the necessary time to achieve infiltration, the vadose zone storage and resultant recharge would likely be greater for S1 than for S4. The unique topography at Umoja provides this opportunity in S1.

Connectivity with the riparian zone

Overall, S4 provides for much greater connectivity between the stream channel and the riparian zone than S1 (see Fig. 4.18). Sandier soils with higher hydraulic conductivity permit subsurface water to flow more freely from the channel and sand dams to the riparian zone. Within the channel, there is little difference between the S1 and S4 change in groundwater elevation over the course of the study. However, beyond the channel banks, S4 groundwater elevations increase by as much as 2 m more than in S1. Connectivity between the stream channel and the riparian zone is important to permit subsurface flow from the channel into the banks, where it can further recharge the groundwater or be taken up for use by vegetation. In addition, a sand dam that is well-connected to its channel margins can be recharged by subsurface flow. Sand dams that are repeatedly recharged by subsurface flows will store water for much longer into the dry season (Quinn et al., 2019).

4.7 General Discussion and Considerations

The model of the Chididimo watershed and four simulations that were run provide some guidance on land and climate features that will increase the performance of a sand dam. The Chididimo watershed only contains three sand dams that are in a cascading arrangement, so the general discussion included here is not conclusive. However, the findings of this study are the first of their kind and provide value to the sand dam community through their insights.

The simulation results for the base case (S1) revealed that stream width and sinuosity have little impact on the change in groundwater elevation within a sand dam's area of influence. While this is generally true, the total volume of a sand dam reservoir likely has a significant impact on the length of time that a sand dam stores water. The volume of the sand reservoir that develops upstream of a sand dam will depend on the stream width, the depth of the sandy streambed pre-construction, the slope of the streambed, and the height of the sand dam spillway. While these factors

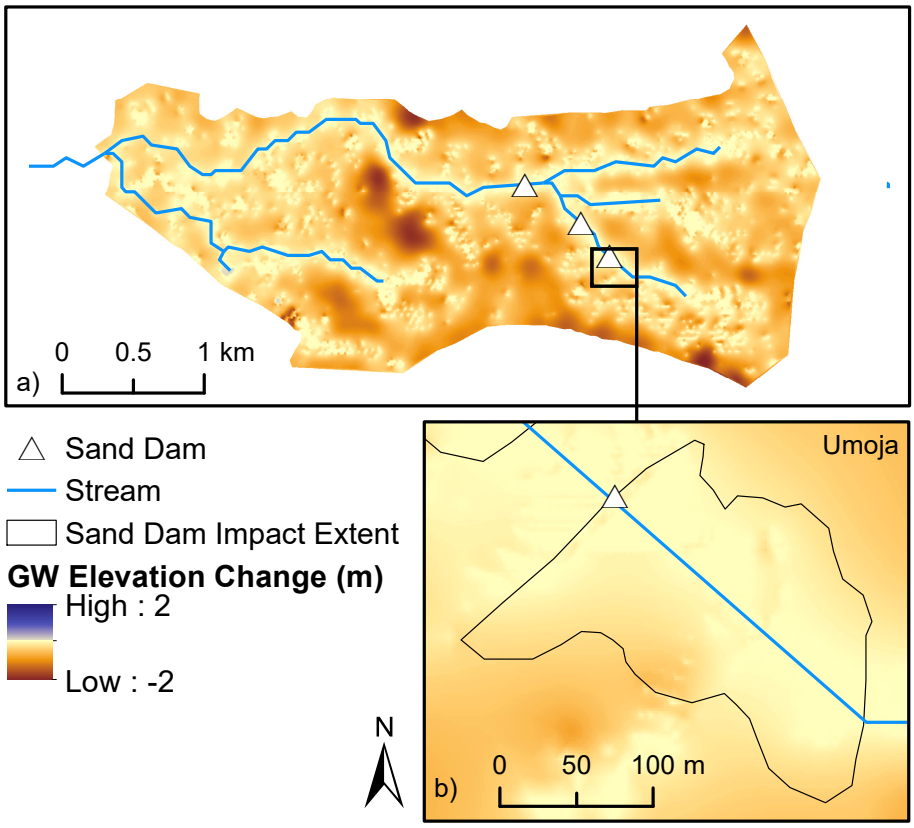

Figure 4.18. The difference between S1 and S4 groundwater (GW) elevation change at the end of the simulation period for a) the Chididimo watershed and b) the Umoja sand dam. A positive value indicates S1 produced a more desirable change in GW elevation relative to S4.

will influence the volume and duration of stored water, the depth of the resultant sand reservoir, dependent upon the depth of the sandy streambed and the height of the spillway, is likely the most important factor. Deeper sand reservoirs will lose less of their water to ET (Hellwig, 1973; Quinn, Parker, & Rushton, 2018). Stream width is somewhat correlated to stream depth, but the relationship depends largely on local geology and the location of the reach within the greater stream network.

The slope of the surrounding land may indicate whether a sand dam would successfully store water into the dry season. S1 showed that locations within u-shaped valleys are most likely to be inundated, thus providing ample water to saturate a

sand dam. While it will not always be feasible to build a sand dam in a u-shaped valley, sand dam performance will likely benefit from careful consideration of the surrounding topography. Sand dams should be built in areas with a reasonably large upstream catchment such that sufficient runoff is generated and directed to the sand dam reservoir.

Somewhat unexpectedly, S2 revealed that sand dams should likely be built in an area that is highly cultivated with low-water demand crops. Typically, actual ET is significantly reduced for crops during the initial and final stages of the growing season relative to the reference ET (Allen et al., 1998). Conversely, while crop coefficients have not been well-studied for ecosystems with natural vegetation, most studies indicate that natural vegetation ET is nearly equal to reference ET (Corbari et al., 2017; Nagler et al., 2007). Thus, the extended periods of reduced ET in areas that are heavily cropped allow for greater vadose zone storage and recharge during the growing season. These benefits outweigh the negative affects of the limited period of increased ET during the middle of the growing season. Therefore, sand dams constructed in areas that are cultivated with low-water stress crops will likely store water longer into the dry season than a sand dam constructed in an area with primarily natural vegetation.

The additional rainfall concentrated in fewer large events over a longer rainy season in S3 did not result in greater sand dam performance beyond increased vadose zone storage. Additional vadose zone storage provides more water for plants to use in transpiration but would not increase the water available to local communities. Interestingly, the additional vadose zone storage in S3 results in greater ET losses in S3 compared to S1, despite S3's lower potential ET. The additional rainfall that falls on the highly productive Kenyan sand dams is not what increases their performance above that of the Tanzanian sand dams, but rather it is the overall cycle of dry and rainy seasons. At the end of the study period, there was an insignificant difference between recharge in S1 (Tanzanian rainfall) and in S3 (Kenyan rainfall). However, in Kenya, another rainy season would begin within a couple of weeks. In Dodoma,

Tanzania, the next rainy season would not begin for at least another three to four months. Thus, Kenya's dry seasons are much shorter than those of Dodoma, and sand dams can store water for the entire duration of a Kenyan dry season. Sand dams constructed in areas with three to four month-long dry seasons will be better able to provide water to the local communities for the entire dry season. Conversely, communities in locations with extended dry seasons will require an additional water source after the sand dam dries.

Sandier soils resulted in more groundwater recharge and greater connectivity between the sand dam and channel margins. The additional recharge raises the local groundwater table, which helps to rejuvenate the ecosystem by making water available to vegetation. The increased connectivity with the riparian zone also increases the sand dam's area of impact. A sand dam that is well-connected to its channel margins will have a greater positive impact on the vitality of the surrounding land. When possible, sand dams should likely be built in a location where the soil textures in the riparian zone permit high connectivity with the sand dam reservoir.

4.8 Future Work

The guidelines developed here will be expanded and further refined by modeling five additional sand dams in the nearby Soweto watershed. Three of the five Soweto watershed sand dams are also in a cascading system. However, the cascading Soweto sand dams are much more productive than those included in this study. The Soweto watershed also includes two isolated sand dams. The five Soweto sand dams will increase the diversity of sand dams used to develop the siting guidelines and will therefore improve overall utility of the guidelines.

5. SYNTHESIS

The results of this dissertation show that sand dams have a complicated record of success as a solution to rural water security in sub-Saharan Africa. Understanding and accepting the underlying issues that pervade sand dams is the first step to identifying strategies for increasing their effectiveness. Continuing to turn a blind eye to sand dam-related failures enables the the myth of their being a panacea to rural water security to be perpetuated. Ramping up sand dam construction while issues remain unaddressed may lead to a situation where millions of dollars are invested in rural sub-Saharan Africa only to litter the region with expensive man-made waterfalls that intermittently flow during the rainy season.

This dissertation aims to begin developing a scientific understanding of the wide range of sand dam impacts and to initiate a discussion of feasible strategies for improving their effectiveness. A summary of related findings is included below.

5.1 Regional impacts of sand dams on water storage and vegetation

Three adjacent counties (SDC) in southeastern Kenya are already home to an estimated 3,000 sand dams, each with an area of impact up to 2 km^2. While many non-governmental organizations (NGOs) and published research has discussed local impacts of sand dams, the regional impacts have not been described. This study investigated whether the high density of sand dams in the SDC have an additive effect on water storage or vegetation as recorded in remotely sensed datasets. The Gravity Recovery and Climate Experiment (GRACE) dataset only recorded significantly more storage in the SDC during the two months of highest rainfall each year, one month in each of the two rainy seasons. The GRACE data is likely too low resolution to detect an expected small-magnitude regional impact on water storage. Not only is GRACE

data low resolution, but the published 2 km^2 area of impact for sand dams is likely generous. While the regional impacts of sand dams on water storage could not be directly detected and quantified, an analysis of normalized difference vegetation index (NDVI) indicated that sand dams have a consistently positive impact on regional vegetation. Groundwater elevations are often correlated with vegetation cover and health. Therefore, the positive relationship between sand dams and vegetation hints that a positive relationship between sand dams and regional water storage also exists. These findings may provide the foundation of a methodology for quantifying sand dam performance, wherein a sand dam with a relatively greater increase in NDVI captures and stores water more effectively than a sand dam with a relatively smaller increase in NDVI.

5.2 Local impacts of sand dams

Most published research on sand dam impacts is focused on a single, highly-effective sand dam in southeastern Kenya or analyses high-level surveys of sand dams. This has created a limited understanding of the local impacts of sand dams with minimal recognition of potential negative impacts. This study sought to expand the scientific information and analysis available on the environmental responses to sand dams. A year-long field study of three sand dams in Tanzania was conducted to examine sand dams in relation to groundwater elevation, vegetative cover, streambank erosion, and macroinvertebrates. Only two of the three studied sand dams were functioning. The sand dams studied have a positive impact on groundwater levels, but this impact is more limited in time and space than previously believed. Sand dams in Tanzania are only able to store water for the first few months of the dry season, rather than the oft-claimed entire dry season. Sand dams do, however, effectively increase the duration of water storage by reducing the rate of evapotranspiration to below that of surface water. Improved vegetative cover around the two functioning sand dams was also observed. The magnitude of the impact seems limited by the slope of the riparian

zone. It was observed that relatively flat channel margins led to a greater increase in vegetative cover. Streambank erosion was not a significant factor at the functioning sand dams, however mass bank failure downstream of the non-function sand dam was recorded. The non-functioning sand dam's poor positioning within the reach likely contributed to the instability, and thus mass failures, of its banks. Unfortunately, sand dams do not appear to be a suitable habitat for microinvertebrates. Overall, analysis of the environmental responses to sand dams provided some insight into overland characteristics that are likely to have a significant impact on sand dam performance, such as land slope, rainfall, and streambank stability.

5.3 Siting a sand dam based on surface characteristics

Based on published estimates of the sand dam failure rate, more research on mitigation strategies for common sand dam failure traps is essential. One frequently cited trap that is supported by both anecdotes and experience is that of constructing sand dams in ill-suited reaches or watersheds. This study built an integrated surface flow and groundwater model of three cascading sand dams and explored how different overland factors affect groundwater elevation and various flow quantities, such as groundwater recharge and vadose zone storage. This research identified basic siting guidelines that will likely lead to increased sand dam performance. For example, U-shaped valleys seem to be particularly suited to sand dams, because they are more likely than other topography to have periods of inundation. Many sand dams are recharged via flash floods, so inundation is desirable for this purpose. In addition, higher cultivation rates of low-water requirement crops and ET variability during the growing season led to increased rainy season vadose zone storage and groundwater recharge. The analysis revealed that the amount of rain that falls during the rainy season is not as important as the length of the dry season for ensuring sand dams provide water for a community throughout the dry season. Lastly, sand dams in catchments with sandier soils produce greater recharge and have greater connectivity

with their channel margins. The work included in this study should be expanded to include a greater diversity of sand dams to increase the applicability and strength of the findings.

5.4 Limitations and future work

While every attempt was made to develop robust methodologies for the studies included in this dissertation, limitations of the work must be acknowledged. First, the information about constructed sand dams is limited. Most of the assumptions in this dissertation were based on anecdotes that are occasionally inconsistent across sources. Assumptions ranged from the quantity to the locations to the subsurface conditions of sand dams. Second, climatic, geologic, and land surface data is sparse for sub-Saharan Africa. Low resolution datasets were employed where no better options exist. This adds a high level of uncertainty to the results of studies that relied heavily upon such datasets. However, this uncertainty must be endured until better data for the African continent becomes freely available for research purposes.

Future work on this topic will focus on expanding findings from the field study in Tanzania and on developing more robust site selection guidelines based on diverse sand dams. Factors affecting the area of a sand dam's impact will be explored along with the interactions between the sand dam and local geology. Groundwater dynamics around the sand dams will be further investigated to develop a greater understanding of the role of ET in sand dam drawdown. Lastly, five additional sand dams will be modeled in ICPR to further inform the development of site selection guidelines for sand dams.

REFERENCES

A, G., Wahr, J., & Zhong, S. (2013). Computations of the viscoelastic response of a 3-D compressible Earth to surface loading: an application to Glacial Isostatic Adjustment in Antarctica and Canada. *Geophysical Journal International*, *192*(2), 557–572. doi: 10.1093/gji/ggs030

Aerts, J., Lasage, R., Beets, W., de Moel, H., Mutiso, G., Mutiso, S., & de Vries, A. (2007). Robustness of sand storage dams under climate change. *Vadose Zone Journal*, *6*(3), 572. doi: 10.2136/vzj2006.0097

Allen, R. G., Pereira, L. S., Raes, D., Smith, M., et al. (1998). Crop evapotranspiration-guidelines for computing crop water requirements-fao irrigation and drainage paper 56. *FAO*, *300*(9), D05109.

Anderson, W. B., Zaitchik, B. F., Hain, C. R., Anderson, M. C., Yilmaz, M. T., Mecikalski, J., & Schultz, L. (2012). Towards an integrated soil moisture drought monitor for East Africa. *Hydrology and Earth System Sciences*, *16*(8), 2893–2913. doi: 10.5194/hess-16-2893-2012

Anselin, L. (2002). Under the hood Issues in the specification and interpretation of spatial regression models. *Agricultural Economics*, *27*(3), 247–267. doi: 10.1016/S0169-5150(02)00077-4

Beaudoing, H., & Rodell, M. (2016). Nasa/gsfc/hsl. *GLDAS Noah Land Surface Model L4 monthly 0.25 x 0.25 degree*, *2*.

Behailu, M., & Haile, M. (2002). Water harvesting in northern Ethiopia: Environmental, health and socio-economic impacts. In *Integrated water and land management research and capacity building priorities for Ethiopia* (pp. 185–191).

Beswetherick, S., Carrière, M., Legendre, V., Mather, W., Perpes, T., & Saunier, B. (2018). *Guidelines for the siting of sand dams* (Master's thesis, Cranfield University, Cranfield, UK). Retrieved from `https://www.cranfield.ac.uk/~/media/files/research_case-study_project_files/final-sand-dam-group-report(1).ashx`

Biazin, B., Sterk, G., Temesgen, M., Abdulkedir, A., & Stroosnijder, L. (2012). Rainwater harvesting and management in rainfed agricultural systems in sub-Saharan Africa–a review. *Physics and Chemistry of the Earth, Parts A/B/C*, *47*, 139–151.

Borst, L., & de Haas, S. (2006). *Hydrology of sand storage dams: A case study in the Kiindu catchment, Kitui District, Kenya* (Master's thesis, Vrije Universiteit Amsterdam, Amsterdam, Netherlands). Retrieved from `https://www.samsamwater.com/library.php`

Boulton, A., Stanley, E., Fisher, S., & Lake, P. (1992). Over-summering strategies of macroinvertebrates in intermittent streams in Australia and Arizona. In *Aquatic Ecosystems in Semi-arid Regions: Implications for Resource Management* (pp. 227–237). Saskatoon, Canada: NHRI Symposium Series 7. (Eds. R. Robarts and M. Bothwell)

Bouma, J. A., Hegde, S. S., & Lasage, R. (2016). Assessing the returns to water harvesting: A meta-analysis. *Agricultural Water Management*, *163*, 100–109. doi: 10.1016/j.agwat.2015.08.012

Cao, Y., Nan, Z., & Cheng, G. (2015). GRACE gravity satellite observations of terrestrial water storage changes for drought characterization in the arid land of Northwestern China. *Remote Sensing*, *7*(1), 1021–1047. doi: 10.3390/rs70101021

Cheng, M., Ries, J. C., & Tapley, B. D. (2011). Variations of the Earth's figure axis from satellite laser ranging and GRACE. *Journal of Geophysical Research*, *116*(B1). doi: 10.1029/2010JB000850

Chow, V. T. (1959). *Open channel flow.* London: McGRAW-HILL.

Corbari, C., Ravazzani, G., Galvagno, M., Cremonese, E., & Mancini, M. (2017). Assessing crop coefficients for natural vegetated areas using satellite data and eddy covariance stations. *Sensors*, *17*(11), 2664.

Crowley, J. W., Mitrovica, J. X., Bailey, R. C., Tamisiea, M. E., & Davis, J. L. (2006). Land water storage within the Congo Basin inferred from GRACE satellite gravity data. *Geophysical Research Letters*, *33*(19). doi: 10.1029/2006GL027070

de Trincheria, J., Leal, W. F., & Otterpohl, R. (2018). Towards a universal optimization of the performance of sand storage dams in arid and semi-arid areas by systematically minimizing vulnerability to siltation: A case study in Makueni, Kenya. *International Journal of Sediment Research*, *33*(3), 221–233. doi: 10.1016/j.ijsrc.2018.05.002

de Trincheria, J., Nissen-Petersen, E., Filho, W., & Otterphol, R. (2015). Factors affecting the performance and cost-efficiency of sand storage dams in southeastern Kenya. In *Deltas of the future and what happens upstream, 36th IAHR World Congress.* The Hague, Netherlands.

Didan, K. (2015). *MOD13A3 MODIS/Terra vegetation Indices Monthly L3 Global 1km SIN Grid V006.* NASA EOSDIS Land Processes DAAC. Retrieved 02-14-2019, from `https://lpdaac.usgs.gov/node/840` doi: 10.5067/MODIS/MOD13A3.006

Didan, K., Barreto-Munoz, A., Solano, R., & Huete, A. (2015). *MODIS vegetation index user's guide: MOD 13 series (Version 3.00).* Retrieved from `https://lpdaac.usgs.gov/sites/default/files/public/product_documentation/mod13_user_guide.pdf`

Dormann, C. F., McPherson, J. M., Araújo, M. B., Bivand, R., Bolliger, J., Carl, G., ... Wilson, R. (2007). Methods to account for spatial autocorrelation in the analysis of species distributional data: a review. *Ecography*, *30*(5), 609–628. doi: 10.1111/j.2007.0906-7590.05171.x

Drechsel, P., & Gyiele, L. (1999). The economic assessment of soil nutrient depletion. *Analytical issues for framework development. International Board for Soil Research and Management Issues in Sustainable Land Management*, *7*.

Duan, X., Wang, Z., & Tian, S. (2008). Effect of streambed substrate on macroinvertebrate biodiversity. *Frontiers of Environmental Science & Engineering in China*, *2*(1), 122–128. doi: 10.1007/s11783-008-0023-y

Elmore, A., Kaste, J., Okin, G., & Fantle, M. (2008). Groundwater influences on atmospheric dust generation in deserts. *Journal of Arid Environments*, *72*(10), 1753–1765. doi: 10.1016/j.jaridenv.2008.05.008

Ertsen, M., & Hut, R. (2009). Two waterfalls do not hear each other. Sand-storage dams, science and sustainable development in Kenya. *Physics and Chemistry of the Earth, Parts A/B/C*, *34*(1-2), 14–22. doi: 10.1016/j.pce.2008.03.009

FAO. (2002). *Multipurpose Landcover Database for Kenya - AFRICOVER* [Digital map]. Rome, Italy: Food and Agriculture Organization of the United Nations.

Fick, S. E., & Hijmans, R. J. (2017). WorldClim 2: new 1-km spatial resolution climate surfaces for global land areas: New climate surfaces for global land areas. *International Journal of Climatology*, *37*(12), 4302–4315. doi: 10.1002/joc.5086

Fischer, G., Nachtergaele, F., Prieler, S., van Velthuizen, H., Verelst, L., & Wiberg, D. (2008). *Global Agro-ecological Zones Assessment for Agriculture* [Digital map]. Laxenburg, Austria & Rome, Italy: International Institute for Applied Systems Analysis & Food and Agricultural Organization of the United Nations.

Garfì, M., Ferrer-Martí, L., Bonoli, A., & Tondelli, S. (2011). Multi-criteria analysis for improving strategic environmental assessment of water programmes. A case study in semi-arid region of Brazil. *Journal of Environmental Management*, *92*(3), 665–675. doi: 10.1016/j.jenvman.2010.10.007

Gupta, S. (2011). Demystifying 'tradition': The politics of rainwater harvesting in rural Rajasthan, India. *Water Alternatives*, *4*(3), 347–364.

Hachborn, E., Berg, A., Levison, J., & Ambadan, J. T. (2017). Sensitivity of GRACE-derived estimates of groundwater-level changes in southern Ontario, Canada. *Hydrogeology Journal*, *25*(8), 2391–2402. doi: 10.1007/s10040-017-1612-2

Hekala, W. (2012). Why donors should care more about project management. *Devex*. Retrieved from `http://www.devex.com/en/news/why-donors-shouldcare-more-about-project/77595`

Hellwig, D. (1973). Evaporation of water from sand, 4: The influence of the depth of the water-table and the particle size distribution of the sand. *Journal of Hydrology*, *18*(3-4), 317–327. doi: 10.1016/0022-1694(73)90055-3

Hengl, T., Mendes de Jesus, J., Heuvelink, G. B. M., Ruiperez Gonzalez, M., Kilibarda, M., Blagotić, A., ... Kempen, B. (2017). SoilGrids250m: Global gridded soil information based on machine learning. *PLOS ONE*, *12*(2), e0169748. doi: 10.1371/journal.pone.0169748

Henry, C. M., Allen, D. M., & Huang, J. (2011). Groundwater storage variability and annual recharge using well-hydrograph and GRACE satellite data. *Hydrogeology Journal*, *19*(4), 741–755. doi: 10.1007/s10040-011-0724-3

Henry, M., Baldwin, G., & Quathamer, G. (2015). Designing a Community-based Water Harvesting System: Understanding Water Use in Endallah, Tanzania. *Journal of Purdue Undergraduate Research*, *5*(1), 38–47. doi: 10.5703/jpur.05.1.05

Herman, J., Davis, A., Chin, K., Kinzler, M., Scholz, S., & Steinhoff, M. (2012). Life with a weak heart: Prolonging the GRACE mission despite degraded batteries. In *12th International Conference on Space Operations.* Stockholm, Sweden.

Hoogmoed, M. (2007). *Analyses of impacts of a sand storage dam on groundwater flow and storage: Groundwater flow modelling in Kitui District, Kenya* (Unpublished master's thesis). Vrije Universiteit Amsterdam, Amsterdam, Netherlands. (Dept. of Hydrogeology)

Hooke, J. (1979). An analysis of the processes of river bank erosion. *Journal of Hydrology*, *42*(1-2), 39–62. doi: 10.1016/0022-1694(79)90005-2

Huang, J., Halpenny, J., van der Wal, W., Klatt, C., James, T. S., & Rivera, A. (2012). Detectability of groundwater storage change within the Great Lakes Water Basin using GRACE: Detectability of groundwater using GRACE. *Journal of Geophysical Research: Solid Earth*, *117*(B8). doi: 10.1029/2011JB008876

Hut, R., Ertsen, M., Joeman, N., Vergeer, N., Winsemius, H., & van de Giesen, N. (2008). Effects of sand storage dams on groundwater levels with examples from Kenya. *Physics and Chemistry of the Earth, Parts A/B/C*, *33*(1-2), 56–66. doi: 10.1016/j.pce.2007.04.006

Ika, L. A. (2012). Project management for development in Africa: Why projects are failing and what can be done about it. *Project Management Journal*, *43*(4), 27–41. doi: 10.1002/pmj.21281

Jaber, J., & Mohsen, M. (2001). Evaluation of non-conventional water resources supply in Jordan. *Desalination*, *136*(1-3), 83–92. doi: 10.1016/S0011-9164(01)00168-0

Julian, R. (2016). Is it for donors or locals? The relationship between stakeholder interests and demonstrating results in international development. *International Journal of Managing Projects in Business*, *9*(3), 505–527. doi: 10.1108/IJMPB-09-2015-0091

Kosugi, K., Katsura, S., Katsuyama, M., & Mizuyama, T. (2006). Water flow processes in weathered granitic bedrock and their effects on runoff generation in a small headwater catchment: Water flow processes in weathered bedrock. *Water Resources Research*, *42*(2). doi: 10.1029/2005WR004275

Kumar, S., Holmes, T., Mocko, D., Wang, S., & Peters-Lidard, C. (2018). Attribution of flux partitioning variations between land surface models over the continental U.S. *Remote Sensing*, *10*(5), 751. doi: 10.3390/rs10050751

Landerer, F. W., & Swenson, S. C. (2012). Accuracy of scaled GRACE terrestrial water storage estimates: Accuracy of GRACE-TWS. *Water Resources Research*, *48*(4). doi: 10.1029/2011WR011453

Lasage, R., Aerts, J., Mutiso, G.-C., & de Vries, A. (2008). Potential for community based adaptation to droughts: Sand dams in Kitui, Kenya. *Physics and Chemistry of the Earth, Parts A/B/C*, *33*(1-2), 67–73. doi: 10.1016/j.pce.2007.04.009

Lasage, R., Aerts, J. C. J. H., Verburg, P. H., & Sileshi, A. S. (2015). The role of small scale sand dams in securing water supply under climate change in Ethiopia. *Mitigation and Adaptation Strategies for Global Change*, *20*(2), 317–339. doi: 10 .1007/s11027-013-9493-8

Lasage, R., & Verburg, P. H. (2015). Evaluation of small scale water harvesting techniques for semi-arid environments. *Journal of Arid Environments*, *118*, 48–57. doi: 10.1016/j.jaridenv.2015.02.019

Lautz, L. K. (2008). Estimating groundwater evapotranspiration rates using diurnal water-table fluctuations in a semi-arid riparian zone. *Hydrogeology Journal*, *16*(3), 483–497. doi: 10.1007/s10040-007-0239-0

Lawler, D. M., Grove, J. R., Couperthwaite, J. S., & Leeks, G. J. L. (1999). Downstream change in river bank erosion rates in the Swale-Ouse system, northern England. *Hydrological Processes*, *13*(7), 977–992. doi: 10.1002/(SICI)1099-1085(199905) 13:7⟨977::AID-HYP785⟩3.0.CO;2-5

Le Maitre, D., Scott, D., & Colvin, C. (1999). A review of information on interactions between vegetation and groundwater. *Water SA*, *25*(2), 137–152.

Liu, Z., Merwade, V., & Jafarzadegan, K. (2019). Investigating the role of model structure and surface roughness in generating flood inundation extents using one- and two-dimensional hydraulic models. *Journal of Flood Risk Management*, *12*(1), e12347.

Luhunga, P. M., & Djolov, G. (2017). Evaluation of the Use of Moist Potential Vorticity and Moist Potential Vorticity Vector in Describing Annual Cycles of Rainfall over Different Regions in Tanzania. *Frontiers in Earth Science*, *5*. doi: 10.3389/feart.2017.00007

Lutes, D., Keane, R., Caratti, J., Key, C., Benson, N., Sutherland, S., & Gangi, L. (2006). *FIREMON: Fire effects monitoring and inventory system* (Gen. Tech. Rep. No. RMRS-GTR-164-CD). Fort Collins, Colorado: U.S. Department of Agriculture, Forest Service, Rocky Mountain Research Station.

MacDonald, A. M., Bonsor, H. C., Dochartaigh, B. É. Ó., & Taylor, R. G. (2012). Quantitative maps of groundwater resources in africa. *Environmental Research Letters*, *7*(2), 024009.

Makin, J., Schilstra, J., & Theisen, A. A. (1969). The nature and genesis of certain aridisols in Kenya. *Journal of Soil Science*, *20*(1), 111–125. doi: 10.1111/j.1365 -2389.1969.tb01560.x

Mallik, A. U., & Richardson, J. S. (2009). Riparian vegetation change in upstream and downstream reaches of three temperate rivers dammed for hydroelectric generation in British Columbia, Canada. *Ecological Engineering*, *35*(5), 810–819. doi: 10.1016/j.ecoleng.2008.12.005

Manzi, H., & Kuria, D. (2011). The use of satellite images to monitor the effect of sand dams on stream bank land cover changes in Kitui District. *Journal of Agriculture, Science and Technology*, *13*(2), 133–150.

Maranz, D. E. (2001). *African friends and money matters: Observations from Africa*. International Academic Bookstore.

Martínez, J. (1989). Simulación matemática de cuencas subterráneas: flujo impermanente bidimensional. *Monografía, Facultad de Ingeniería Civil, Instituto Superior Politécnico José Antonio Echeverría, Ciudad de la Habana, Cuba*.

Mata-González, R., McLendon, T., Martin, D. W., Trlica, M. J., & Pearce, R. A. (2012). Vegetation as affected by groundwater depth and microtopography in a shallow aquifer area of the Great Basin. *Ecohydrology*, *5*(1), 54–63. doi: 10.1002/eco.196

McConville, J. R., & Mihelcic, J. R. (2007). Adapting life-cycle thinking tools to evaluate project sustainability in international water and sanitation development work. *Environmental Engineering Science*, *24*(7), 937–948.

McNally, A., Arsenault, K., Kumar, S., Shukla, S., Peterson, P., Wang, S., ... Verdin, J. P. (2017). A land data assimilation system for sub-Saharan Africa food and water security applications. *Scientific Data*, *4*, 170012. doi: 10.1038/sdata.2017.12

Moyo, D. (2009). *Dead aid: Why aid is not working and how there is a better way for Africa*. Macmillan.

Msongaleli, B. M., Tumbo, S. D., Kihupi, N. I., & Rwehumbiza, F. B. (2017). Performance of sorghum varieties under variable rainfall in Central Tanzania. *International Scholarly Research Notices*, *2017*, 1–10. doi: 10.1155/2017/2506946

Mueller, N. D., Gerber, J. S., Johnston, M., Ray, D. K., Ramankutty, N., & Foley, J. A. (2012). Closing yield gaps through nutrient and water management. *Nature*, *490*(7419), 254–257.

Nagler, P., Glenn, E., Kim, H., Emmerich, W., Scott, R., Huxman, T., & Huete, A. (2007). Relationship between evapotranspiration and precipitation pulses in a semiarid rangeland estimated by moisture flux towers and modis vegetation indices. *Journal of Arid Environments*, *70*(3), 443–462.

NASA JPL. (2013). *NASA Shuttle Radar Topography Mission Global 1 arc second V003.* Retrieved 09-22-2018, from `https://lpdaac.usgs.gov/node/527`

NASA/GSFC/HSL, A. M. (2016). *FLDAS Noah Land Surface Model L4 monthly 0.1 x 0.1 degree for Southern Africa (MERRA-2 and CHIRPS), version 001.* NASA Goddard Earth Sciences Data and Information Services Center. Retrieved 02-14-2019, from `https://disc.gsfc.nasa.gov/datacollection/FLDAS_NOAH01_C_SA_M_001.html` (type: dataset) doi: 10.5067/8LPWNKCBUDA6

Naumburg, E., Mata-gonzalez, R., Hunter, R. G., Mclendon, T., & Martin, D. W. (2005). Phreatophytic vegetation and groundwater fluctuations: A review of current research and application of ecosystem response modeling with an emphasis on Great Basin vegetation. *Environmental Management*, *35*(6), 726–740. doi: 10.1007/s00267-004-0194-7

Ngigi, S. N., Savenije, H. H., Thome, J. N., Rockström, J., & de Vries, F. P. (2005). Agro-hydrological evaluation of on-farm rainwater storage systems for supplemental irrigation in Laikipia district, Kenya. *Agricultural Water Management*, *73*(1), 21–41. doi: 10.1016/j.agwat.2004.09.021

Nissen-Petersen, E. (2006). *Water from dry riverbeds* (Technical handbook for DANIDA). Retrieved from http://www.faoswalim.org/resources/water/Water_for_arid_land/Water_from_dry_riverbeds.pdf

Palmer, J. A., Schilling, K. E., Isenhart, T. M., Schultz, R. C., & Tomer, M. D. (2014). Streambank erosion rates and loads within a single watershed: Bridging the gap between temporal and spatial scales. *Geomorphology*, *209*, 66–78. doi: 10.1016/j.geomorph.2013.11.027

Peel, M. C., Finlayson, B. L., & McMahon, T. A. (2007). Updated world map of the Köppen-Geiger climate classification. *Hydrology and Earth System Sciences*, *11*(5), 1633–1644. doi: 10.5194/hess-11-1633-2007

Pioneers of sand dams. (n.d.). Retrieved 05-26-2020, from https://sswm.info/sites/default/files/reference_attachments/ED%20Editor%20ny%20Pioneers%20of%20Sand%20Dam.pdf

Platts, P. J., Omeny, P. A., & Marchant, R. (2015). AFRICLIM: high-resolution climate projections for ecological applications in Africa. *African Journal of Ecology*, *53*(1), 103–108. doi: 10.1111/aje.12180

Previati, M., Bevilacqua, I., Canone, D., Ferraris, S., & Haverkamp, R. (2010). Evaluation of soil water storage efficiency for rainfall harvesting on hillslope micro-basins built using time domain reflectometry measurements. *Agricultural Water Management*, *97*(3), 449–456. doi: 10.1016/j.agwat.2009.11.004

Qadir, M., Jiménez, G., Farnum, R., Dodson, L., & Smakhtin, V. (2018). Fog water collection: Challenges beyond technology. *Water*, *10*(4), 372. doi: 10.3390/w10040372

Quilis, R. O., Hoogmoed, M., Ertsen, M., Foppen, J. W., Hut, R., & de Vries, A. (2009). Measuring and modeling hydrological processes of sand-storage dams on different spatial scales. *Physics and Chemistry of the Earth, Parts A/B/C*, *34*(4-5), 289–298. doi: 10.1016/j.pce.2008.06.057

Quinn, R., Avis, O., Decker, M., Parker, A., & Cairncross, S. (2018). An Assessment of the Microbiological Water Quality of Sand Dams in Southeastern Kenya. *Water*, *10*(6), 708. doi: 10.3390/w10060708

Quinn, R., Parker, A., & Rushton, K. (2018). Evaporation from bare soil: Lysimeter experiments in sand dams interpreted using conceptual and numerical models. *Journal of Hydrology*, *564*, 909–915. doi: 10.1016/j.jhydrol.2018.07.011

Quinn, R., Rushton, K., & Parker, A. (2019). An examination of the hydrological system of a sand dam during the dry season leading to water balances. *Journal of Hydrology X*, *4*, 100035. doi: 10.1016/j.hydroa.2019.100035

Rawls, W. J., & Brakensiek, D. L. (1982). Estimating soil water retention from soil properties. *Journal of the Irrigation and Drainage Division*, *108*(2), 166–171.

Rawls, W. J., Brakensiek, D. L., & Saxton, K. E. (1982). Estimation of soil water properties. *Transactions of the ASAE*, *25*(5), 1316–1320. doi: 10.13031/2013.33720

Rawls, W. J., Gimenez, D., & Grossman, R. (1998). Use of soil texture, bulk density, and slope of the water retention curve to predict saturated hydraulic conductivity. *Transactions of the ASAE*, *41*(4), 983–988. doi: 10.13031/2013.17270

Reversing Land Degradation and Desertification. (n.d.). Retrieved 07-01-2019, from https://www.excellentdevelopment.com/reversing-land-degradation-and-desertification

Reyer, C. P. O., Rigaud, K. K., Fernandes, E., Hare, W., Serdeczny, O., & Schellnhuber, H. J. (2017). Turn down the heat: regional climate change impacts on development. *Regional Environmental Change*, *17*(6), 1563–1568. doi: 10.1007/s10113-017-1187-4

Rodell, M., Chen, J., Kato, H., Famiglietti, J. S., Nigro, J., & Wilson, C. R. (2007). Estimating groundwater storage changes in the mississippi river basin (usa) using grace. *Hydrogeology Journal*, *15*(1), 159–166.

Rodell, M., Houser, P., Jambor, U., Gottschalck, J., Mitchell, K., Meng, C.-J., ... others (2004). The global land data assimilation system. *Bulletin of the American Meteorological Society*, *85*(3), 381–394.

Ryan, C., & Elsner, P. (2016). The potential for sand dams to increase the adaptive capacity of East African drylands to climate change. *Regional Environmental Change*, *16*(7), 2087–2096. doi: 10.1007/s10113-016-0938-y

Saksena, S., Dey, S., Merwade, V., & Singhofen, P. J. (2020). A computationally efficient and physically based approach for urban flood modeling using a flexible spatiotemporal structure. *Water Resources Research*, *56*(1), e2019WR025769. doi: 10.1029/2019WR025769

Saksena, S., Merwade, V., & Singhofen, P. J. (2019). Flood inundation modeling and mapping by integrating surface and subsurface hydrology with river hydrodynamics. *Journal of Hydrology*, *575*, 1155–1177. doi: 10.1016/j.jhydrol.2019.06.024

Sakumura, C., Bettadpur, S., & Bruinsma, S. (2014). Ensemble prediction and intercomparison analysis of GRACE time-variable gravity field models. *Geophysical Research Letters*, *41*(5), 1389–1397. doi: 10.1002/2013GL058632

Salant, N. L., Schmidt, J. C., Budy, P., & Wilcock, P. R. (2012). Unintended consequences of restoration: Loss of riffles and gravel substrates following weir installation. *Journal of Environmental Management*, *109*, 154–163. doi: 10.1016/j.jenvman.2012.05.013

Sand Dams. (n.d.). Retrieved 2019-07-01, from https://thewaterproject.org/sand-dams

Saynor, M. J., & Erskine, W. D. (2006). Spatial and temporal variations in bank erosion on sand-bed streams in the seasonally wet tropics of northern Australia. *Earth Surface Processes and Landforms*, *31*(9), 1080–1099. doi: 10.1002/esp.1310

Seeyan, S., Merkel, B., & Abo, R. (2014). Investigation of the relationship between groundwater level fluctuation and vegetation cover by using NDVI for Shaqlawa Basin, Kurdistan Region – Iraq. *Journal of Geography and Geology*, *6*(3). doi: 10.5539/jgg.v6n3p187

Shangguan, W., Hengl, T., Mendes de Jesus, J., Yuan, H., & Dai, Y. (2017). Mapping the global depth to bedrock for land surface modeling: Global map of depth to bedrock. *Journal of Advances in Modeling Earth Systems*, *9*(1), 65–88. Retrieved 05-16-2020, from http://doi.wiley.com/10.1002/2016MS000686 doi: 10.1002/2016MS000686

Shemsanga, C., Muzuka, A. N. N., Martz, L., Komakech, H., & Mcharo, E. (2018). Indigenous knowledge on development and management of shallow dug wells of Dodoma Municipality in Tanzania. *Applied Water Science*, *8*(2). doi: 10.1007/s13201-018-0697-7

Shen, H., Schumm, S., & Doehring, D. (1979). Stability of stream channel patterns. *Transportation Research Record*(736).

Shlens, J. (2014). *A tutorial on principal component analysis* (Tech. Rep.). Ithaca, NY: Cornell University.

Sprecher, S. (2008). *Installing monitoring wells in soils (Version 1.0)*. Lincoln, Nebraska: National Soil Survey Center, Natural Resources Conservation Service, USDA.

Stott, T. (1997). A comparison of stream bank erosion processes on forested and moorland streams in the Balquhidder Catchments, central Scotland. *Earth Surface Processes and Landforms*, *22*(4), 383–399. doi: 10.1002/(SICI)1096-9837(199704)22:4⟨383::AID-ESP695⟩3.0.CO;2-4

Streamline Technologies. (2018). *ICPR4 technical reference manual*. Winter Springs, Florida: Streamline Technol. Inc.,. Retrieved from `www.streamnologies.com/misc/ICPR4_DOCS.zip`

Stromberg, J., Tiller, R., & Richter, B. (1996). Effects of groundwater decline on riparian vegetation of semiarid regions: The San Pedro, Arizona. *Ecological Applications*, *6*(1), 113–131.

Stubbington, R., Greenwood, A. M., Wood, P. J., Armitage, P. D., Gunn, J., & Robertson, A. L. (2009). The response of perennial and temporary headwater stream invertebrate communities to hydrological extremes. *Hydrobiologia*, *630*(1), 299–312. doi: 10.1007/s10750-009-9823-8

Swenson, S., Chambers, D., & Wahr, J. (2008). Estimating geocenter variations from a combination of GRACE and ocean model output: Estimating geocenter variations. *Journal of Geophysical Research: Solid Earth*, *113*(B8). doi: 10.1029/2007JB005338

Swenson, S., & Wahr, J. (2006). Post-processing removal of correlated errors in GRACE data. *Geophysical Research Letters*, *33*(8). doi: 10.1029/2005GL025285

Taniguchi, H., & Tokeshi, M. (2004). Effects of habitat complexity on benthic assemblages in a variable environment. *Freshwater Biology*, *49*(9), 1164–1178. doi: 10.1111/j.1365-2427.2004.01257.x

Tapley, B. D., Bettadpur, S., Watkins, M., & Reigber, C. (2004). The gravity recovery and climate experiment: Mission overview and early results: GRACE mission overview and early results. *Geophysical Research Letters*, *31*(9). doi: 10.1029/2004GL019920

TELLUS. (2012). *GRACE MONTHLY LAND WATER MASS GRIDS NETCDF RELEASE 5.0.* NASA PO.DAAC. Retrieved 02-14-2019, from `http://podaac.jpl.nasa.gov/dataset/TELLUS_LAND_NC_RL05` doi: 10.5067/TELND-NC005

Tobler, W. R. (1970). A computer movie simulating urban growth in the Detroit region. *Economic Geography*, *46*, 234. doi: 10.2307/143141

Ulsaker, L., & Kilewe, A. (1983). Runoff and soil erosion for an Alfisol in Kenya. *East African Agricultural and Forestry Journal*, *44*, 210–241.

United Republic of Tanzania National Bureau of Statistics. (2015). *Migration and urbanization report: 2012 Population and housing census* (Tech. Rep.). Dar es Salaam, Tanzania. (Volume IV)

Verdonschot, R. C. M., van Oosten-Siedlecka, A. M., ter Braak, C. J. F., & Verdonschot, P. F. M. (2015). Macroinvertebrate survival during cessation of flow and streambed drying in a lowland stream. *Freshwater Biology*, *60*(2), 282–296. doi: 10.1111/fwb.12479

Viducich, J. (2015). *Spillway staging and selective sediment deposition in sand storage dams* (Master's thesis, Oregon State University, Corvallis, OR). Retrieved from `https://ir.library.oregonstate.edu/concern/graduate_thesis_or_dissertations/1z40kx51c`

Wang, P., Zhang, Y., Yu, J., Fu, G., & Ao, F. (2011). Vegetation dynamics induced by groundwater fluctuations in the lower Heihe River Basin, northwestern China. *Journal of Plant Ecology*, *4*(1-2), 77–90. doi: 10.1093/jpe/rtr002

Wilson, G., Fredlund, D., & Barbour, S. (1997). The effect of soil suction on evaporative fluxes from soil surfaces. *Canadian Geotechnical Journal*, *34*, 145–155.

World Bank. (2013). Turn down the heat: Climate extremes, regional impacts, and the case for resilience. *A Report for the World Bank by the Potsdam Institute for Climate Impact Research and Climate Analytics*.

Yeomans, K. A., & Golder, P. A. (1982). The Guttman-Kaiser Criterion as a predictor of the number of common factors. *The Statistician*, *31*(3), 221. doi: 10.2307/2987988

Yilmaz, M. T., Anderson, M. C., Zaitchik, B., Hain, C. R., Crow, W. T., Ozdogan, M., ... Evans, J. (2014). Comparison of prognostic and diagnostic surface flux modeling approaches over the Nile River basin: Prognostic and diagnostic modeling over Nile. *Water Resources Research*, *50*(1), 386–408. doi: 10.1002/2013WR014194

Yohan, I., Oteng'i, S., & Lukorito, C. (2006). Assessment of the growing season over the unimodal rainfall regime region of Tanzania. *Tanzania Journal of Agricultural Sciences*, *7*(1), 16–26.

Youker, R. (2003). The nature of international development projects. In *Proceedings of PMI Global Congress 2003 – North America.* Baltimore, Maryland.

VITA

Jessica Eisma was born in Lansing, Michigan. She graduated from Michigan State University with a B.S. in civil engineering in 2012. After completing an extended internship in water resources at Barr Engineering in Minneapolis, Minnesota, Jessica began her M.S. in civil engineering at Purdue University, graduating in 2015. Jessica received the National Science Foundation Graduate Research Fellowship to support her doctoral studies, completed at Purdue University. During her doctoral studies, Jessica spent one year conducting field work in Tanzania at the Nelson Mandela African Institute of Science and Technology supported by a Fulbright U.S. Student grant and the Borlaug Graduate Student Grant for Global Food Security. Jessica also spent a semester developing a Bayesian inference model to study the error structure of citizen science data at Delft University of Technology in the Netherlands supported by the National Science Foundation Graduate Research Opportunities Worldwide program.

Jessica will begin her academic career as an Assistant Professor in the Department of Civil Engineering at the University of Texas at Arlington.